Structures Research
Report 2016/00112484-
00112485

UF University of Florida
Civil and Coastal Engineering

University of Florida
Civil and Coastal Engineering

Final Report **April 2016**

Determination of Barge Impact Probabilities for Bridge Design

Principal investigator:
Gary R. Consolazio, Ph.D.

Research assistant:
George C. Kantrales

Department of Civil and Coastal Engineering
University of Florida
P.O. Box 116580
Gainesville, Florida 32611

Sponsor:
Florida Department of Transportation (FDOT)
William Potter, P.E. – Project manager

Contract:
UF Project No. 00112484 & 00112485
FDOT Contract No. BDV31-977-21

DISCLAIMER

The opinions, findings, and conclusions expressed in this publication are those of the authors and not necessarily those of the Florida Department of Transportation or the U.S. Department of Transportation.

SI (MODERN METRIC) CONVERSION FACTORS

*APPROXIMATE CONVERSIONS **TO** SI UNITS*

SYMBOL	WHEN YOU KNOW	MULTIPLY BY	TO FIND	SYMBOL
LENGTH				
in	inches	25.4	millimeters	mm
ft	feet	0.305	meters	m
yd	yards	0.914	meters	m
mi	miles	1.61	kilometers	km
AREA				
in^2	square inches	645.2	square millimeters	mm^2
ft^2	square feet	0.093	square meters	m^2
yd^2	square yard	0.836	square meters	m^2
ac	acres	0.405	hectares	ha
mi^2	square miles	2.59	square kilometers	km^2
VOLUME				
fl oz	fluid ounces	29.57	milliliters	mL
gal	gallons	3.785	liters	L
ft^3	cubic feet	0.028	cubic meters	m^3
yd^3	cubic yards	0.765	cubic meters	m^3
NOTE: volumes greater than 1000 L shall be shown in m^3				
MASS				
oz	ounces	28.35	grams	g
lb	pounds	0.454	kilograms	kg
T	short tons (2000 lb)	0.907	Megagrams	Mg (or "t")
TEMPERATURE (exact degrees)				
^oF	Fahrenheit	5(F-32)/9 or (F-32)/1.8	Celsius	^oC
ILLUMINATION				
fc	foot-candles	10.76	lux	lx
fl	foot-Lamberts	3.426	$candela/m^2$	cd/m^2
FORCE and PRESSURE or STRESS				
kip	1000 pounds force	4.45	kilonewtons	kN
lbf	pounds force	4.45	newtons	N
lbf/in^2	pounds force per square inch	6.89	kilopascals	kPa
psf	pounds force per square foot	47.88	pascals	Pa

1. Report No.	2. Government Accession No.	3. Recipient's Catalog No.

4. Title and Subtitle	5. Report Date
Determination of Barge Impact Probabilities for Bridge Design	April 2016
	6. Performing Organization Code
	8. Performing Organization Report No.
7. Author(s) G. R. Consolazio, G.C. Kantrales	2016/112484-112485
9. Performing Organization Name and Address University of Florida Department of Civil & Coastal Engineering P.O. Box 116580 Gainesville, FL 32611-6580	10. Work Unit No. (TRAIS)
	11. Contract or Grant No. BDV31-977-21
12. Sponsoring Agency Name and Address Florida Department of Transportation Research Management Center 605 Suwannee Street, MS 30 Tallahassee, FL 32301-8064	13. Type of Report and Period Covered Final Report
	14. Sponsoring Agency Code

15. Supplementary Notes

16. Abstract

Waterway bridges in the United States are designed to resist vessel collision loads according to design provisions released by the American Association of State Highway and Transportation Officials (AASHTO). These provisions provide detailed procedures for calculating design vessel impact loads within the context of a comprehensive risk assessment. One of the primary subcomponents of this process is the calculation of probabilities that estimate the likelihood that a barge-to-bridge impact event will occur. However, the expressions used to predict the frequency of barge-to-bridge collisions were developed from a limited number of data sets. Furthermore, the technology employed by the maritime industry at the time the original AASHTO provisions were developed—in the early 1990s—has been significantly improved in subsequent decades. As a consequence of these factors, current estimates of barge-to-bridge collision probabilities may differ from presently-employed AASHTO estimates. The focus of the research described in this report was the development of a revised barge impact probability expression particularly applicable for the design of bridge structures located on Florida waterways. Specifically, the existing AASHTO expression for the base aberrancy rate (*BR*)—used to estimate the likelihood that a barge flotilla will stray from the intended transit path—was recalibrated and updated. Barge flotilla traffic data and barge-to-bridge collision (casualty) data for Florida bridge locations were collected and used to compute historical barge-to-bridge collision probabilities. These probabilities were then utilized in conjunction with additional supplementary parameters specified in AASHTO—quantified using bridge site-specific information—to back-calculate *BR* values for each bridge location. A subset of *BR* estimates from several bridge sites were then utilized to produce a single design value of *BR* that may be used in risk assessments for new and existing bridge structures. Based on results from the recalibration process, the updated *BR* estimate was 55% smaller than the current value prescribed by AASHTO. To demonstrate the effect of the recalibrated *BR* parameter, annual frequency (*AF)* of collapse values from risk assessments of two previously-investigated bridge structures—the Bryant Grady Patton Bridge (Apalachicola Bay, FL) and the LA-1 Bridge (Leeville, LA)—were recomputed using the updated *BR* expression. Despite the reduction in *BR*, values of *AF* estimated using UF/FDOT methods and the updated *BR* expression remained high relative to *AF* estimates produced by existing AASHTO methods. It was noted in this study that bridge locations with low volumes of barge traffic corresponded to high estimates of *BR*. This finding was a consequence of utilizing less data in the statistical calibration process, which reduced the accuracy of the resulting predictions. Consequently, only Florida bridge locations with significant levels of barge flotilla traffic were utilized to produce the recommended design value of *BR*. However, additional out-of-state locations exist with more highly trafficked bridge locations, as well as a more comprehensive source of barge traffic data. Inclusion of such locations in a similar recalibration effort could result in a lower design value of *BR*.

17. Key Words	18. Distribution Statement
Barge, impact, collision, bridge pier, risk assessment, probability of impact, aberrancy rate, bridge design specifications	No restrictions.

19. Security Classif. (of this report)	20. Security Classif. (of this page)	21. No. of Pages	22. Price
Unclassified	Unclassified	119	

Form DOT F 1700.7 (8-72). Reproduction of completed page authorized

ACKNOWLEDGEMENTS

The authors thank the Florida Department of Transportation (FDOT) for providing the funding that made this research project possible. The authors also thank the United States Coast Guard (USCG) and the United States Army Corps of Engineers (USACE) for providing the data necessary to complete this work. Specific thanks are extended to Ms. Amy Tujague (USACE Waterborne Commerce Statistics Center), Capt. Timothy McGill (St. Johns Bar Pilot Association), Capt. Gary Bryan, and Capt. Clyde Wolfe for their individual contributions.

EXECUTIVE SUMMARY

Waterway bridges in the United States are designed to resist vessel collision loads according to design provisions released by the American Association of State Highway and Transportation Officials (AASHTO). These provisions provide detailed procedures for calculating design vessel impact loads within the context of a comprehensive risk assessment. One of the primary subcomponents of this process is the calculation of probabilities that estimate the likelihood that a barge-to-bridge impact event will occur. However, the expressions used to predict the frequency of barge-to-bridge collisions were developed from a limited number of data sets. Furthermore, the technology employed by the maritime industry at the time the original AASHTO provisions were developed—in the early 1990s—has been significantly improved in subsequent decades. As a consequence of these factors, current estimates of barge-to-bridge collision probabilities may differ from presently-employed AASHTO estimates.

The focus of the research described in this report was the development of a revised barge impact probability expression particularly applicable for the design of bridge structures located on Florida waterways. Specifically, the existing AASHTO expression for the base aberrancy rate (*BR*)—used to estimate the likelihood that a barge flotilla will stray from the intended transit path—was recalibrated and updated. Barge flotilla traffic data and barge-to-bridge collision (casualty) data for Florida bridge locations were collected and used to compute historical barge-to-bridge collision probabilities. These probabilities were then utilized in conjunction with additional supplementary parameters specified in AASHTO—quantified using bridge site-specific information—to back-calculate *BR* values for each bridge location. A subset of *BR* estimates from several bridge sites were then utilized to produce a single design value of *BR* that may be used in risk assessments for new and existing bridge structures.

Based on results from the recalibration process, the updated *BR* estimate was 55% smaller than the current value prescribed by AASHTO. To demonstrate the effect of the recalibrated *BR* parameter, annual frequency (*AF)* of collapse values from risk assessments of two previously-investigated bridge structures—the Bryant Grady Patton Bridge (Apalachicola Bay, FL) and the LA-1 Bridge (Leeville, LA)—were recomputed using the updated *BR* expression. Despite the reduction in *BR*, values of *AF* estimated using UF/FDOT methods and the updated *BR* expression remained high relative to *AF* estimates produced by existing AASHTO methods.

It was noted in this study that bridge locations with low volumes of barge traffic corresponded to high estimates of *BR*. This finding was a consequence of utilizing less data in the statistical calibration process, which reduced the accuracy of the resulting predictions. Consequently, only Florida bridge locations with significant levels of barge flotilla traffic were utilized to produce the recommended design value of *BR*. However, additional out-of-state locations exist with more highly trafficked bridge locations, as well as a more comprehensive source of barge traffic data. Inclusion of such locations in a similar recalibration effort could result in a lower design value of *BR*.

TABLE OF CONTENTS

LIST OF FIGURES

LIST OF TABLES

CHAPTER 1
INTRODUCTION

1.1 Introduction

A critical component of the design process for waterway bridges is the consideration of structural loads related to barge-to-bridge impact events. Such scenarios are considered extreme events in the design process and may result in considerable damage and loss of life if care is not taken in evaluating the structural collapse risks associated with them. Historical examples, such as the collapse of the I-40 bridge in Webbers Falls, Oklahoma (NTSB 2004), illustrate the importance of both predicting the frequency with which bridges are struck by barges, and designing bridges to resist the forces associated with such collisions.

1.2 Motivation

Within the United States, the American Association of State Highway and Transportation Officials (AASHTO) regularly releases design guidance and specifications dealing with vessel impact-resistant design methodologies. Methodologies described in these documents include expressions for predicting the likelihood that a vessel (ship or barge) will collide with a given bridge structure, and static load models that may be used to design bridges to resist the loads imparted by vessel collisions. The majority of the current AASHTO specifications dealing with vessel impact loads were formulated using research conducted prior to 1990, at which time limited information was available relating to barge-to-bridge collision events.

The University of Florida (UF), working in conjunction with the Florida Department of Transportation (FDOT), has performed prior research to improve existing design methods for barge impact loading of bridges. These efforts have resulted in revised barge impact analysis methodologies (Consolazio and Cowan 2005), load models (Consolazio et al. 2009, Getter and Consolazio 2011), and design expressions (Consolazio et al. 2010, Davidson et al. 2013). However, since the original release of the AASHTO provisions, only limited research has been conducted on alternative methods for predicting the likelihood that a barge-to-bridge impact event will occur. Current AASHTO expressions used for this purpose were developed from a relatively small number of investigations focused primarily on ship-to-bridge impact events and other types of vessel casualties such as barge groundings and strandings. In addition, numerous maritime technological advances have taken place in the decades following first release of the AASHTO provisions; many of these technologies have an influence on the ease of vessel pilotage through coastal and inland areas where bridges are constructed. Consequently, in the present study, a new barge impact probability expression was developed that is derived from recent and extensive barge-to-bridge collision data sets and that is more representative of the current state of the barge towing industry.

1.3 Objectives

The primary objective of the research presented in this report was to develop a revised probability expression to predict the frequency of occurrence associated with barge-to-bridge collisions. This was achieved through a recalibration of the AASHTO base aberrancy rate (BR) for barge flotillas, which is employed as a component of AASHTO expressions presently used to predict the likelihood of a barge-to-bridge impact event occurring. To ensure that the revised

expression is particularly applicable for bridges in Florida, data collection and analysis efforts were focused on barge traffic and collision data associated with Florida waterways.

1.4 Scope of Work

- Literature review of existing methods to predict barge impact events: A literature review was conducted to examine current design procedures to predict the frequency of barge-to-bridge collisions. Specific attention was given to the AASHTO Bridge Design Specifications, employed by design engineers both in the United States and internationally, as well as Eurocode provisions, which are utilized internationally. Relevant research pertaining to the prediction of vessel impact events was also summarized.
- Collection of data to quantify barge impact probabilities for Florida bridges: Data needed to compute historical barge impact probabilities for Florida bridge structures throughout the state were collected, including barge traffic and barge-to-bridge collision data. In addition, supplementary information needed in the computation of AASHTO-specified probabilities and modification factors, such as bridge plans and water current velocity data, were also assembled.
- Recalibration of existing AASHTO *BR* expression: Using information collected for bridges crossing Florida waterways, the AASHTO *BR* expression was recalibrated to exclusively reflect barge-to-bridge collision data. Recalibration was accomplished through calculation of historical barge-to-bridge impact probabilities and AASHTO-specified expressions for 13 different bridge locations. The computed parameters were then employed in a back-calculation framework to compute *BR* estimates for each bridge based on eight different sets of conditions relating to potential barge flotilla configurations and bridge protection levels. A subset of *BR* estimates was then used to compute a single recalibrated *BR* expression for use in bridge design.
- Risk assessments on bridge structures using recalibrated *BR* expression: Risk assessments were conducted on the Bryant Grady Patton Bridge over Apalachicola Bay, FL and the Louisiana Highway-1 (LA-1) Bridge in Leeville, LA using the recalibrated design *BR* expression developed in this study as well as information from a previous investigation. Comparisons were made between annual frequency of collapse estimates derived from existing AASHTO procedures and estimates produced from methods more recently developed through UF/FDOT research.
- Code language for UF/FDOT barge impact design provisions: Code language was developed for UF/FDOT *BR* and probability of collapse expressions in addition to the UF/FDOT barge impact load prediction model.

CHAPTER 2
LITERATURE AND BACKGROUND REVIEW

2.1 Introduction

As described in Chapter 1, aberrant barges which strike bridge piers or waterline pile caps can result in costly and catastrophic instances of structural collapse. Consequently, care must be taken in the design process, including evaluating the likelihood of impact events occurring and determining the structural loads associated with them. To provide guidance to design engineers on these issues, AASHTO and the European Committee for Standardization (CEN) have developed design specifications which directly address the topic of vessel collision. These documents, along with related research investigations, are summarized in this chapter. Portions of published works that address the prediction of barge impact events are emphasized. It is important to note that while the 7th edition of the AASHTO Bridge Design Specifications (AASHTO 2014) was used for reference purposes throughout this study, notes for the 2015 and 2016 interim revisions were reviewed and no relevant changes to the specifications dealing with vessel impact loading were identified.

2.2 AASHTO LRFD Bridge Design Specifications

To design waterway bridges for vessel collision events, the AASHTO LRFD Bridge Design Specifications (AASHTO 2014) allow for the use of several different design methodologies, two of which—Method I and Method III— require special circumstances and the permission of the bridge owner to employ.

Method I, a semi-deterministic procedure, is the simplest and most conservative of the three methodologies. In this procedure, a single 'design vessel' is selected for use in assessing the adequacy of the bridge structure; the design vessel is intended to represent one of the largest vessels typical of the waterway. AASHTO recommends that Method I only be used in situations where the waterway is too shallow to allow large ship traffic to pass, or for locations where accurate vessel traffic data is not readily available.

Method II, a comprehensive risk assessment procedure, is considerably more complicated than Method I, requiring significant data collection. In Method II, the annual frequency of bridge collapse (AF) is calculated using a database—developed by the design engineer—that provides a full description of the vessels that typically transit the waterway near the bridge, as well as the number of transits per vessel type. Due to the level of rigor required to conduct a Method II risk assessment, it is the most accurate of the available analysis methods. As such, Method II is considered the default approach for bridge design, and is the only procedure which does not require explicit approval from the bridge owner before being considered for use.

Method III is a cost-benefit analysis procedure that may be employed in situations where a Method II analysis results in design criteria which cannot be feasibly met, given various project constraints. Note that a Method II analysis must first be conducted prior to considering Method III as a possible option.

As Method II is considered the default risk analysis procedure, it is the focus of the present study. As noted above, Method II requires the design engineer to compute the annual frequency of structural collapse—due to vessel collision—for each individual bridge element

(pier, span) that is at risk for impact. Computation of the annual frequency of structural collapse is achieved by applying the following equation on a per-element basis:

$$AF = N(PA)(PG)(PC)(PF) \tag{2.1}$$

where N is the number of vessel transits per year for a particular vessel group, PA is the probability of vessel aberrancy (the probability that a vessel will deviate from the intended transit path), PG is the geometric probability (the 'conditional probability' that a vessel will strike a particular bridge element should deviation from the intended transit path occur), PC is the probability of structural collapse (conditional upon the bridge being struck), and PF is a protection factor used to account for protective obstructions (sandbars, fenders, dolphins, etc.) in the waterway which could prevent collisions with certain bridge elements.

Following the Method II analysis procedures, a unique AF value must be calculated using Eqn. 2.1 for each major vessel group that transits the waterway. Vessel groups may be categorized as one of two types—ships or barges—and are further divided into sub-types based on various criteria (external dimensions, weight, etc.) so that each vessel within a particular group should elicit similar structural demands upon impact. Calculated AF values are compared to AASHTO-specified limits to determine the acceptability of the design. For typical bridge structures this limit is 0.001 (1/1000), whereas, for critical/essential bridges, the limit is 0.0001 (1/10,000).

A particular focus of the present study is on the combined influence of the terms PA, PG, and PF (as used to compute AF), which collectively predict the probability that a given vessel will strike a bridge element. Details regarding these terms are provided in the following sub-sections. Specifics regarding the computation of barge impact forces and other supplementary topics are organized in Appendix A.

2.2.1 Probability of aberrancy

PA, the probability of aberrancy (Eqn. 2.2), is a measure of the likelihood that a vessel will deviate from its intended transit path:

$$PA = BR(R_B)(R_C)(R_{XC})(R_D) \tag{2.2}$$

where BR is the base aberrancy rate, and R_B, R_C, R_{XC}, and R_D are modification factors that amplify the base aberrancy rate to account for various waterway conditions. Such conditions include: the location of the bridge relative to turns or bends in the waterway (R_B); currents acting parallel to the intended transit path of the vessel (R_C); cross-currents acting perpendicular to the intended transit path of the vessel (R_{XC}); and the density of vessel traffic in the immediate vicinity of the bridge (R_D). The magnitude of BR is dependent on the vessel type being considered (0.00006 for ships and 0.00012 for barges) to reflect the relative difficulty of pilotage.

R_B is calculated by first examining the geometry of the waterway in the vicinity of the bridge structure to determine whether or not the bridge is located within, or immediately adjacent to, either a turn or a bend in the waterway. Should the bridge be located immediately adjacent to either a turn or a bend, the bridge is classified as being in a 'transition region' (Fig. 2.1). The angle of the turn or bend (θ) is then calculated (as shown in Fig. 2.1) and used in one of the following equations:

$$R_B = \left(1 + \frac{\theta}{45^\circ}\right) \tag{2.3}$$

$$R_B = \left(1 + \frac{\theta}{90^\circ}\right) \tag{2.4}$$

Eqn. 2.3 is employed if the bridge under consideration is directly within a turn or bend, and Eqn. 2.4 is used if the bridge is located within a transition region. If no turn or bend is present in the waterway near the bridge (i.e., the waterway is straight), R_B is taken as 1.0.

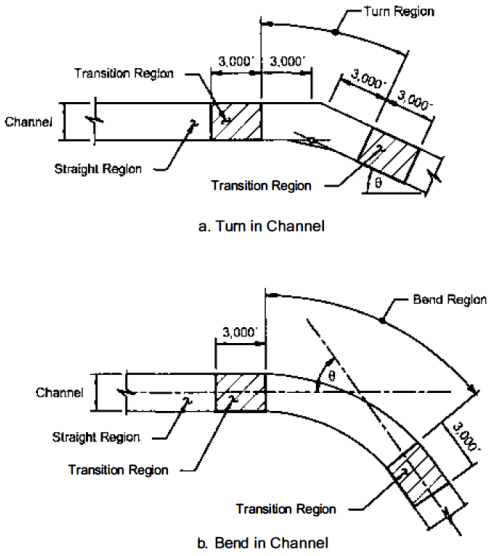

Figure 2.1 Methodology for classifying geometric characteristics of a waterway that are used in the calculation of R_B (Source: AASHTO 2014)

Determining the current and cross-current modification factors (R_C and R_{XC}, respectively) involves calculating waterway velocities parallel (V_C) and perpendicular (V_{XC}) to the intended vessel transit path. Such velocity determinations are commonly done through hydraulic and hydrologic analysis, but may also be obtained from other sources. Eqns. 2.5 and 2.6 are then used to determine appropriate impact risk amplification factors.

$$R_C = \left(1 + \frac{V_C}{10}\right) \tag{2.5}$$

$$R_{XC} = \left(1 + V_{XC}\right) \tag{2.6}$$

Unlike other modification factors noted above, the vessel traffic density factor R_D is selected solely based on the judgment of the design engineer. R_D can take one of three values, depending on the vessel traffic density category selected:

- Low density ($R_D = 1.0$)
- Average density ($R_D = 1.3$)
- High density ($R_D = 1.6$)

Selection of the vessel traffic density category is related to the frequency at which vessels encounter (cross or pass) each other in the vicinity of the bridge. A rough determination of vessel traffic density can be performed by examining the geometry of the waterway, and the relative numbers and sizes of vessels that typically transit the waterway near the bridge, over a span of several years. This information can then be used by an experienced design engineer to select a representative value for R_D .

2.2.2 Geometric probability

To assess the likelihood that an aberrant vessel will strike a particular component of a bridge structure, AASHTO (2014) utilizes a conditional probability term entitled 'geometric probability' (PG). It is important to note that this term includes the probabilistic distribution of location for a given *aberrant* vessel along the width of the waterway. Consequently, PG is not used to represent probable locations of vessels that are tracking 'normally' along an intended transit path.

Calculation of PG for a specific bridge element is performed by integrating a probability density function (PDF) that models the distribution of probable (aberrant) vessel locations across the waterway over a desired range (Fig. 2.2). This range is related to the width of the bridge pier (or pile cap) as well as the beam (width) of the vessel being considered. As a consequence, a unique value of PG must be determined for each combination of pier and vessel type. Detailed in Fig. 2.2, the PDF which describes possible locations of the aberrant vessel within the waterway is normally distributed about a mean which represents the centerline of the intended vessel transit path. The standard deviation of the PDF is taken as the overall vessel length (LOA); a unique LOA must be computed for each type of vessel considered in the risk analysis. AASHTO recommends that any bridge elements located outside a distance of 3 x LOA from the centerline of the vessel transit path (computed using the LOA of the largest design vessel) be omitted from the risk analysis. It should be noted that the normal distribution assumed for PG , as well as the parameters that define its shape, were developed from historical records of *ship*-to-bridge collisions; nevertheless the same PG distribution is also used to assess risks associated with *barge*-to-bridge collisions.

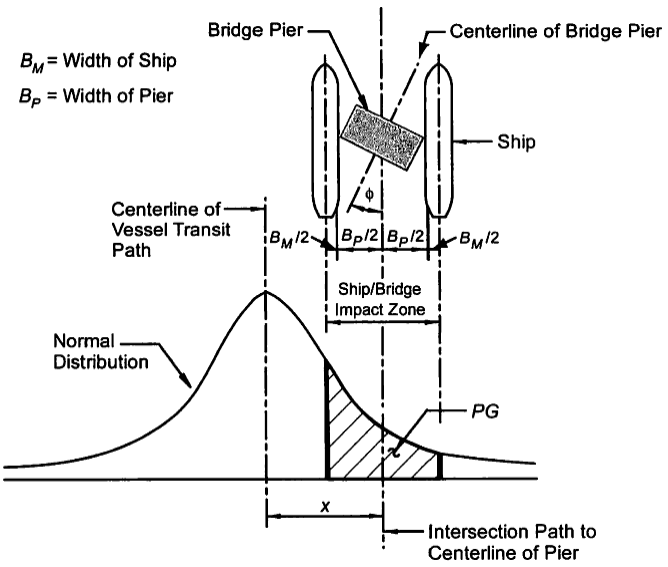

Figure 2.2 Methodology for calculating the geometric probability, *PG*
(Source: AASHTO 2014)

2.2.3 Protection factor

Since the probability of a barge impacting a particular bridge pier or pile cap can be influenced by the presence of impassable waterway features (shallow sand bars or protective systems such as dolphins or fenders), the AASHTO provisions include a term which modifies *AF* to reflect the reduction in impact probability that is associated with shielding a bridge element. This term, called a protection factor (*PF*), is employed on a per-element basis using the following equation:

$$PF = 1 - (\%\ Protection\ Provided / 100) \tag{2.7}$$

Note that the methodology used to calculate the percentage of protection provided by a barrier or protective system is based on the judgment of the design engineer, and will vary depending on the characteristics of the individual protective system under consideration.

2.2.4 Limitations

The probability expressions currently implemented in AASHTO (2014) to predict the occurrence of barge-to-bridge impact events are based on research conducted before 1991. At that time, comprehensive data sets associated with such events were not widely available. As a consequence, a relatively small collection of vessel casualty statistics were used to calibrate parameters in both *PA* and *PG* . Moreover, as opposed to considering only vessel casualties that involved vessels striking bridge elements, *all* types of impact events were considered, including vessel *groundings* and *vessel-to-vessel* collisions. Between 1991 and present, significant advances in navigational technology have occurred, including the wide-spread utilization of global positioning systems (GPS), automatic identification systems (AIS), and electronic chart display and information systems (ECDIS). Advances in vessel mechanical systems, such as azimuth thrusters for multi-directional propulsion, have also seen increased use in modern tugs and towboats. Furthermore, in addition to technological advances, there have also

been significant changes in the training and certification requirements for tug and pushboat operators. It is probable that the combined effects of technological advances and improved training requirements has resulted in a decrease in vessel aberrancy rates relative to pre-1991 levels.

2.3 Previous UF/FDOT Research

For over a decade, the University of Florida (UF) has been working in conjunction with the Florida Department of Transportation (FDOT) to complete a series of research projects related to barge-to-bridge impact design. This research has resulted in the development of several notable tools for use by bridge designers, including comprehensive dynamic analysis procedures and revised load-prediction models for barge types common to U.S. waterways. Findings from each of these projects have been incorporated into proposed revisions to the current AASHTO risk analysis framework. Detailed information regarding previous UF/FDOT studies is summarized in Appendix B.

2.4 Eurocode 1: Actions on Structures

In contrast to the AASHTO specifications, European standards for vessel collision design—developed by the European Committee for Standardization—are more loosely organized with more flexibility afforded to individual nations. Primary design guidelines and concepts for vessel collision are organized in *Eurocode 1: Actions on Structures (EN 1991), Part 1-7: General Actions - Accidental Actions* (CEN 2006). Each nation that adopts EN 1991 determines specific quantities for many of the variables mentioned in the provisions. This information is then detailed in a nation-specific supplementary document called a 'national annex'. The general organization and design approach of EN 1991 is outlined in this section. Additional discussions pertaining to risk assessment methodologies are also provided. Supplementary topics relating to the computation of impact forces are summarized in Appendix A.

2.4.1 General principles

EN 1991 divides accidental actions, such as vessel collisions, into three categories based on a qualitative measure of consequence in the event of a failure: CC1 (low-level consequences); CC2 (moderate-level consequences); and CC3 (high-level consequences). These categories are coupled to recommendations on design and analysis methods in increasing order of complexity. In the case of a design situation classified as a CC1 event, no *specific* action to mitigate failure is recommended (beyond designing for general robustness and stability, as provided in EN 1990 – EN 1991). For CC2 events, equivalent-static analyses or prescriptive designing/detailing procedures are recommended. Finally, for CC3 events, EN 1991 specifies that a comprehensive risk assessment incorporating nonlinear-dynamic structural analysis methods may be necessary. More specific recommendations can also be provided in national annexes, as deemed appropriate by individual nations.

In the event that the threat posed by vessel collision is significant enough to merit independent consideration (CC2 and CC3), EN 1991 provisions recommend that only dynamic or 'equivalent static' design forces be used to represent vessel collision events. The use of purely static design forces without implicit inclusion of dynamic effects is not considered an adequate approach for design. Moreover, it is assumed that the impacting vessel dissipates a considerable

majority of impact energy through plastic deformation (also called a 'hard impact'). EN 1991 §4.6 outlines additional areas that should be considered by a design engineer, including: (1) the characteristics of the waterway (geometry, currents, depth); structural characteristics (stiffness, mass, ability to dissipate energy); and vessel characteristics (type, dimensions, force-deformation behavior under impact conditions). Vessels are divided by the Eurocode into two major design categories: (1) vessels which commonly transit inland waterways and (2) ocean-going vessels. Inland vessels are further organized into a series of classes according to the European Conference of Ministers of Transport (ECMT) classification system (Table 2.1). In contrast, ocean-going vessels are classified according to unique systems outlined in individual national annexes. Representative categories for such vessels, along with relevant design values, are provided in Table 2.2.

For each vessel being included in the design process, two *separate* loading cases should be considered: (1) a head-on (frontal) impact, resulting in an impact force parallel to the direction of travel (F_{dx}); and (2) a lateral impact, resulting in an impact force perpendicular to the direction of travel (F_{dy}) coupled with a friction force (F_R). Further details relating to the computation of design forces are provided in Appendix A.

Table 2.1 ECMT vessel classifications (Source: CEN 2006)

CEMT[a] Class	Reference type of ship	Length ℓ (m)	Mass m (ton)[b]	Force F_{dx}[c] (kN)	Force F_{dy}[c] (kN)
I		30-50	200-400	2 000	1 000
II		50-60	400-650	3 000	1 500
III	"Gustav König"	60-80	650-1 000	4 000	2 000
IV	Class „Europe"	80-90	1 000-1 500	5 000	2 500
Va	Big ship	90-110	1 500-3 000	8 000	3 500
Vb	Tow + 2 barges	110-180	3 000-6 000	10 000	4 000
VIa	Tow + 2 barges	110-180	3 000-6 000	10 000	4 000
VIb	Tow + 4 barges	110-190	6 000-12 000	14 000	5 000
VIc	Tow + 6 barges	190-280	10 000-18 000	17 000	8 000
VII	Tow + 9 barges	300	14 000-27 000	20 000	10 000

[a] CEMT: European Conference of Ministers of Transport, classification proposed 19 June 1992, approved by the Council of European Union 29 October 1993.

[b] The mass m in tons (1 ton = 1 000 kg) includes the total mass of the vessel, including the ship structure, the cargo and the fuel. It is often referred to as the displacement tonnage.

[c] The forces F_{dx} and F_{dy} include the effect of hydrodynamic mass and are based on background calculations, using expected conditions for every waterway class.

Table 2.2 Representative classifications for ocean-going vessels (Source: CEN 2006)

Class of ship	Length ℓ= (m)	Mass m[a] (ton)	Force F_{dx}[b,c] (kN)	Force F_{dy}[b,c] (kN)
Small	50	3 000	30 000	15 000
Medium	100	10 000	80 000	40 000
Large	200	40 000	240 000	120 000
Very large	300	100 000	460 000	230 000

[a] The mass m in tons (1 ton = 1 000 kg) includes the total mass of the vessel, including the ship structure, the cargo and the fuel. It is often referred to as the displacement tonnage. It does not include the added hydraulic mass.

[b] The forces given correspond to a velocity of about 5,0 m/s. They include the effects of added hydraulic mass.

[c] Where relevant the effect of bulbs should be accounted for.

2.4.2 Risk analysis methodology

In some instances, structural failure due to vessel impact can have severe consequences (e.g., failure of a pier for a major highway bridge). For these cases, per EN 1991 recommendations, a comprehensive risk assessment (i.e., risk analysis) may be necessary. The general approach for such an analysis (Fig. 2.3) is iterative in nature and contains both qualitative and (if sufficient data are available) quantitative components.

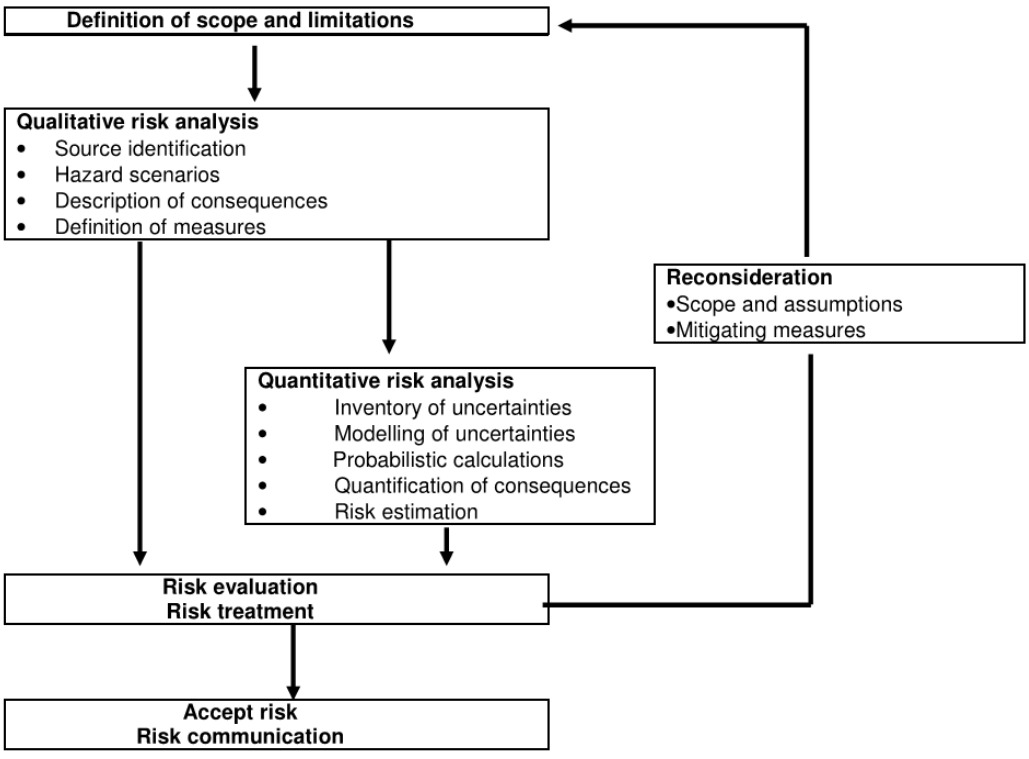

Figure 2.3 Risk analysis methodology (Source: CEN 2006)

Evaluating risk using EN 1991 procedures first involves defining the boundaries (purpose, assumptions, and objectives) of the risk analysis. Following this, a qualitative analysis is conducted, which includes determining the sources of potential hazards as well as any environmental factors which could contribute to hazard severity. If feasible, a quantitative analysis is subsequently performed. A general approach for quantifying the risk posed to a structural system is provided in the form of Eqn. 2.8.

$$R = \sum_{i=1}^{N_H} p(H_i) \sum_{j=1}^{N_D} \sum_{k=1}^{N_S} p(D_j \left| H_i \right.) p(S_k \left| D_j \right.) C(S_k) \tag{2.8}$$

where R is the calculated risk, N_H is the number of hazards considered, $p(H_i)$ is the probability of occurrence for hazard H_i, N_D is the number of different ways that hazard H_i can damage the structural system, N_S is the number of adverse states for the structural system, $p(D_j \left| H_i \right.)$ is the conditional probability that damage state D_j will occur for a given hazard H_i, $p(S_k \left| D_j \right.)$ is the conditional probability that adverse state S_k will occur given that damage state D_j is present, and $C(S_k)$ is the consequence associated with adverse state S_k.

In addition to the general approach presented in Eqn. 2.8, EN 1991 provides a procedure more specific to vessel collision (Eqn. 2.9) that may be used to quantify the probability of failure for a given structural system:

$$P_f(T) = n\lambda T(1 - p_a) \int P(F_{dyn}(x) > R) dx \tag{2.9}$$

where $P_f(T)$ is the probability that the structural system fails over a selected time period T, n is the number of vessel passages per unit of time, λ is the probability that a navigational or equipment failure occurs in the vessel per unit of travel, p_a is the probability that a collision with the structure is avoided by human intervention, and $P(F_{dyn}(x))$ is the probability that the dynamic impact force imparted by the vessel, $F_{dyn}(x)$, is greater than the resistance of the structure, R. Note that the dynamic impact force is a function of x, the distance between the structure and the point in the waterway where equipment failure occurred.

While the Eurocode provides some guidance on how to estimate the dynamic impact force, F_{dyn} (see Appendix A), no specific information is provided on how to determine any of the other parameters provided in Eqn. 2.9.

2.5. Related Research

In addition to the methods proposed by CEN (2006) and AASHTO (2014), several other procedures have been developed by researchers to predict the occurrence of vessel impact events. The most relevant of these investigations are summarized below.

Larsen (1993) proposed a methodology (Eqn. 2.10) to determine the number of annual vessel-bridge collisions resulting in failure (F) that is similar in form to the AASHTO AF expression, but without the additional modification factors that are incorporated into AASHTO:

$$F = \sum N_i \times P_{c,i} \times \sum P_{G,i,k} \times P_{F,i,k} \tag{2.10}$$

where N_i represents the number of vessels belonging to class i, $P_{c,i}$ is the 'causation probability', or the probability that a vessel from class i will be unable to avoid collision, $P_{G,i,k}$ is the 'geometrical probability', or the probability that a vessel from class i will strike the k'th bridge element, and $P_{F,i,k}$ is the 'failure' probability associated with the k'th bridge element if it is struck by a vessel from class i. Larsen recommends that vessels be classified into groups depending on a variety of vessel characteristics, including: draft; air draft; and structural characteristics (which relate to collision-induced loads).

Kunz (1998) presented a model (Eqn. 2.11) to determine the probability of vessel-structure collision (ν) for a given path of travel (s), which shares some basic similarities with Eqn. 2.9:

$$\nu = N \int \frac{d\lambda}{ds} \times W_1(s) \times W_2(s) ds \tag{2.11}$$

where N is the number of vessel transits per unit of time, $\frac{d\lambda}{ds}$ is the rate of vessel failure (navigational or mechanical) per unit of travel, $W_1(s)$ is the probability of a particular collision course occurring, and $W_2(s)$ is the probability that the vessel will not be able to come to a stop before colliding with the structure. $W_1(s)$ may be quantified by employing the following equations:

$$W_1(s) = F_\varphi(\varphi_1) - F_\varphi(\varphi_2) \tag{2.12}$$

$$F_\varphi(\varphi) = \frac{1}{\sqrt{2\pi}\sigma_\varphi} \int_{-\infty}^{\varphi} \exp\left(\frac{(\varphi - \bar{\varphi})^2}{2\sigma_\varphi^2} \right) d\varphi \tag{2.13}$$

where, φ is a normally-distributed random variable representing the angle of deviation from the planned path of travel. Values of φ_1 and φ_2 for a particular maneuvering path and bridge pier may be determined through graphical means (Fig. 2.4).

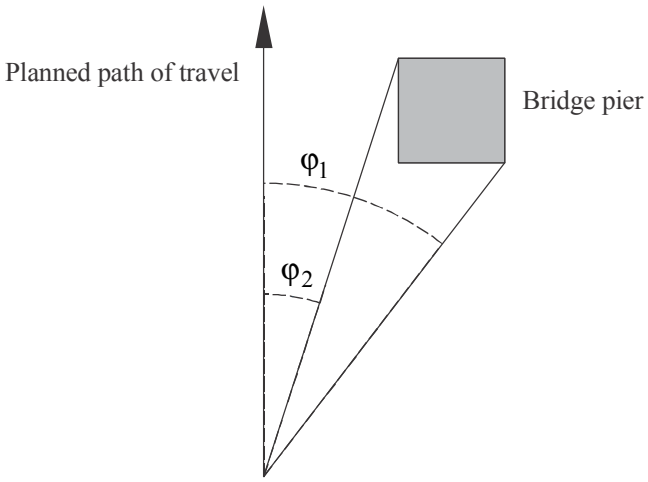

Figure 2.4 Determination of deviation angles for a particular bridge pier and maneuvering path

$W_2(s)$ may be quantified by employing the following relationships:

$$W_2(s) = 1 - F_x(s) \tag{2.14}$$

$$F_x(x) = \frac{1}{\sqrt{2\pi}\sigma_x} \int_{-\infty}^{x} \exp\left(\frac{(x-\bar{x})^2}{2\sigma_x^2} \right) dx \tag{2.15}$$

where x is a normally-distributed random variable representing the 'stopping distance', or the distance over which the operators of the vessel recognize that a collision is possible and attempt to bring the vessel to a halt. Note that Eqn. 2.11, similar to Eqn. 2.9, contains a parameter which describes the probability that a failure will occur in the vessel per unit of travel. Kunz notes that estimation of this parameter is not trivial, as it relates to a number of variables. One recommendation is to use an estimated failure time rate (failures/vessel/year) in conjunction with the known navigational distance (to safely transit underneath the bridge) to come up with a desired failure rate per unit of travel. Additional complications associated with this approach are related to the estimation of the parameters which describe the assumed normal distributions ($\bar{\varphi}$, σ_φ, $\bar{x}$, and σ_x).

Wang and Wang (2014) took general concepts from the Kunz model and expanded the approach to account for several factors not directly addressed by Kunz which can significantly influence vessel impact probabilities: 'meandering' navigation channels (nonlinear waterways); seasonal variations in water level; and waterway obstacles. (Recall that the AASHTO provisions also incorporate probability expressions to address both nonlinear waterway geometry [R_B] as well as waterway obstacles [PF]). Organized as a series of summations, the model proposed by Wang and Wang (Eqn. 11) takes the following general form:

$$P_{clsn} = \sum_{i=1}^{I_W} \sum_{j=1}^{J_V^S} \sum_{n=1}^{N_C} P_{i,j,n} \tag{2.16}$$

where P_{clsn} is the total vessel-bridge collision probability, I_W is the number of water level intervals considered, J_V^S is the number of vessel groups, N_C is the number of navigation channels, and $P_{i,j,n}$ is the collision probability associated with the i^{th} water level interval, the j^{th} vessel group, and the n^{th} navigation channel. $P_{i,j,n}$ is determined as follows:

$$P_{i,j,n} = \int_{h_{i-1}}^{h_i} \left\{ \int_{w_{j-1}^S}^{w_j^S} f_n^{DWT}(w) \left[\sum_{l=1}^{L_S(n)} P_{n,l}(h,w) \right] dw \right\} \times f_H(h) dh \tag{2.17}$$

where h_{i-1} and h_i are the lowest and highest values of the i^{th} water level interval, w_{j-1}^S and w_j^S are the lowest and highest dead weight tonnages associated with the j^{th} vessel group, $f_n^{DWT}(w)$ is the frequency of vessel traffic as a function of vessel tonnage for channel n, and $L_S(n)$ is the number of straight segments that channel n can be divided into so that nonlinear waterway geometry can be approximately represented. $f_H(h)$ is a PDF which describes the distribution of water levels, and $P_{n,l}(h,w)$ is the vessel-bridge collision probability for the l^{th} segment of the n^{th} channel, which is calculated using the following:

$$P_{n,l}(h,w) = \lambda \int_{x_{n,(l-1)}}^{x_{n,l}} \int_{y_{n,l,1}(x)}^{y_{n,l,2}(x)} f_{n,l}^{TD}(y) G\left(x, y \mid h_i, w_j^S\right) dxdy \tag{2.18}$$

where λ is the vessel aberrancy rate per unit of travel, $x_{n,(l-1)}$ and $x_{n,l}$ are the x-coordinates of the beginning and ending points of the l^{th} segment of the n^{th} navigation channel, $y_{n,l,1}(x)$ and $y_{n,l,2}(x)$ are the y-coordinates of the same points (as a function of x), and $f_{n,l}^{TD}(y)$ is the PDF of vessel positions perpendicular to the channel centerline for the l^{th} segment of the n^{th} channel. $G\left(x, y \mid h_i, w_j^S\right)$ is the probability of collision from position (x,y) for a vessel with tonnage w_j^S and water level h_i, determined as follows:

$$G\left(x, y \mid h_i, w_j^S\right) = \int_{\theta_{\min}(x,y,w_j^S)}^{\theta_{\max}(x,y,w_j^S)} f_{DA}\left(\theta \mid w_j^S\right) F\left(\theta \mid x, y, w_j^S\right) d\theta \tag{2.19}$$

where $\theta_{\min}(x, y, w_j^S)$ and $\theta_{\max}(x, y, w_j^S)$ are the minimum and maximum yaw angles of a vessel with tonnage w_j^S at a position (x,y). $f_{DA}\left(\theta \mid w_j^S\right)$ is the PDF of the vessel yaw angle for tonnage category w_j^S, and $F\left(\theta \mid x, y, w_j^S\right)$ is the probability that a vessel with tonnage w_j^S, position (x,y), and yaw angle θ will not be able to evade striking a bridge element, calculated by:

$$F\left(\theta \mid x, y, w_j^S\right) = 1 - \int_0^s \phi\left(z \mid w_j^S\right) dz \tag{2.20}$$

where $\phi\left(z \mid w_j^S\right)$ is a normally-distributed PDF representing the distance the vessel travels from the onset of aberrancy until stoppage, and s is the distance from the point at which vessel aberrancy is initiated until a bridge element is struck.

While the approach developed by Wang and Wang accounts for several important factors which contribute to the occurrence of vessel impact events, it is considerably more complicated than the mostly empirical approach adopted by AASHTO. Furthermore, the effects of certain highly influential factors considered by AASHTO, such as currents and vessel traffic density are not explicitly represented. It is possible, however, that careful selection of an appropriate value of λ could *implicitly* capture the influence of such variables.

Statistical parameters (mean and standard deviation) which define each normal distribution in the method proposed by Wang and Wang need to be calibrated using relevant data; data for such calibrations can be difficult to collect in some cases. Wang and Wang illustrated the calibration process by computing parameters for the Jiujiang Bridge in the Guangdong province of China using data collected from local port authorities. In their example, λ was determined by utilizing vessel casualty and traffic data collected within 10 km of the bridge over a two-year period of time.

Several other investigations of note have also addressed various aspects of vessel collision analysis, including: development of risk analysis software packages employing established methods (Friis-Hansen and Simonsen 2002); use of real-time (Gucma 2003) and Monte-Carlo based (Hutchinson et al. 2003) vessel maneuvering simulations coupled with vessel tracking experiments to predict aberrancy rates; the influence of turbulent zones (Zhang 2013); and potential effects of wind and flow-induced vessel drift (Zhou et al. 2011).

2.6 AASHTO Provision Historical Background

To ensure that the updated provisions developed in the present study were made in full awareness of the historical background of the existing AASHTO provisions, a discussion was held with the principal author of the AASHTO vessel impact design provisions. The purpose of the discussion was to review the historical basis of portions of the AASHTO provisions that relate specifically to *barge-to-bridge* impact design. During the discussion, the UF research team was briefed on historical information relating to several key issues:

- The types of vessel casualties (i.e., groundings, collisions, etc.) that were included in the 1980s-1990s studies from which the AASHTO probability of aberrancy (*PA*) term was produced;

- The general approach that was used to arrive at the design base aberrancy rate (*BR*) values that are specified by AASHTO for ships and barges;

- Calibration procedures that were adopted in formulating the AASHTO modification factors R_B, R_C, R_{XC}, and R_D;

- Factors which have likely influenced changes in the base aberrancy rate since 1991 (e.g., changes in GPS technology, etc.)

2.7 Observations

Consideration of vessel impact loads is a critical component of the overall bridge design process, requiring careful attention to numerous variables. While design standards (AASHTO 2014, CEN 2006) provide methodologies to predict the frequency of vessel impact events, and researchers (Larsen 1993, Kunz 1998, Wang and Wang 2014) have developed alternative strategies to address this topic, there remains a need for a widely-applicable and simply-structured methodology which distinguishes between a vessel-to-bridge collision and other types of vessel casualties (strandings, groundings, etc.). Furthermore, due to numerous differences between the mechanical systems and pilotage of ships versus barge tows, a study which focuses specifically on the latter is needed to improve existing barge impact load prediction methodologies. Additionally, while empirical methods are able to capture the influence of variables that are not readily characterized probabilistically (e.g., human error), the existing empirical AASHTO method was calibrated using a limited number of data sets and may not reflect changes in navigational technology, vessel mechanical systems, and operator/pilot training that have occurred since 1991.

CHAPTER 3
METHODOLOGY

3.1 Introduction

As described in the Chapter 2, the current AASHTO (2014) specifications for barge impact design were formed from a series of vessel accident studies conducted prior to 1991 and may not reflect changes that have occurred in the barge towing industry over the past twenty-five (25) years. Moreover, due to the limited availability of accident data prior to 1991, development of the AASHTO barge impact design provisions relied on data spanning not solely, or specifically, barge-to-bridge impacts, but rather more general vessel-to-vessel impacts (e.g., ship-to-ship), vessel-to-bridge impacts, and vessel groundings. Therefore, the primary objective of the present study was to develop a revised, and updated, barge impact probability expression based on comprehensive, up-to-date barge casualty data. Accident data used in formulating the new impact probability expression were limited to *barge*-to-bridge collisions (i.e., ship impacts and vessel groundings were excluded), and were reflective of historical barge traffic (density) and accident-rate statistics specific to Florida waterways.

3.2 Approach

Prior to developing a detailed approach to revise existing AASHTO (2014) expressions for predicting the occurrence of barge-to-bridge impact events, it was necessary to gain additional insight into factors that could have affected barge aberrancy rates since 1991. To do this, industry professionals were consulted to identify advances that have been made in vessel technology (navigational and mechanical) and personnel training since 1991, and the potential influence of such advances on barge flotilla aberrancy rates. The outcome of these interviews—the details of which are discussed in subsequent sections—revealed that technological advances and modern training requirements could have significantly reduced barge flotilla aberrancy rates, relative to pre-1991 levels. As a consequence of this initial finding, a full investigation was carried out to quantify an updated aberrancy rate reflective of the current state of the barge towing industry (Chapter 5).

Revised aberrancy rates were obtained through the use of expressions in the current AASHTO formulation for AF (Eqn. 2.1). The AF component terms PA, PG, and PF, when multiplied together, represent the probability that a vessel will strike the bridge. This probability will be referred to as the 'probability of impact' (PI):

$$PI = (PA)(PG)(PF) \tag{3.1}$$

Substitution of the full expression for PA (Eqn. 2.2) into Eqn. 3.1 produces:

$$PI = (BR)(R_B)(R_C)(R_{XC})(R_D)(PG)(PF) \tag{3.2}$$

where, BR is the base aberrancy rate, and R_B, R_C, R_{XC}, and R_D are modification factors that amplify the base aberrancy rate to account for: the location of the bridge relative to turns or bends in the waterway (R_B); currents acting parallel to the intended transit path of the vessel (R_C); cross-currents acting perpendicular to the intended transit path of the vessel (R_{XC}); and

the density of vessel traffic in the immediate vicinity of the bridge (R_D). *PG* is the geometric probability, and *PF* is the protection factor. Rearranging the terms in Eqn. 3.2, *BR* may be expressed as follows:

$$BR = \frac{PI}{(R_B)(R_C)(R_{XC})(R_D)(PG)(PF)} \tag{3.3}$$

Eqn. 3.3 may be used to calculate base aberrancy rates for individual bridge locations, provided that PI, PG, PF, R_B, R_C, R_{XC}, and R_D can all be quantified. This process was achieved in the present investigation through the collection of data obtained from several federal and state agencies, as well as a notable amount of site-specific data analysis. Specific steps included:

- Consultation with industry professionals regarding advances that have been made in vessel technology and training since the 1990s, and the potential influence of these advances on barge flotilla aberrancy rates;
- Collection of all barge-to-bridge accident data that were available for Florida bridge structures;
- Development of a list of Florida bridges included in the study, each of which has significant levels of barge flotilla traffic;
- Collection of supporting information for each suitable Florida bridge site, including: bridge plans; annual barge traffic data; and hydraulic/hydrologic data;
- Calculation of historical barge impact probabilities, AASHTO-specified protection factors, aberrancy modification factors, and geometric probabilities for individual bridge sites;
- Recalibration of the base barge aberrancy rate for bridge design using the calculated parameters noted above.

In the sections that follow, general methodologies that were used to satisfy each of the requirements listed above are discussed in detail. More specific methods used in data collection and data analysis are discussed in Chapters 4 and 5, respectively.

3.3 Data Sources

Data collection for this study was performed in several phases, beginning with interviews of professionals working in the maritime barge transportation industry. Since the outcome of these interviews confirmed the need for a revised barge impact probability expression, several government entities were contacted regarding the collection of data pertinent to several components of this study, including: barge-to-bridge collision data and associated accident reports (United States Coast Guard [USCG]); barge traffic data (USACE); bridge plans and hydraulic reports (FDOT); and water current predictions (National Oceanic and Atmospheric Administration [NOAA]).

3.3.1 Interviews

To qualitatively assess the relative influence that advances in maritime technology and operator training have had on barge flotilla pilotage over the past two decades, it was necessary to consult industry professionals who have significant familiarity with the navigation of barge flotillas. Consulted entities included tug captains with decades of experience navigating Florida waterways. Consulted professionals indicated that the primary tools currently utilized in maritime navigation include: radio detection and ranging (RADAR), global positioning systems (GPS), automatic identification systems (AIS), and electronic chart display and information systems (ECDIS).

RADAR is used by maritime navigators to detect the distance and bearing of vessels or other objects in close proximity to the piloted vessel through transmission and reflection of radio waves. These systems are used primarily for collision avoidance and navigation during limited-visibility conditions (e.g., during night hours or foggy conditions).

GPS employs receivers to interface with multiple orbiting satellites that are able to provide real-time latitude and longitude coordinates identifying the location of the user. Initially developed as a military tool, GPS was used increasingly in civilian sectors beginning in the 1990s. However, with recent advancements in GPS technology, and the removal of (military) restrictions on the quality of GPS predictions in the year 2000, the reliability of GPS technology has increased considerably since it was initially developed (Kumar and Moore 2002).

AIS serves as a means by which vessels navigating within a common waterway may share vessel-specific information, such as call signs, transits speeds, bearings, and vessel dimensions. This information is communicated through maritime very high frequency (VHF) radio and interpreted via receivers on properly equipped vessels. AIS data are commonly visualized on a map of the waterway (example shown in Fig. 3.1), with the position of each vessel represented as a clearly defined marker. Unlike RADAR, or other older navigational technologies, AIS was not regularly employed until after the year 2000. However, although the technology is relatively new, the USCG has mandated that vessels meeting certain specifications (e.g., specified minimum lengths and horsepower) must have AIS devices installed in order to operate within US waterways.

ECDIS (Fig. 3.2) is used to synthesize all available navigational information into one unit for convenient display. Such information includes not only GPS and AIS data, but also information that is typically contained in navigational charts, such as water depths and channel marker information. Consequently, ECDIS systems can serve as a replacement for conventional paper navigational charts. While ECDIS units are not universally employed by maritime navigators, interviewees stated that such units are becoming increasingly popular due to the high level of convenience attributed to them.

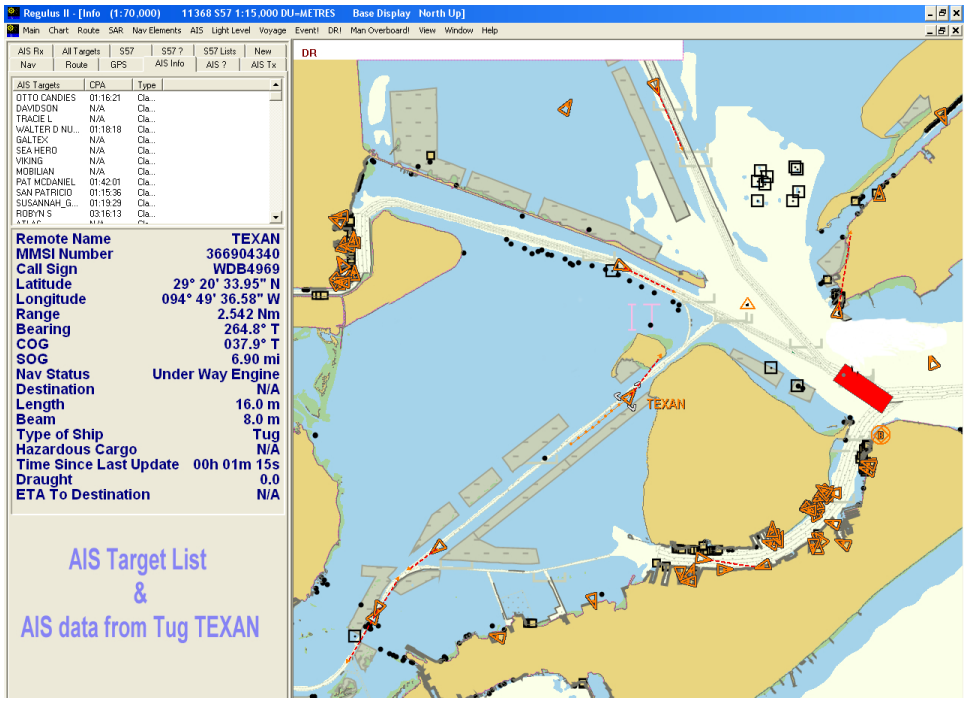

Figure 3.1 Visualization of sample AIS data (Adapted from: http://www.navcen.uscg.gov)

Figure 3.2 ECDIS display on-board a NOAA vessel (Source: http://www.ncep.noaa.gov)

In addition to developments in navigational technology, interviews revealed that the mechanical technologies commonly employed to maneuver tugs and pushboats have also changed since the early 1990s. Specifically, consulted industry professionals indicated that azimuth thrusters are becoming more common on modern tugs. Azimuth thrusters enhance vessel control and maneuverability by allowing the direction of propulsion to change by means of a rotating propeller that can align to any horizontal angle. However, despite the navigational

advantages afforded by this technology, interviewees indicated that it is unlikely that most older tugs used in barge transportation have azimuth thrusters equipped.

Supplementing technological advances, it was also noted that training requirements for tug operators have changed since the early 1990s. This includes increased formal and continuing educational requirements as well as the implementation of more regular training drills. It was noted that these increased requirements have made it more difficult for seamen without formal maritime training to become licensed tug operators, which may have an effect on the quality of barge flotilla navigators operating throughout the United States.

According to the consulted industry professionals, significant improvements in the accuracy and reliability of all four navigational tools discussed above (RADAR, GPS, AIS, and ECDIS) have been achieved since 1990. Indeed, certain technologies, such as AIS, have only recently seen widespread use in industry. Based on this finding, it was determined that a revised barge impact probability expression developed from recent (2000-2014) barge-to-bridge collision data sets will be much more likely to capture the influence of recent advances in technology and training methods than the expression currently employed in AASHTO design specifications.

3.3.2 Barge-to-bridge collisions

Collisions between barge flotillas and bridge structures are investigated by the USCG, and are classified as 'vessel casualty events'. For each such event, the captain of the vessel responsible for the collision must file an accident report with the USCG. Based on the information contained in these reports, the USCG has constructed a 'Maritime Information for Safety and Law Enforcement' (MISLE) database of reported vessel casualties. Each entry (collision event) in the MISLE database contains the following information:

- Date, time, and location of the event
- Classification of the event (e.g., collision, grounding)
- Classifications (e.g., tug, barge, ship), tonnages, and dimensions of each vessel involved
- Name or designation of the bridge struck
- Narrative describing how the event occurred

While the level of detail provided in the event narratives is variable, generally, each discussion provides a statement regarding the perceived cause(s) of the collision as determined by the investigating officer. In addition, if available, the conditions at the time of the event are also stated in the report, including: water current and wind conditions, visibility, and air temperature.

Researchers are permitted to request extracted data sets from the MISLE database for specific regions through the USCG Office of Investigations and Casualty Analysis (CG-INV). In addition, the original (detailed) accident reports from which the MISLE database was constructed may also be requested from the same office. Consequently, all barge-to-bridge collision data collected for this study (see Section 4.2 and Appendix C) were obtained through CG-INV.

3.3.3 Barge traffic

Commercial barge and tug traffic in U.S. waterways is monitored by the USACE, and may be made available to engineers and researchers upon request. For this investigation, barge and tug traffic data were collected for all regions in the state of Florida with reasonable traffic levels (see Section 4.3 and Appendix D). It is important to note that the USACE does not monitor vessel traffic associated with a *non-commercial* purposes (e.g., movement of construction barges). Commercial barge and tug traffic data are recorded as vessel passages ('trips'), either upstream or downstream, that pass by a specified geographic location. Such data may be organized by vessel type or vessel draft (example shown in Table 3.1). The USACE also maintains information regarding the types of commodities that are shipped, and the payload tonnages associated with vessel movements. In order to request vessel traffic data for a given year, or a range of years, it is necessary to provide the USACE with specific mile marker information for the location(s) of interest. Unmarked waterways, or waterways without *commercial* traffic, will not likely have recorded data available for request.

Table 3.1 Extract from Waterborne Commerce of the United States (WCUS) illustrating the organization of USACE vessel traffic data (Source: USACE 2012)

Trips and Drafts of Vessels, 2012
(draft in feet)

Draft	Self Propelled Vessels				Non-Self Propelled Vessels		Self Propelled Vessels				Non-Self Propelled Vessels	
	Total	Dry Cargo	Tanker	Tow or Tug	Dry Cargo	Tanker	Total	Dry Cargo	Tanker	Tow or Tug	Dry Cargo	Tanker
GULF INTRACOASTAL WATERWAY BETWEEN APALACHEE BAY, FL AND THE MEXICAN BORDER (CONSOLIDATED REPORT)												
	Upbound						Downbound					
Grand Total	**94,146**	**14,793**	**13**	**30,411**	**15,813**	**33,116**	**93,758**	**15,018**	**4**	**30,684**	**14,922**	**33,130**
DOMESTIC												
Total	**94,146**	**14,793**	**13**	**30,411**	**15,813**	**33,116**	**93,758**	**15,018**	**4**	**30,684**	**14,922**	**33,130**
15	236	—	1	230	—	5	284	1	1	268	—	14
14	371	10	—	333	2	26	358	5	—	332	3	18
13	232	15	—	188	17	12	322	14	—	201	20	87
12	1,100	116	—	303	237	444	900	141	1	272	144	342
11	2,146	42	—	571	610	923	1,592	46	—	547	258	741
10	6,529	1,991	—	1,797	504	2,237	6,123	2,016	—	1,818	693	1,596
9	15,051	289	4	2,904	4,137	7,717	14,189	273	—	2,969	3,912	7,035
8	15,398	665	7	7,647	2,927	4,152	13,527	986	—	7,582	1,944	3,015
7	12,508	2,527	—	8,536	651	794	12,415	2,127	—	8,583	467	1,238
≤ 6	40,575	9,138	1	7,902	6,728	16,806	44,048	9,409	2	8,112	7,481	19,044
										Total trips:		**187,904**
GULF INTRACOASTAL WATERWAY, APALACHEE BAY TO PANAMA CITY, FL (INCLUDED IN GULF INTRACOASTAL WATERWAY CONSOLIDATED REPORT)												
	Upbound						Downbound					
Grand Total	**321**	**1**	**—**	**80**	**31**	**209**	**329**	**3**	**—**	**81**	**34**	**211**
DOMESTIC												
Total	**321**	**1**	**—**	**80**	**31**	**209**	**329**	**3**	**—**	**81**	**34**	**211**
12	1	—	—	—	—	1	—	—	—	—	—	—
11	22	—	—	—	—	22	—	—	—	—	—	—
10	25	—	—	3	1	21	7	—	—	7	—	—
9	66	1	—	50	2	13	52	—	—	52	—	—
8	48	—	—	5	9	34	8	3	—	5	—	—
7	47	—	—	15	5	27	13	—	—	13	—	—
≤ 6	112	—	—	7	14	91	249	—	—	4	34	211
										Total trips:		**650**

3.3.4 Bridge plans

In order to determine the geometric probability, PG, of a collision between an aberrant barge and a structural component of a bridge, it is necessary to have a detailed description of the geometry of the bridge relative to the waterway it crosses over. Since the FDOT maintains a catalogue of pertinent design drawings and reports for Florida bridges, which were the focus of the present investigation, appropriate FDOT personnel were contacted to supply information that was used to describe the footprint of a bridge structure in a given waterway.

3.3.5 Water currents

Two of the modification factors used to calculate the probability of aberrancy, PA, relate to the current (R_C) and cross-current (R_{XC}) of the waterway in the vicinity of the bridge. Unlike barge collision incident data or barge traffic data, no single government-maintained database contained all of the water current data (e.g. flow velocities) that were needed in this study. Instead, such data were acquired from multiple sources. In most cases, individual barge collision accident reports contained flow-velocity and directional information for the day and time of the impact event. In addition, current predictions were also available for certain bridge locations through NOAA. NOAA current predictions do not include the influence of certain ambient conditions like wind and water salinity. However, unlike information typically supplied in accident reports, NOAA tidal current predictions may be obtained for longer records of time. The most rigorous method of producing a water current estimation for a specific bridge location is through detailed hydraulic simulations that include the influence of both tides and ambient conditions (e.g., wind). While predictions derived from such simulations are generally more accurate than tidal current predictions, hydraulic simulations are also vastly more demanding in terms of model preparation, input data collection, and computation. As a consequence, the utilization of hydraulic simulations was not feasible for this study. Resultantly, only current data associated with accident reports and NOAA tidal current predictions were utilized in the computation of water current-related parameters.

3.4 General Data Analysis Methods

Following the collection of raw data from the sources mentioned in the preceding sections, it was necessary to initially screen each data set to remove data points that represented conditions which fell outside the scope of this investigation (e.g., removing barge groundings from the full data set of barge casualties). Once this process was completed, calculations were performed on the screened sets of data in order to calculate each of the terms in Eqn. 3.3.

3.4.1 Bridge locations

Bridge locations suitable for this study were determined based on availability of both barge-to-bridge collision data as well as barge traffic data. For the state of Florida, the majority of commercial barge traffic moves through the Gulf Intracoastal Waterway (GIWW) from Pensacola to Panama City. Other regions of moderate commercial barge traffic include the Atlantic Intracoastal Waterway (AIWW), near Jacksonville, FL, and the Tampa Bay area. These general regions are indicated on the map in Fig. 3.3.

Bridge structures that were selected for this investigation (from the regions shown in Fig. 3.3) were those with a known history of recorded *barge-to-bridge* impacts. Since vessel

groundings and vessel-to-vessel collisions may occur under considerably different circumstances than barge-to-bridge impacts, aberrancy rates associated with groundings and vessel-to-vessel collisions are not necessarily pertinent for the prediction of barge-to-bridge impact probabilities. Consequently, this study considered only bridge locations at which barge-to-bridge collisions have occurred.

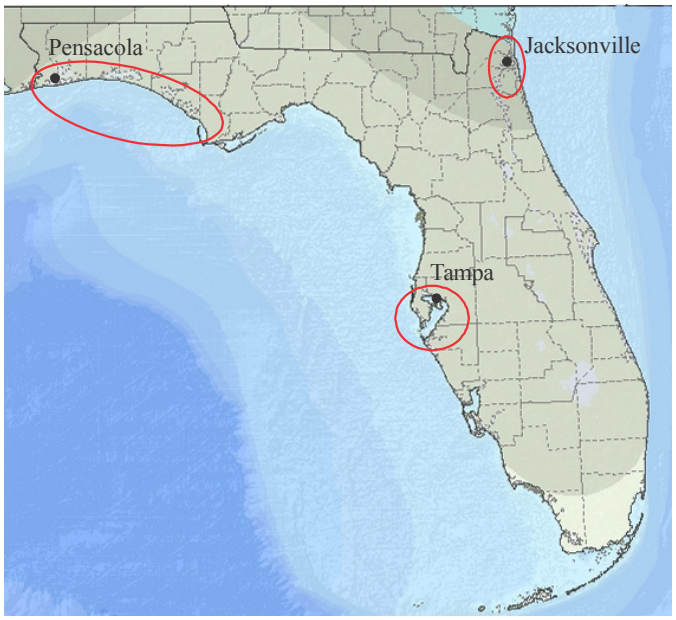

Figure 3.3 Regions of Florida waterways that, per USACE data, carry notable commercial barge traffic (Map adapted from: the United States Geological Survey [USGS])

3.4.2 Probability of impact

The probability of a barge-to-bridge impact event occurring per vessel passage (*PI*) was assumed to be reasonably constant over the time-frame considered for this investigation, since any meaningful variation in *PI*, associated with the influence of significant technological advances or changes in waterway geometry, may only be quantified over a much longer record of time. Furthermore, since this investigation was only concerned with quantifying *PI* values reflective of the *current* state of the barge towing industry, determining the historical variation in *PI*, although useful, was not a central goal of this research. Therefore, a value of *PI* for a given bridge site and transit direction was estimated from collected accident data by summing the number of barge-to-bridge collisions which occurred over the time-frame of interest and dividing this sum by the total number of barge flotilla passages during that same time:

$$PI = \frac{\sum_{t=t_i}^{t=2014} BC_t}{N_T} \tag{3.4}$$

where, t_i is the first year in which barge casualty data were utilized, BC_t is the number of barge casualties that occurred in year t, and N_T is the number of barge flotilla transits in the direction

of interest from the year t_i to the year 2014. Based on conversations that took place between UF and the USACE, it was ascertained that the preparation (by the USACE) of annual vessel traffic data sets for specific bridge locations and times (calendar years) is a work-intensive process. As such, it was not feasible to obtain barge and tug traffic data (from the USACE) for every *individual* year within the span of time over which collision data (from the USCG) were available (2002-2014). Thus, while collision data were available for each year from 2002-2014, it was necessary to restrict the request of barge and tug traffic data to every other year from 2002-2012, and for the year 2013. Data for the year 2014 were not available at the time this investigation was conducted. To make full use of available USCG barge-to-bridge collision data, temporal curve fitting procedures were employed to estimate barge flotilla traffic counts for years where USACE-provided traffic data were unavailable, including hindcast and forecast predictions (Fig. 3.4). Specific details regarding the curve fitting methods employed in this investigation are presented in Section 5.2.

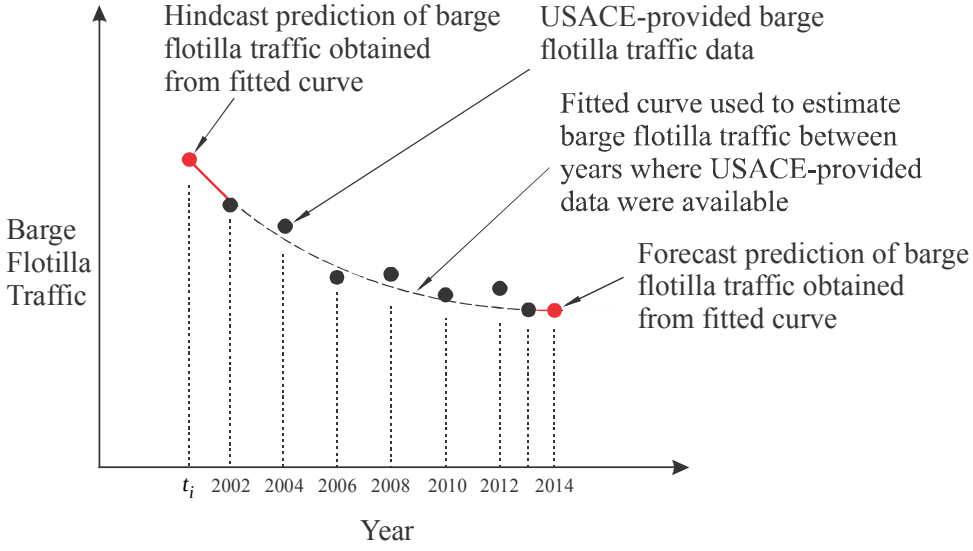

Notes: 1) Barge accident data were available from 1992-2014
2) Barge flotilla traffic data were available every other year from 2002-2012 and for 2013
3) Data utilized for this research spanned every year from t_i to 2014

Figure 3.4 Curve-fitting approach for the estimation of barge flotilla traffic data

3.4.3 Geometric probability

Determination of the *geometric* probability of a barge-to-bridge collision event occurring at a particular *bridge site* (PG_{br}), in a given direction, was performed by summing the individual geometric probabilities calculated for each pier within 3xLOA of the centerline of the vessel transit path (recall that LOA is the overall flotilla length):

$$PG_{br} = \sum_{i=1}^{n} \left(PG_i \right) \tag{3.5}$$

where PG_i is the geometric probability associated with the i^{th} pier, and n is the number of piers within a distance of 3xLOA from the centerline of the vessel transit path. The calculation of PG_i was accomplished for a single pier by superimposing a normal (Gaussian) distribution over the waterway with the mean value of the distribution coinciding with the centerline of the channel (intended vessel transit path) and the standard deviation of the distribution being equal to the LOA of the vessel group under consideration. The width of the area integrated under the distribution for a single pier was equivalent to the combined widths of the barge flotilla (B_M) and the pier (B_P), as shown in Fig. 3.5. Note that fender systems were ignored in the PG calculation process. Details regarding the specific barge flotilla sizes used in the calculation of PG_{br} for individual bridge sites are provided in Appendix F.

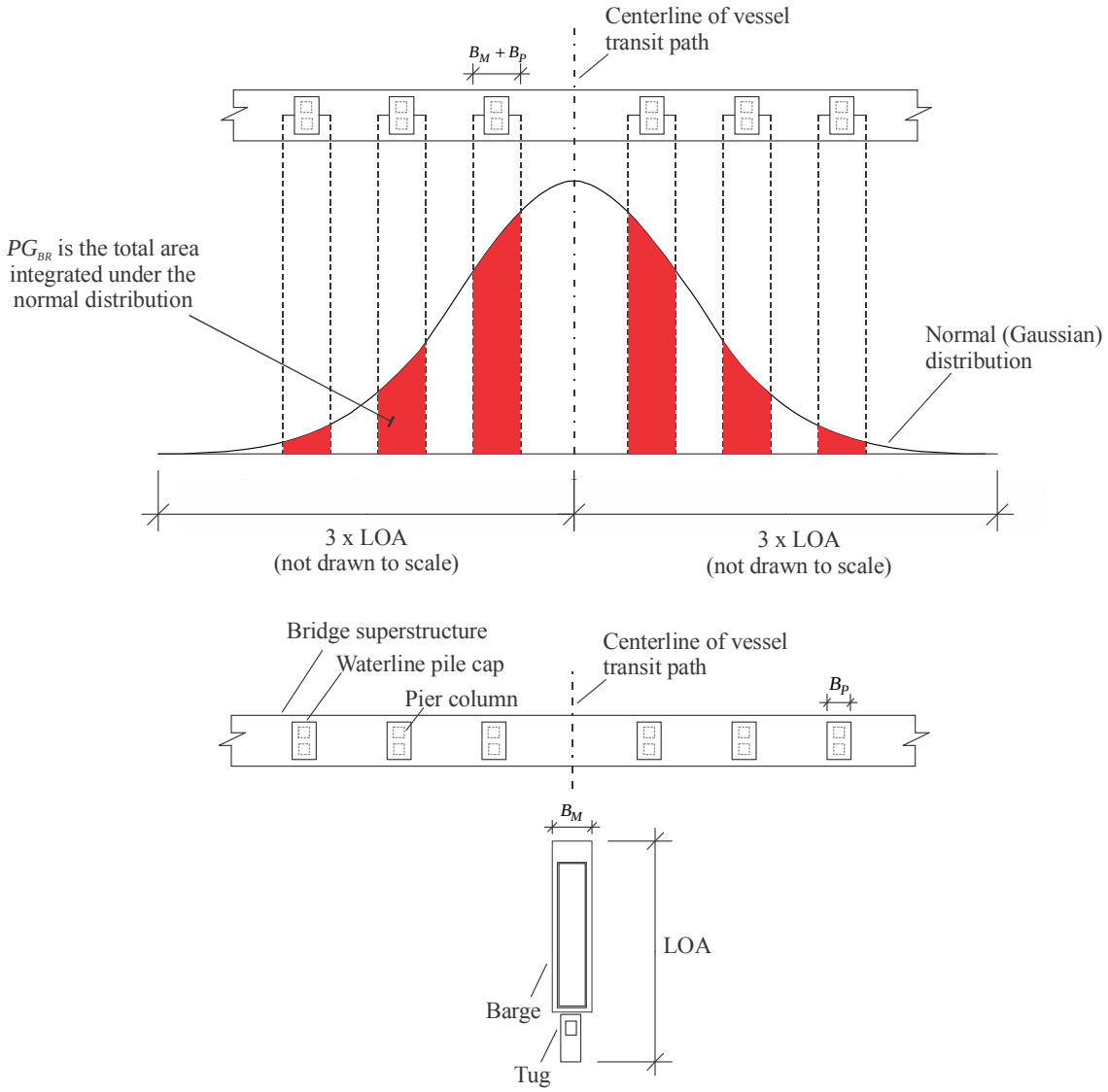

Figure 3.5 Calculation of the geometric probability for a single bridge location,

3.4.4 Protection factor

Impassable waterway features, such as sand bars or dolphins, near individual bridge locations included in this study were examined using satellite imagery to determine the number of piers shielded from impact in the upstream and downstream directions. This process was site specific, and included features that shielded the entire bridge (Fig. 3.6), bodies of land that could provide protection to specific piers (Fig. 3.7), or shallow water regions in the vicinity of the bridge that could influence vessel navigation (Fig. 3.8). In some cases, certain features (typically adjacent bridges) were close enough to the bridge of interest that they would have little to no major effect on the intended transit path of a barge flotilla (e.g., the adjacent bridge shown in Fig. 3.6). These features were therefore excluded from the calculation of protection factors. *PF* values for individual bridges were determined by computing *PG* values for each protected pier, dividing the sum of these values by the sum of all pier *PG* values (PG_{br}), and subtracting the resulting value from one:

$$PF_{br} = 1 - \left(\frac{\sum_{i=1}^{n} \left(\left(PG_p \right)_i \right)}{PG_{br}} \right) \tag{3.6}$$

where PF_{br} is the protection factor for a given bridge site, PG_{br} is the geometric probability of collision for that same bridge, $\left(PG_p \right)_i$ is the area integrated under the *PG* normal distribution (i.e., the *PG* value) associated with the *i*'th protected pier, and *n* is the number of protected bridge piers.

Figure 3.6 Bridge piers protected by adjacent low-rise railroad bridge
(Source: https://www.flickr.com)

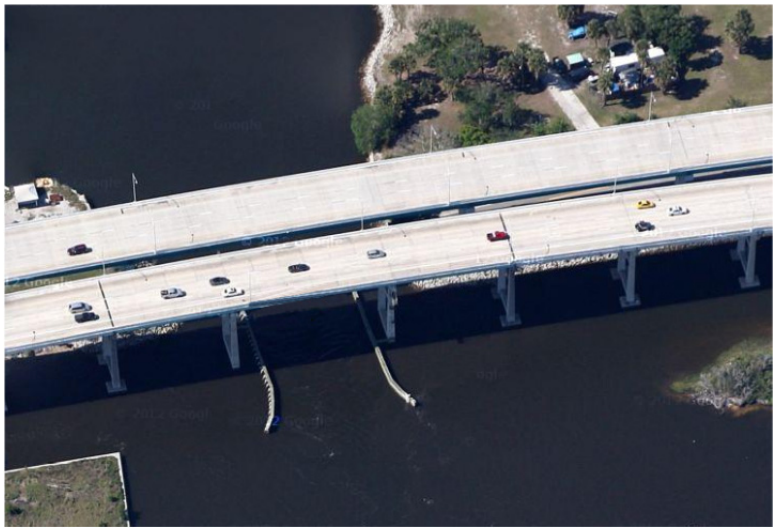

Figure 3.7 Bridge piers protected by land bodies
(See lower left and upper right of image; Source: Google)

Figure 3.8 Shallow water regions near bridge
(See lightly-colored regions in the central portion of the waterway; Source: Google)

3.4.5 Modification factors

Each of the modification factors used in the calculation of *PA*—specifically, R_B, R_C, R_{XC}, and R_D—were computed using the general procedures outlined in this section; specific values for each modification factor are tabulated and discussed in Section 5.3.2. R_B, the modification factor which accounts for the presence of any bends or turns in the waterway that could induce vessel aberrancy, was determined on a site-specific basis using satellite imagery (Fig. 3.9). Consideration was provided for each potential transit path through the bridge site. Calculation of R_B first involved mapping the centerline of each transit path, demarcating the beginning and end of all turns or bends, and noting the bounds of the transition regions on either side of the bridge. A bend or turn angle (θ) associated with each path was calculated and

employed in the appropriate AASHTO equations to determine R_B, depending on whether or not the bridge location was within the turn or bend (Eqn. 2.3), or within a transition region (Eqn. 2.4). For bridge locations with multiple potential transit paths (Fig. 3.9), the path that resulted in the smallest value of R_B was selected for use in a particular direction, since smaller R_B values corresponded to more conservative (larger) estimates of *BR* (see Eqn. 3.3).

Figure 3.9 Calculation of the bridge location modification factor, R_B
(Image adapted from: Google)

Current and cross-current modification factors (R_C and R_{XC}, respectively) were calculated directly from data representing waterway velocities parallel (V_C) and perpendicular (V_{XC}) to the intended vessel transit path (Eqns. 2.5 and 2.6). Water velocity data were obtained through one of the methods discussed previously (accident reports and tidal current predictions), and were intended to represent average current conditions at individual bridge sites.

In order to determine R_D (the vessel traffic density modification factor) for a given bridge site, a ratio of the average annual *vessel* (ship and barge) traffic at that location to the width of the navigable waterway near the bridge was calculated:

$$VDF = \frac{\mu_N}{W} \tag{3.7}$$

where, μ_N is the average annual vessel traffic, W (ft) is the width of the waterway near the bridge location, and VDF is the 'vessel density factor'. VDF values were used as general quantitative measures of vessel traffic density, and were employed in conjunction with data from a previously-conducted AASHTO risk assessment example to select appropriate values of R_D for individual bridge locations (Section 5.3.3).

3.4.6 Base aberrancy rate

Barge flotilla *BR* values specifically calibrated to each bridge site considered in this study were calculated using the methods described in the preceding sections and Eqn. 3.3. To assess variation among the calibrated *BR* values, confidence bounds were fit to various subsets of bridge site *BR* values (Section 5.5). Based on the findings from this process, recommendations were made regarding a single *BR* estimate that may be used in barge-to-bridge impact risk analyses of new and existing bridge structures in Florida waterways.

CHAPTER 4
DATA COLLECTION

4.1 Introduction

Detailed in Chapter 3, the methodology for the present study required the use of several categories of data in the calibration process for the revised barge flotilla *BR* estimate. Required data included barge accident and traffic data, employed in the calculation of barge impact probabilities, and supplementary site-specific data, including waterway velocity data and geometric bridge layouts. This chapter outlines specific data collection procedures used to assemble the required information, as well as methods employed to process data into a form that was appropriate for use in the *BR* calibration framework.

4.2 Barge collision data

As discussed previously, barge collision data are a primary component used in the computation of probability of impact (*PI*) terms for each bridge site of interest (see Eq. 3.4). Barge collision data collected for the present study were obtained from the USCG for every year from 2002-2014. Additional data corresponding to earlier years—as early as 1992—were also obtained from the USCG for certain areas in the panhandle region of Florida.

4.2.1 Organization

Two sources of data were used to obtain information relating to barge impact events at each bridge location in the present study—vessel casualty data and individual barge-to-bridge collision accident (incident) reports. Vessel casualty data (Fig. 4.1), the first set of information obtained from the USCG, consisted of a catalogue of vessel-to-bridge impact events throughout the state of Florida. Since Florida is divided into two USCG districts (Fig. 4.2)—District 8 (northwest Florida) and District 7 (central, south, and east Florida)—two separate sets of vessel casualty data were obtained (one for each district). Each entry (impact event) was classified by a unique number, referred to as an activity ID, which was used by the USCG for reference purposes.

	A	B	C	D	E	F	G
1	Facility.Activity ID	MISLE Facility ID	Involved Facility Name	Facility Description	Involved Facility Type	State	Waterway
2	1673024	1225	ESCAMBIA RIVER BRIDGE	Also known as: HWY 90 BRIDGE-PENSACOLA	Bridge	FL	
3	1842150	93003725	DUPONT BRIDGE	Also known as: EAST BAY DUPONT BRIDGE, US 98/FL SR 30 BRIDGE, 295.5 ICW; Unit Abbr 080BR changed to PCDD.	Bridge	FL	GULF INTRACOASTAL WATERWAY
4	1900158	93003725	DUPONT BRIDGE	Also known as: EAST BAY DUPONT BRIDGE, US 98/FL SR 30 BRIDGE, 295.5 ICW; Unit Abbr 080BR changed to PCDD.	Bridge	FL	East Bay
5	1967164		Jackson Rail Road Bridge	UNSPECIFIED	Bridge		TOMBIGBEE RIVER
6	2026361	1225	ESCAMBIA RIVER BRIDGE	Also known as: HWY 90 BRIDGE-PENSACOLA	Bridge	FL	GICW- East Choctawhatchee Bay through West Bay
7	2074374	95000770	PENSACOLA BEACH BRIDGE	Also known as: BOB SYKES BRIDGE	Bridge	FL	GULF INTRACOASTAL WATERWAY
8	2097878		HATHAWAY BRIDGE	UNSPECIFIED	Bridge		Panama City Harbor
9	2294661	95000770	PENSACOLA BEACH BRIDGE	Also known as: BOB SYKES BRIDGE	Bridge	FL	GULF INTRACOASTAL WATERWAY
10	2306623	96001711	GULF BEACH BRIDGE	Also known as: ST 292	Bridge	FL	GULF INTRACOASTAL WATERWAY

(a)

	AV	AW	AX	AY	AZ
1	MISLE Investigations by Invol.Latitude	MISLE Investigations by Invol.Longitude	Activity Title	Case Title	Initial Event Type
2	30.541490000000000	-87.198333333333000	UNKNOWN VESSEL; ALLISION		Allision
3	30.070833333333000	-85.509444500000000	[redacted]Barge/Bridge Allision		Allision
4	30.070833333333000	-85.509443333333000	[redacted]; Dupont Bridge Allision		Allision
5	31.758091000000000	-88.126633000000000	[redacted]; ALLISION	M Allision/[redacted] 1429/[redacted] [redacted]/12/13/2003 01:	Allision
6	30.398030000000000	-86.521740000000000	[redacted]; ALLISION	M Allision/[redacted]/ESCAMBIA RIVER/[redacted]/ 00 00.0 S 000 00.0 W	Allision
7	30.149660000000000	-85.686680000000000	[redacted]; ALLISION	M Allision/[redacted] [redacted]/PENSACOLA BEACH BRIDGE/Santa Rosa Sound/[redacted]	Allision
8	30.149660000000000	-85.686680000000000	[redacted]/ALLISION/HATHAWAY BRIDGE	M Allision/[redacted]/ 30 11.2362 N 085 44.5266 W/06/04/2004 01:40:00 PM	Vessel Maneuverability
9	30.149660000000000	-85.686680000000000	[redacted]; ALLISION	M Allision/[redacted]/GICW-Big Lagoon-Santa Rosa Sound-The Narrows/Warrior & Gul	Allision
10	30.283550000000000	-87.756850000000000	[redacted]; ALLISION	M Allision/[redacted]/GULF INTRACOASTAL WATERWAY/ Waterway Name: GULF INTRACOASTAL	Material Failure (Vessels)

(b)

Figure 4.1 Selected portions of USCG vessel casualty data set: (a) bridge and waterway information; (b) event information

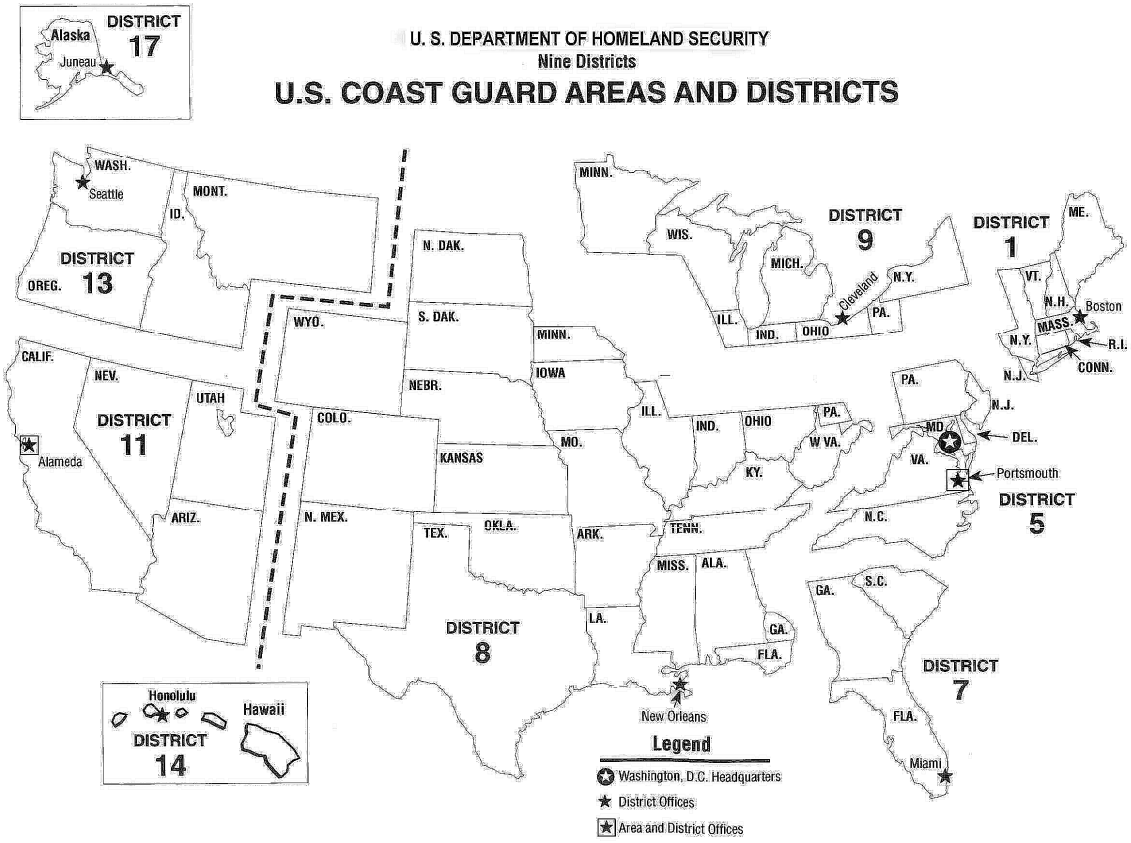

Figure 4.2 USCG districts (Source: http://www.uscg.mil)

After reviewing the vessel casualty data sets obtained from the USCG, it was determined that the records for certain barge-to-bridge impact events were incomplete. As a consequence, original (i.e., 'raw') accident reports (example portion shown in Fig. 4.3) for each impact event of interest were obtained from the USCG to supplement the vessel casualty data. Using both sources of information, it was generally possible to assemble a complete record of each barge impact event. Raw accident reports were obtained through a Freedom of Information Act (FOIA) request submitted to the USCG. The FOIA request process was initiated by sending the USCG a complete list of requested reports organized by activity ID. In response, electronic copies of each available report were provided by the USCG on a CD-ROM, which was delivered by mail a few months after the initial request was made.

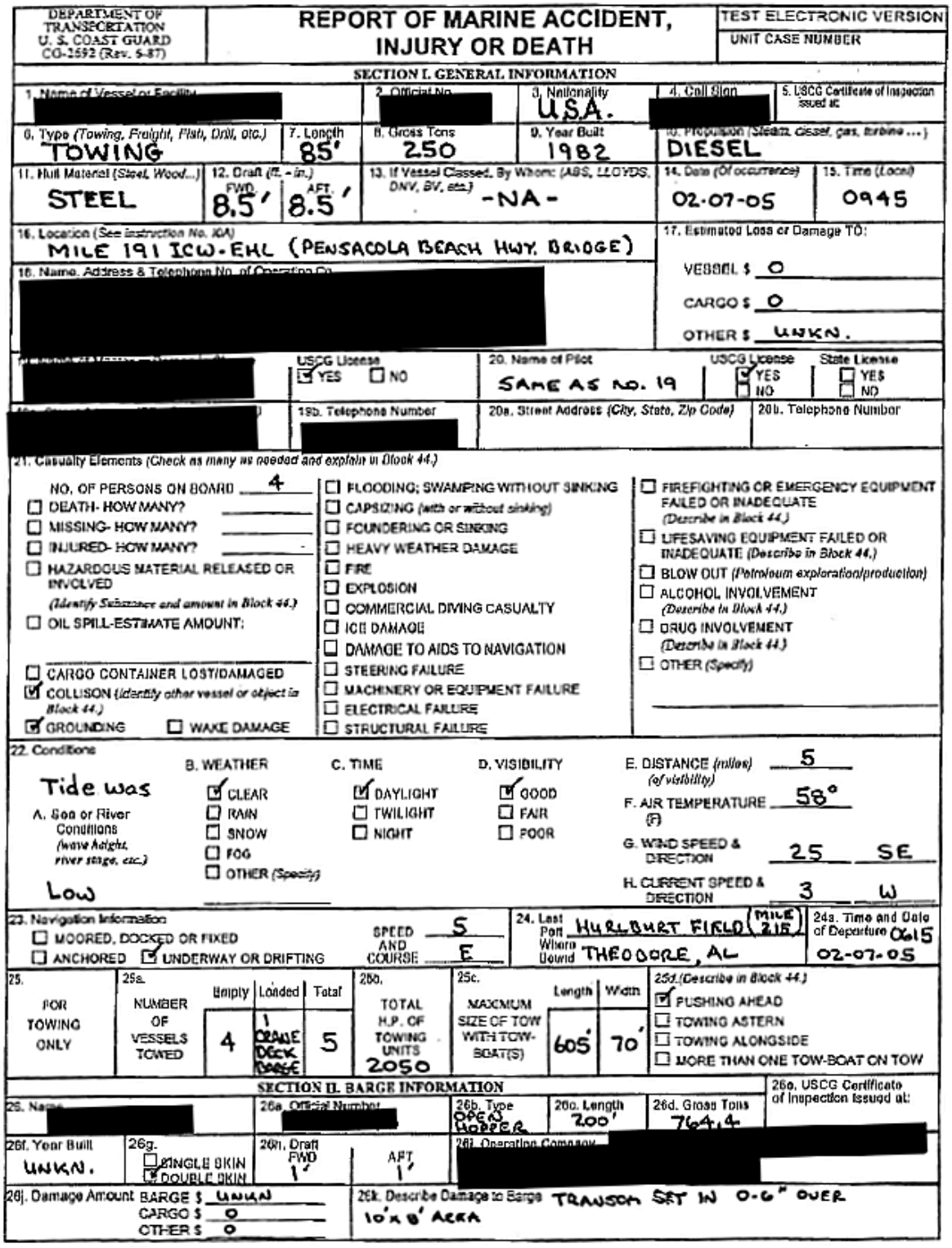

DEPARTMENT OF TRANSPORTATION
U. S. COAST GUARD
CG-2692 (Rev. 6-87)

REPORT OF MARINE ACCIDENT, INJURY OR DEATH

TEST ELECTRONIC VERSION
UNIT CASE NUMBER

SECTION I. GENERAL INFORMATION

1. Name of Vessel or Facility	2. Official No.	3. Nationality	4. Call Sign	5. USCG Certificate of Inspection issued at:
[redacted]	[redacted]	USA.	[redacted]	

6. Type (Towing, Freight, Fish, Drill, etc.)	7. Length	8. Gross Tons	9. Year Built	10. Propulsion (Steam, diesel, gas, turbine ...)
TOWING	85'	250	1982	DIESEL

11. Hull Material (Steel, Wood...)	12. Draft (ft. - in.) FWD	AFT	13. If Vessel Classed, By Whom: (ABS, LLOYDS, DNV, BV, etc.)	14. Date (Of occurrence)	15. Time (Local)
STEEL	8.5'	8.5'	-NA-	02-07-05	0945

16. Location (See instruction No. 16A)
MILE 191 ICW-EHL (PENSACOLA BEACH HWY. BRIDGE)

17. Estimated Loss or Damage TO:
VESSEL $ 0
CARGO $ 0
OTHER $ UNKN.

18. Name, Address & Telephone No. of Operating Co.
[redacted]

[redacted]	USCG License ☑ YES ☐ NO	20. Name of Pilot	USCG License ☑ YES ☐ NO	State License ☐ YES ☐ NO
		SAME AS NO. 19		

[redacted]	19b. Telephone Number	20a. Street Address (City, State, Zip Code)	20b. Telephone Number
	[redacted]		

21. Casualty Elements (Check as many as needed and explain in Block 44.)

NO. OF PERSONS ON BOARD 4
☐ DEATH- HOW MANY?
☐ MISSING- HOW MANY?
☐ INJURED- HOW MANY?
☐ HAZARDOUS MATERIAL RELEASED OR INVOLVED (Identify Substance and amount in Block 44.)
☐ OIL SPILL-ESTIMATE AMOUNT:
☐ CARGO CONTAINER LOST/DAMAGED
☑ COLLISON (Identify other vessel or object in Block 44.)
☑ GROUNDING ☐ WAKE DAMAGE

☐ FLOODING; SWAMPING WITHOUT SINKING
☐ CAPSIZING (with or without sinking)
☐ FOUNDERING OR SINKING
☐ HEAVY WEATHER DAMAGE
☐ FIRE
☐ EXPLOSION
☐ COMMERCIAL DIVING CASUALTY
☐ ICE DAMAGE
☐ DAMAGE TO AIDS TO NAVIGATION
☐ STEERING FAILURE
☐ MACHINERY OR EQUIPMENT FAILURE
☐ ELECTRICAL FAILURE
☐ STRUCTURAL FAILURE

☐ FIREFIGHTING OR EMERGENCY EQUIPMENT FAILED OR INADEQUATE (Describe in Block 44.)
☐ LIFESAVING EQUIPMENT FAILED OR INADEQUATE (Describe in Block 44.)
☐ BLOW OUT (Petroleum exploration/production)
☐ ALCOHOL INVOLVEMENT (Describe in Block 44.)
☐ DRUG INVOLVEMENT (Describe in Block 44.)
☐ OTHER (Specify)

22. Conditions

A. Sea or River Conditions (Wave height, river stage, etc.): Tide was Low

B. WEATHER: ☑ CLEAR ☐ RAIN ☐ SNOW ☐ FOG ☐ OTHER (Specify)

C. TIME: ☑ DAYLIGHT ☐ TWILIGHT ☐ NIGHT

D. VISIBILITY: ☑ GOOD ☐ FAIR ☐ POOR

E. DISTANCE (miles) (of visibility): 5
F. AIR TEMPERATURE (F): 58°
G. WIND SPEED & DIRECTION: 25 SE
H. CURRENT SPEED & DIRECTION: 3 W

23. Navigation Information
☐ MOORED, DOCKED OR FIXED
☐ ANCHORED ☑ UNDERWAY OR DRIFTING
SPEED AND COURSE: 5 E

24. Last Port Where Bound: HURLBURT FIELD (MILE 215) THEODORE, AL
24a. Time and Date of Departure: 0615 02-07-05

25. FOR TtowING ONLY	25a. NUMBER OF VESSELS TOWED	Empty	Loaded	Total	25b. TOTAL H.P. OF TOWING UNITS	25c. MAXIMUM SIZE OF TOW WITH TOW-BOAT(S)	Length	Width	25d. (Describe in Block 44.)
		4	1 CRANE DECK BARGE	5	2050		605'	70'	☑ PUSHING AHEAD ☐ TOWING ASTERN ☐ TOWING ALONGSIDE ☐ MORE THAN ONE TOW-BOAT ON TOW

SECTION II. BARGE INFORMATION

26. Name	26a. Official Number	26b. Type	26c. Length	26d. Gross Tons	26e. USCG Certificate of Inspection issued at:
[redacted]	[redacted]	OPEN HOPPER	200'	764.4	[redacted]

26f. Year Built	26g.	26h. Draft FWD	AFT	26i. Operation Company
UNKN.	☐ SINGLE SKIN ☑ DOUBLE SKIN	1'	1'	[redacted]

26j. Damage Amount: BARGE $ UNKN; CARGO $ 0; OTHER $ 0

26k. Describe Damage to Barge: TRANSOM SET IN 0-6" OVER 10'x8' AREA

Figure 4.3 Selected portion of raw USCG accident report

4.2.2 Description of collected information

USCG collision records contained detailed information regarding the nature of each collision event and the vessel(s) involved. Information that was collected included the location, date, and time of the incident, as reported by the USCG. In addition, vessel-specific information was also included, such as the overall length and width of the flotilla, and the type of vessels from which the flotilla was comprised (e.g., tug, deck barge, hopper barge, etc.). In many cases, details relating to environmental conditions were also provided, such as waterway current speeds and directions, visibility and lighting conditions, and wind speeds (Fig. 4.3). For impact events which resulted in damage to the bridge, estimated repair costs were summarized. In general, two separate narratives of the incident were also recorded—one provided by the captain of the vessel involved in the impact event and one provided by the investigating USCG officer. Each of these narratives briefly described the circumstances surrounding the event and the nature of the collision. While these details varied somewhat between incident records, sufficient information was typically provided to discern the cause of the impact and the general location on the bridge that was struck by the vessel. A summary of collected barge accident data is provided in Appendix C.

4.2.3 Preliminary analysis methods

Since the focus of the present study was on quantifying barge impact probabilities, the analysis procedures outlined in Chapter 3 were intended to be used specifically with barge-to-bridge accident data. Consequently, in the data requests submitted to the USCG, only barge accident records were requested (as opposed to ship impact). However, upon receiving the vessel casualty data sets from the USCG, it was discovered that, in both data sets, other types of vessel collision events had also been included (e.g., passenger craft collisions). As a result, the vessel casualty data sets had to be carefully reviewed to separate those events which involved barges from events that involved other types of vessels, such as pleasure craft or commercial fishing craft. For each bridge site in the state of Florida which possessed at least one confirmed barge-to-bridge impact event, a data catalog was developed that contained individual, processed records for each event. However, for certain impact events, the type of vessel involved was not described in the USCG vessel casualty data sets (example shown in Fig. 4.4). Consequently, it was not possible to fully classify each event without further information. In additional cases, blank data fields were also present (example shown in Fig. 4.5), which left out information that could be of interest to this investigation (e.g., vessel dimensions). To obtain this additional information, the raw (original) accident reports for each potential barge-to-bridge impact event were acquired from the USCG through the FOIA request process described earlier. Each of these reports typically consisted of two parts—a detailed record of the event (CG-2692 form), and, if more than one vessel (e.g., a pushboat and four barges) was involved, an addendum with vessel-specific information (CG-2692A form). Both forms were reviewed for each impact incident to determine the nature of the event so that barge collisions could be identified, and non-barge impacts could be filtered out. Upon completion of this review, incident reports for the barge-to-bridge impact events were used to provide supplementary information (e.g., vessel dimensions, current conditions, incident causes) in processed records.

AB	AC	AD	AE
Involved Vessel Class	Involved Vessel Type	Involved Vessel Subtype	Involved Vessel Service
Towing Vessel	General	General	Towing Vessel
Towing Vessel	General	General	Towing Vessel
Towing Vessel	General	General	Towing Vessel
Towing Vessel	General	General	Towing Vessel
Barge	General	General	Freight Barge
Barge	Deck Barge	General	Freight Barge
Barge	General	General	Freight Barge
Barge	Industrial Barge	Work Platform	Industrial Vessel
Towing Vessel	General	General	Towing Vessel
Barge	General	General	Freight Barge
Towing Vessel	General	General	Towing Vessel
Towing Vessel	General	General	Towing Vessel
Towing Vessel	General	General	Passenger Barge (More Than 6)
Barge	General	General	Freight Barge
Towing Vessel	General	General	Towing Vessel
Towing Vessel	General	General	Towing Vessel
UNSPECIFIED	UNSPECIFIED	UNSPECIFIED	UNSPECIFIED
Towing Vessel	General	General	Towing Vessel
UNSPECIFIED	UNSPECIFIED	UNSPECIFIED	UNSPECIFIED
Towing Vessel	General	General	Towing Vessel
UNSPECIFIED	UNSPECIFIED	UNSPECIFIED	UNSPECIFIED
Towing Vessel	General	General	Towing Vessel

Figure 4.4 Selected portion of USCG vessel casualty data set with unspecified vessel characteristics

AT	AU	AV	AW	AX	AY	AZ
Length (ft)	Breadth (ft)	Depth (ft)	Vessel Age	Activity Role	Damage Status	Event Type
42	18	7	23	Involved in a Marine Casualty	Undamaged	Allision
49.2	15.2	6.4	59	Involved in a Marine Casualty	Undamaged	Allision
64.5	24	8.2	48	Involved in a Marine Casualty	Damaged	Allision
64.7	24	9.1	35	Involved in a Marine Casualty	Undamaged	Allision
0	0	0		Involved in a Marine Casualty	Undamaged	Allision
0	0	0		Involved in a Marine Casualty	Undamaged	Allision
				Involved in a Marine Casualty	Undamaged	Allision
80	0	0	11	Involved in a Marine Casualty	Damaged	Allision
31	14	5	14	Involved in a Marine Casualty	Undamaged	Allision
				Involved in a Marine Casualty	Undamaged	Allision
62.7	20	8.7	50	Involved in a Marine Casualty	Undamaged	Allision
62.7	20	8.7	50	Involved in a Marine Casualty	Undamaged	Allision
25.2	14	4.5	23	Involved in a Marine Casualty	Undamaged	Allision
150	55	9	13	Involved in a Marine Casualty	Undamaged	Allision
84.5	28	10.3	52	Involved in a Marine Casualty	Undamaged	Allision
59.8	19.6	8	57	Involved in a Marine Investigation (non-casualty)	Undamaged	Allision
				Involved in a Marine Investigation (non-casualty)	Undamaged	Allision

Figure 4.5 Selected portion of USCG vessel casualty data set with blank data fields

4.3 Barge traffic data

As mentioned in earlier sections, an individual vessel passage along a marked point in a waterway is referred to as a vessel 'trip'. A collection of observed barge and tugboat trips near a particular bridge location is referred to as the barge traffic data set for that location. Since barge traffic data were required for the computation of *PI* (see Eqn. 3.4), such data were obtained from the USACE for the same bridge sites where barge-to-bridge accident data were obtained from the USCG. A full listing of locations for which barge traffic data were collected is provided in

Appendix D. As discussed earlier, due to the substantial processing effort that such a request translated into for the USACE, it was not feasible to request barge traffic data for every year at which USCG barge collision data were consistently available (2002-2014). Instead, the USACE provided traffic data sets every other year from 2002-2012 and for the year 2013 (i.e., traffic data were obtained for the years 2002, 2004, 2006, 2008, 2010, 2012, and 2013).

4.3.1 Organization

Traffic data provided by the USACE (example shown in Fig. 4.6) were organized by year, with two separate data sets for each year. The first data set provided details regarding the types of commodities that were transported by vessels along the waterway location of interest; the second data set provided information regarding the number of vessel passages along the waterway (trips). Data in both sets were also organized by direction of travel and vessel characteristics: vessel type (e.g., barge, tug, ship, etc.), tonnage, overall length, overall breadth (width), and draft.

	A	B	C	D	E	F	G	H	I	J	K	L	M	N
1	DIRECTION	TTYPE	VTYPE	REG_TONS	CAP_TONS	OVER_LENGTH	OVER_BREADTH	ACTUAL_DRAFT	LOAD_DRAFT	LIGHT_DRAFT	H_F_POINT	YEAR	CONTAINERIZED	TRIPS
2	Downbound	Domestic	04	1758	6017	402.1	100	8	10	5	53	13	1	26
3	Upbound	Domestic	05	791	1290	200	35	12	12.6	2	25	13	0	5
4	Upbound	Domestic	05	885	2200	195	54	9	8.6	2	17	13	N	4
5	Upbound	Domestic	04	1758	6017	402.1	100	8	10	5	53	13	1	23
6	Upbound	Domestic	03	96	999999	60.2	26	8	8	8	31.8	13	0	13
7	Upbound	Domestic	05	001611	4833	274	50	2	12	2	30	13	0	1
8	Downbound	Domestic	03	57	999999	84	20.1	6	7	6	40	13	0	30
9	Downbound	Domestic	05	725	2065	200	36	2	12	2	29	13	N	1
10	Upbound	Domestic	05	003739	16567	362.2	74	10	21	10	74	13	N	1
11	Upbound	Domestic	05	001611	3000	274	50	2	13	2	30	13	0	3
12	Downbound	Domestic	05	791	1290	200	35	12	12.6	2	25	13	0	3
13	Upbound	Domestic	03	91	999999	70	25.2	7	7.7	6.5	37.5	13	0	2
14	Upbound	Domestic	05	002278	4500	274	60	2	12	2	30	13	0	1
15	Upbound	Domestic	03	127	999999	65	26	6	9	5.5	39	13	0	1
16	Downbound	Domestic	03	96	999999	60.2	26	8	8	8	31.8	13	0	12
17	Downbound	Domestic	05	002056	11300	330	74.3	4	19.9	3.8	38	13	N	1
18	Upbound	Domestic	05	001611	4833	274	50	10	12	2	30	13	0	2
19	Upbound	Domestic	05	001611	3000	274	50	7	13	2	30	13	N	3
20	Downbound	Domestic	04	004283	14500	362	74.5	5	23.3	4.6	52	13	N	1
21	Downbound	Domestic	03	85	999999	64.5	24.5	8	8.2	8.2	31.8	13	0	15
22	Upbound	Domestic	03	000133	999999	124	40	7	20	20	87	13	0	4

Figure 4.6 Selected portion of USACE vessel traffic data set for Atlantic Intracoastal Waterway, near Sister's Creek Bridge (Jacksonville, FL)

4.3.2 Preliminary analysis methods

As indicated previously, barge flotilla traffic data were needed for the computation of *PI* using Eqn. 3.4. However, upon receiving the first sets of traffic data from the USACE, it was determined that, in addition to barge and tug traffic, other types of vessel traffic (e.g., ship traffic) were also included. Since the focus of the present investigation is on quantifying barge impact probabilities specifically, it was necessary to separate barge and tug traffic from other—non-pertinent—types of vessel traffic provided by the USACE. Using vessel classification IDs unique to each type of vessel (listed under 'VTYPE' in Fig. 4.6), a Matlab script (program) was developed to sift through each data set, and extract only traffic data specific to tugs and barges. The script was also used to organize traffic by direction (upbound, downbound) and by dimensional ranges (ranges of total length, width, etc.). For individual bridge locations, two traffic totals were computed for each year—one for each direction travel.

4.4 Supporting Information

Supplementing the USCG collision data and USACE traffic data, additional information was collected for each bridge site with a recorded barge-to-bridge collision event: water current velocity data (needed in the computation of the current and cross-current modification factors, R_C and R_{XC}, respectively); bridge plans; and nautical charts. Each of these is described in more detail below.

4.4.1 Current data

Water current data were obtained from two sources: current records included in USCG accident reports and NOAA tidal current predictions (Fig. 4.7). Current data obtained from accident reports, which were available for most bridge sites, included the current speed and direction at the time of the incident. For sites which had NOAA tidal current data available, 52 weeks (one year) of data were collected in order to produce a reasonably representative sample of water current conditions (flow speeds). Such data consisted of peak flood (incoming tide) and ebb (outgoing tide) current speeds and directions (example shown in Fig. 4.7), which were organized by calendar week. Since these data were based solely on tidal predictions, environmental factors that might potentially increase current speeds, including wind and storm conditions, are not reflected in the estimated peak values.

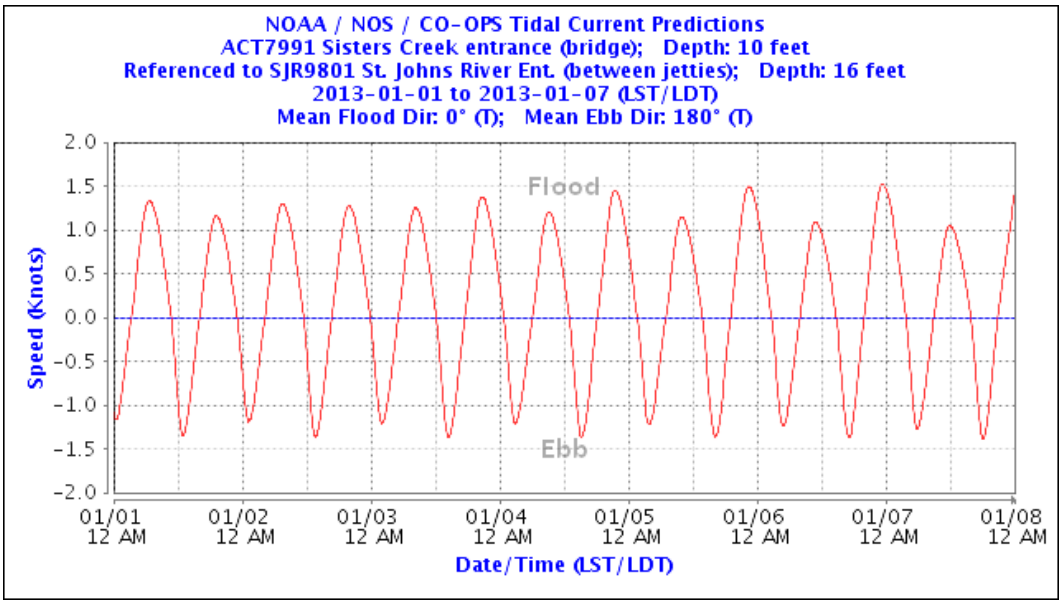

Figure 4.7 Selected sample NOAA tidal current prediction
(Source: http://tidesandcurrents.noaa.gov)

4.4.2 Bridge plans

To compute the geometric probability of collision (*PG*), and protection factors (*PF*) associated with the bridge sites of interest in this study, bridge plans were obtained from the appropriate FDOT district offices. These plans were individually reviewed to develop simplified bridge layouts for reference purposes (Fig. 4.8). Catalogues of bridge pier locations relative to

the centerline of the waterway were also created in order to automate the *PG* calculation process using a series of data processing Matlab scripts.

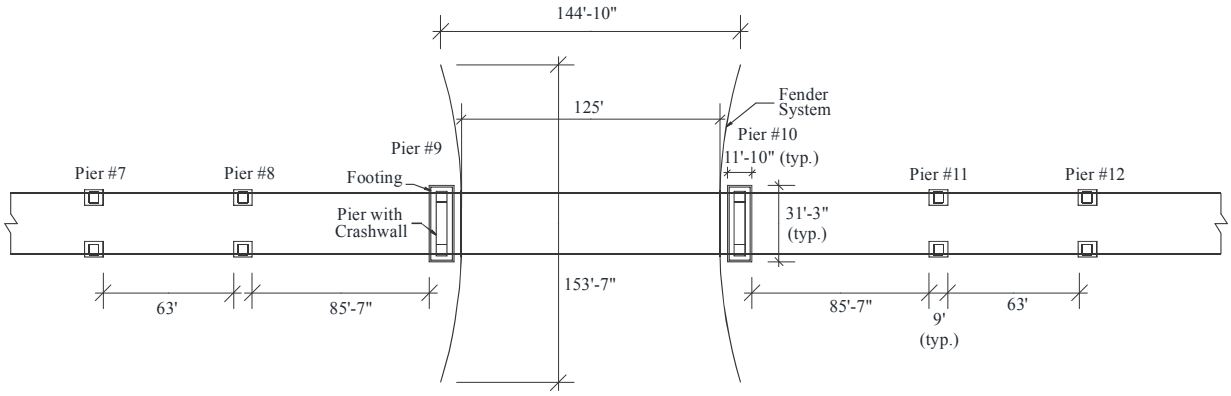

Figure 4.8 Selected portion of simplified bridge layout for the Navarre Beach Bridge over the Gulf Intracoastal Waterway

4.4.3 Nautical charts

While bridge plans included structural layouts, it was also necessary to review nautical charts to collect information specific to the waterway layout, such as the identification of unnavigable shallow water zones, which were also needed in the calculation of both *PG* and *PF*. Nautical charts utilized for this study were obtained from NOAA for all waterways of interest (example shown in Fig. 4.9). Using the NOAA nautical charts, unnavigable shallow water zones, or small islands, close to the bridge site, were identified and used to characterize the level of protection against a collision event. When needed, these documents were also used in the calculation of bridge location modification factors (R_B).

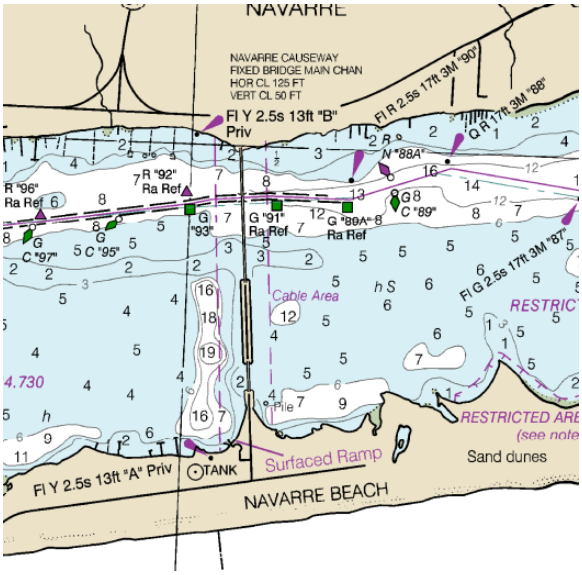

Figure 4.9 Selected portion of NOAA nautical chart (area near Navarre Beach Bridge shown [Source: NOAA])

CHAPTER 5
DATA ANALYSIS

5.1 Introduction

As discussed in earlier chapters, the primary objective of the present study was to reevaluate barge-to-bridge impact probabilities using the general analysis methodology presented in Chapter 3. This chapter summarizes the specific analysis procedures employed in the calculation of base aberrancy rates (*BR* values) for the 13 bridge sites included in this investigation (Table 5.1) and the methods utilized to determine a design *BR* specific to barge flotilla traffic in Florida waterways.

Table 5.1 Bridge locations utilized in present study

Bridge Name	Region	Latitude (deg.)	Longitude (deg.)
Acosta Bridge	Jacksonville, FL	30.21240	-81.66387
Atlantic Blvd. Bridge	Jacksonville, FL	30.32332	-81.43863
Bob Sikes Bridge	Pensacola, FL (panhandle)	30.34832	-87.15365
Brooks Bridge	Fort Walton Beach, FL (panhandle)	30.40122	-86.60056
CSX Railroad Bridge over Escambia Bay	Pensacola, FL (panhandle)	30.52384	-87.14634
Dupont Bridge	Panama City, FL	30.10471	-85.60822
Gandy Bridge	Tampa, FL	27.88797	-82.55168
Highway-90 Bridge over Escambia River	Pensacola, FL (panhandle)	30.54878	-87.19507
Interstate-10 Bridge over Escambia Bay	Pensacola, FL (panhandle)	30.51914	-87.14390
Navarre Beach Bridge	Navarre, FL (panhandle)	30.39717	-86.86330
Pensacola Bay Bridge	Pensacola, FL (panhandle)	30.39451	-87.18487
Sister's Creek Bridge	Jacksonville, FL	30.39402	-81.45990
Theo Baars Bridge	Pensacola, FL (panhandle)	30.31300	-87.42634

Recall that *BR*, as calculated in this study, is a function of several variables:

$$BR = \frac{PI}{(R_B)(R_C)(R_{XC})(R_D)(PG)(PF)} \tag{5.1}$$

where, *BR* is the base aberrancy rate, *PI* is the probability of impact, *PG* is the geometric probability, and *PF* is a protection factor. R_B, R_C, R_{XC}, and R_D are modification factors which account for: the location of the bridge relative to turns or bends in the waterway (R_B); currents acting parallel to the intended transit path of the vessel (R_C); cross-currents acting perpendicular to the intended transit path of the vessel (R_{XC}); and the density of vessel traffic in the immediate vicinity of the bridge (R_D). With the exception of three bridges (CSX Railroad Bridge, Interstate-10 Bridge, and the Theo Baars Bridge), the variables on the right hand side of Eqn. 5.1

were quantified for investigated bridges using the procedures and assumptions described in this chapter. Once quantified, each location-specific set of values was used to calculate a range of *BR* estimates for each bridge location. Since the CSX Railroad Bridge, the Interstate-10 Bridge, and the Theo Baars Bridge did not have any barge-to-bridge collisions documented by the USCG over the period of time considered in this investigation, each of these structures was associated with a *PI* of zero. As a consequence, *BR* estimates for these locations were taken as zero for all analyses considered in this study. A final design *BR* was determined by considering an empirical *BR* distribution comprised of all estimates, including *BR* values of zero associated with the three bridge locations without recorded impact events.

5.2 Probability of Impact

Using historical records of barge-to-bridge collisions, in conjunction with barge and tug traffic data, a probability of impact (*PI*) term was calculated for each bridge site using Eq. 3.4. As described in Chapter 4, barge collision data collected for the present study were obtained from the USCG for every year from 2002-2014, with additional data available for panhandle bridge sites (see Table 5.1) corresponding to earlier years (back to 1992). Barge and tug traffic data sets were obtained from the USACE every other year from 2002-2012, as well as for 2013. Using the curve-fitting methods described in Section 5.2.2, it was ascertained that reasonable estimates of barge and tug traffic counts could be determined for each year from 2000-2014 where vessel traffic data were not available (due to limits on the permissible USACE data requests). Consequently, for bridge locations in the panhandle, where older barge-to-bridge collision data sets were provided, t_i was taken as 2000 in Eqn. 3.4. For bridges located in other regions of Florida, t_i was taken as 2002.

5.2.1 Impact events

In total, 25 barge-to-bridge collision events corresponding to the bridge locations of interest were used in the present investigation (Table 5.2). It should be noted that additional bridge sites in Florida were considered, but these locations were excluded from this investigation due to insufficient vessel traffic data (i.e., barge traffic counts were low). Barge casualties which did not involve a direct collision with a bridge were not included in this study. Since the barge and tug traffic data sets provided by the USACE did not include non-commercial traffic (e.g., construction barges), collision events which involved non-commercial barges also had to be excluded from this investigation.

Table 5.2 Number of barge-to-bridge collision events per bridge location

Bridge name	Number of collisions
Acosta Bridge	1
Atlantic Blvd. Bridge	1
Bob Sikes Bridge	8
Brooks Bridge	2
CSX Railroad Bridge over Escambia Bay	0
Dupont Bridge	3
Gandy Bridge	1
Highway-90 Bridge over Escambia River	3
Interstate-10 Bridge over Escambia Bay	0
Navarre Beach Bridge	3
Pensacola Bay Bridge	1
Sister's Creek Bridge	2
Theo Baars Bridge	0

5.2.2 Analysis of barge traffic data

Traffic data provided by the USACE were initially analyzed using the methods described in Chapter 4 in order to obtain barge and tug traffic counts for each bridge location and direction of travel. However, since the passage of a single multi-barge flotilla through a bridge site would be represented as multiple vessel passages in the traffic data provided by the USACE (where one passage is a single barge or tug), the number of individual barge passages through a bridge location was not, in many cases, an adequate indicator of barge flotilla traffic. Consequently, since many barge flotillas typical to the state of Florida include only a single tug, it was determined that—subject to filtering with the outlier detection algorithm noted below—tug traffic counts were generally a more appropriate basis for the estimation of N_T.

In order to approximate region-specific flotilla sizes, barge-to-tug ratios were calculated for each bridge site by year and direction using the USACE-supplied traffic data. Overall 126 total barge-to-tug ratios were quantified—one for each year (seven years of collected data), waterway (nine total waterways), and direction of travel (two directions). Upon reviewing the calculated ratios, it was noted that for certain years at several bridge locations, barge-to-tug ratios were higher than the largest typical ratio for the waterway (as determined through tug operator interviews). After discussing this observation with the USACE, it was determined that USACE-provided tug traffic counts may be lower than actual values for some years, due to the existence of unreported tug passages. Since the USACE Waterborne Commerce Statistics Center (WCSC) is concerned primarily with tracking the movement of commercial goods in U.S. waterways, data collection emphasis is on commercial barge traffic. In contrast, the tugs used to push barge flotillas do not typically carry commercial goods onboard. Consequently, tugs movements

(passages) along U.S. waterways are not always reported to the USACE Waterborne Commerce Statistics Center with the same accuracy as are barge passages. In order to address the possibility of unreported tug passages, an outlier detection methodology was developed to flag years in which barge-to-tug ratios were significantly higher than typical (indicating a possibility of unreported tug passages). In this methodology, barge-to-tug ratios for each bridge location were normalized by site-specific median values so that normalized barge-to-tug ratios from all bridge locations could be included in a single data set for analysis purposes (Fig. 5.1). For certain years at one bridge site—the Gandy Bridge—barge passages were recorded with no corresponding tug passages; in such cases, barge-to-tug ratios were estimated to be a very large number in the outlier detection analysis (greater than 100). Site median values were used instead of site mean values since the presence of a large number of outliers, or a small number of outliers with very large or small magnitudes (relative to the remainder of the data set), can distort the mean and standard deviation calculated from the data (Leys et al. 2013). Consequently, if normalization of the barge-to-tug ratios had been performed by using site mean values, the significance of outlying values could have been masked in locations with either a large number of outliers, or a small number of significant outliers.

Identification of outlying barge-to-tug ratios was achieved through the use of box plots. Using this approach, originally published by Tukey (1977), data were grouped into four regions using median values referred to as quartiles (Fig. 5.2). The central portion, bounded by the first and third quartiles, is commonly referred to as the ‘box’ portion of the plot. Any data points that fell outside the box, but within the extreme bounds, were termed ‘mild outliers’. Any data points that fell outside the extreme bounds were termed ‘extreme outliers’. For this project, only extreme outliers were flagged for removal; this corresponded to any normalized barge-to-tug ratios that were greater than two (see Fig. 5.1).

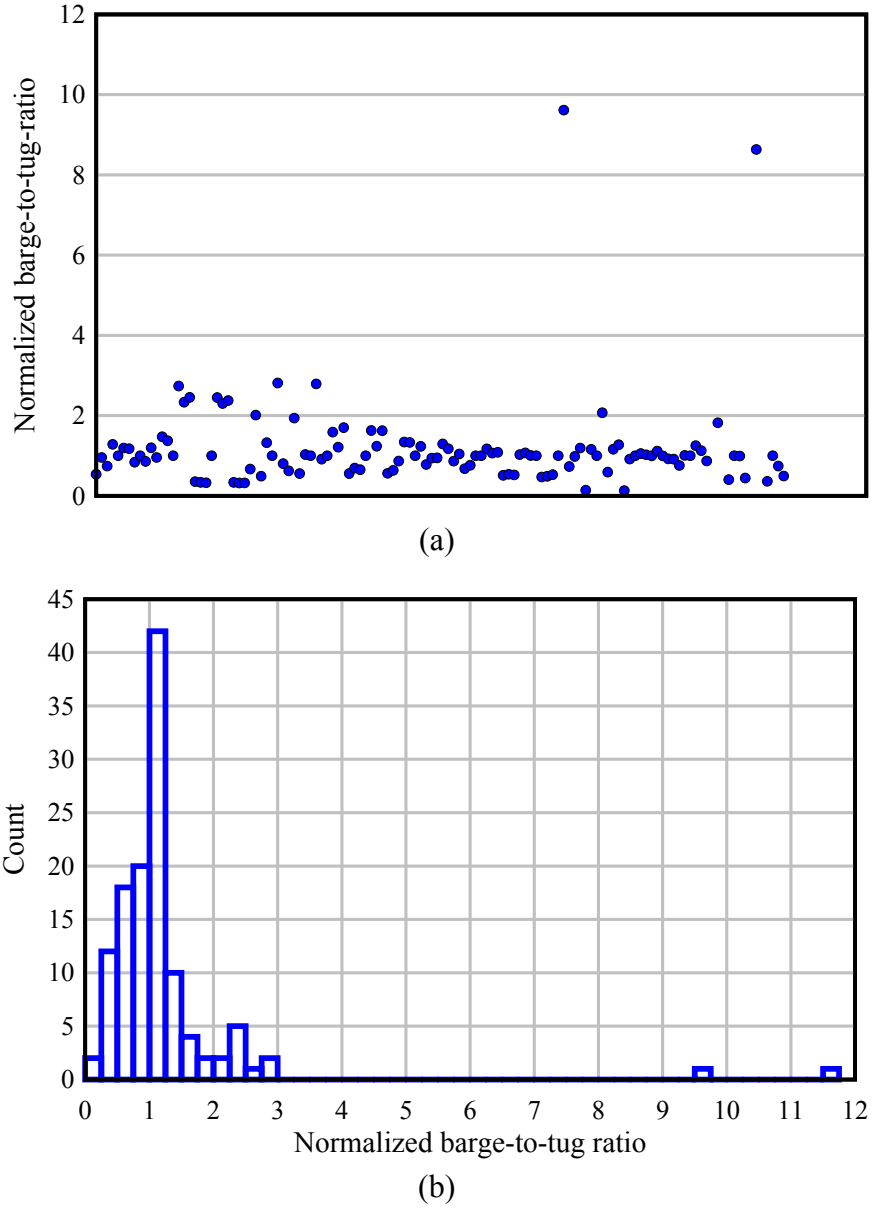

Figure 5.1 Barge-to-tug ratios normalized by bridge site medians: (a) scatterplot; (b) histogram (Note: extreme outliers with barge-to-tug ratios greater than 100 not shown for clarity)

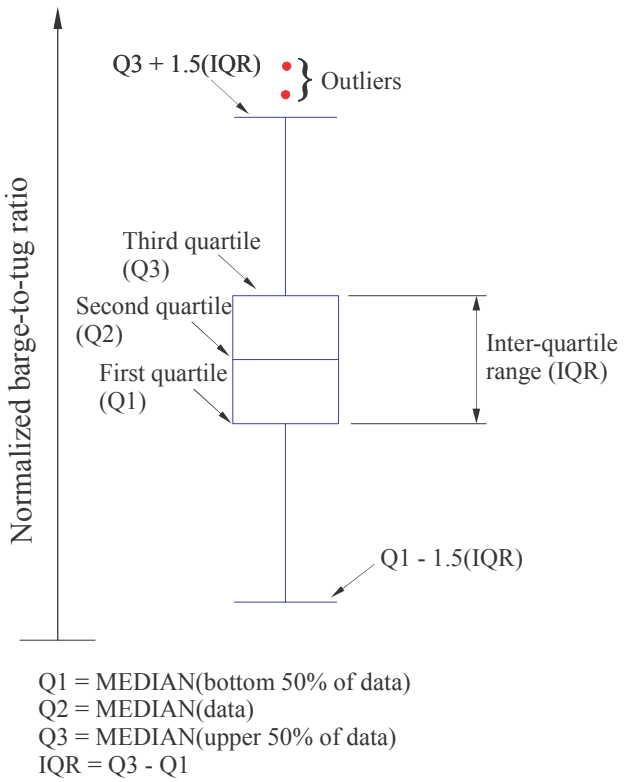

Figure 5.2 Example box plot

Of the bridge locations analyzed in this investigation, seven contained years for which outlying barge-to-tug ratios existed: the Atlantic Blvd. Bridge; the CSX Railroad Bridge; Dupont Bridge; Gandy Bridge; the Highway-90 Bridge; the Interstate-10 Bridge; and the Pensacola Bay Bridge. Overall, this corresponded to 16 outlying barge-to-tug ratios. Three of those 16 outliers were *retained* in the data analysis since the cause of the large barge-to-tug ratios in these cases were related to abrupt increases in the number of observed barge passages, and not due to supposed decreased tug traffic activity. Sudden, and legitimate, increased barge traffic could correspond to a temporary event requiring the movement of more materials (e.g., a construction project). To determine new barge-to-tug ratios for the 13 remaining records in question, for which outlying values were discarded, curve-fitting methods were applied. Several fit types were examined, including linear, quadratic, and exponential fits. Since the exponential fits appeared to approximate data trends the best, exponential fit parameters were used to obtain new barge-to-tug ratios in place of outlying observations (see Appendix E for curve fits). Barge traffic counts for the same locations and years for which outlying barge-to-tug ratios were identified were then divided by the ratios sampled from the curve fits to arrive at new tug traffic counts representative of individual barge flotilla passages. For select locations and years where tug traffic counts exceeded barge traffic counts, the latter (barge traffic counts) were used to represent flotilla traffic. The outlier replacement methodology employed to obtain equivalent barge flotilla traffic counts is summarized in Fig. 5.3.

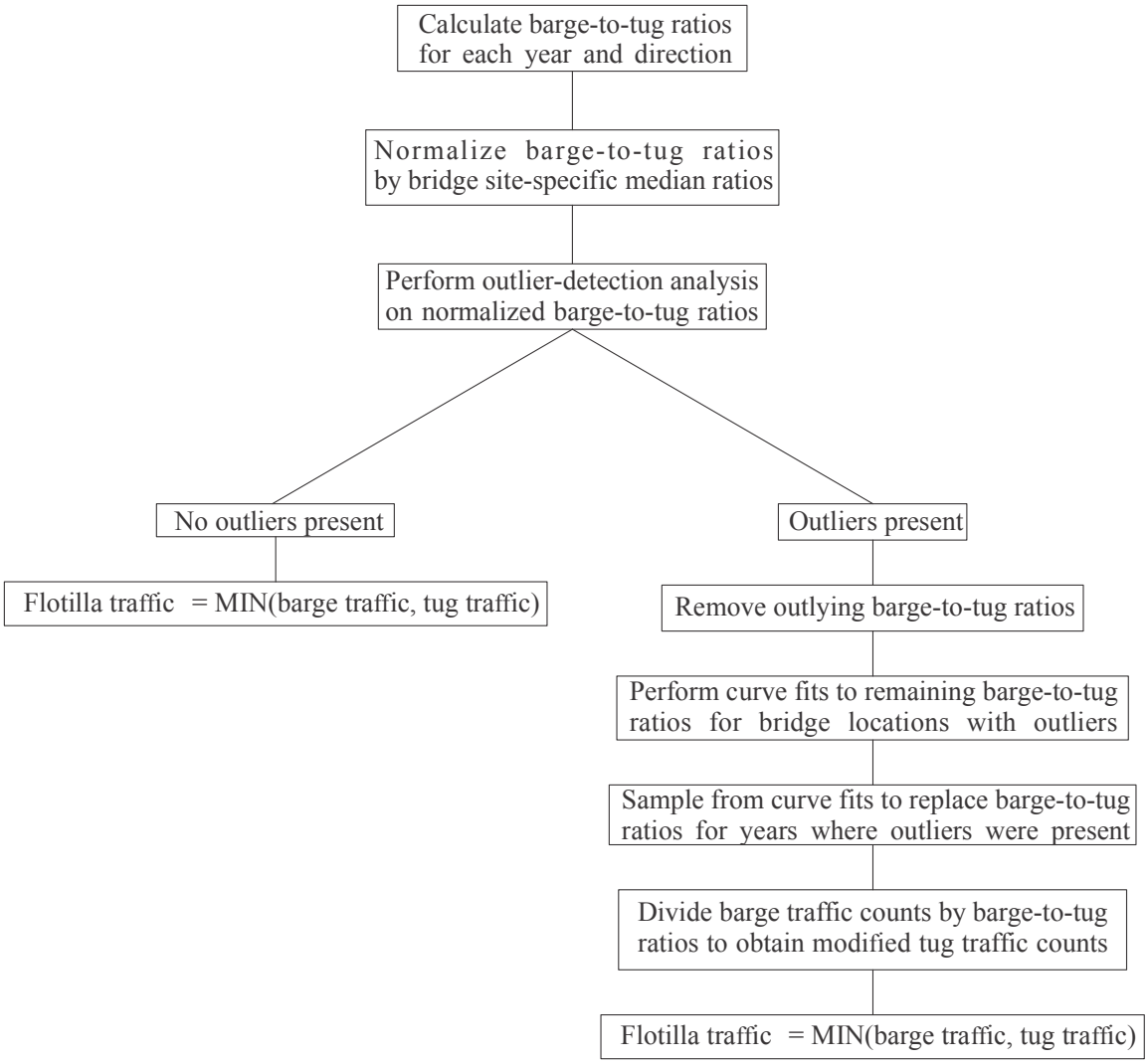

Figure 5.3 Determination of barge flotilla traffic counts for individual bridge locations

The methodology shown in Fig. 5.3 was used to determine barge flotilla traffic counts for each year where USACE vessel traffic data were collected for the bridges analyzed in this study. Additionally, where needed, curve fits were also performed on the analyzed flotilla traffic data in order to estimate flotilla traffic counts for years where USACE data were *not* provided (see Appendix E). During the *BR* calibration procedure, traffic counts were sampled from the fitted curves to calculate estimates of *PI*. Similar to the fits applied to the barge-to-tug ratios, an exponential fit type was selected for the barge flotilla traffic curve fits.

5.2.3 Results

Using the number of barge-to-bridge collisions (Table 5.2) over the time-frame of interest (2000-2014 for panhandle bridges, 2002-2014 for bridges in other regions), and the total number of barge flotilla passages calculated for that same time-frame, values of *PI* were quantified for each bridge location and direction (Table 5.3). The 'inbound' and 'outbound' directional designations were uniquely determined for each bridge site based on the location of nearby ports

and waterway mile markers. Note that a *PI* value of zero indicates that no barge-to-bridge impact events were reported at that particular bridge location in the specified direction.

Table 5.3 Estimated values of *PI*

Bridge name	*PI* (10^{-4}) (inbound)	*PI* (10^{-4}) (outbound)
Acosta Bridge	0.00	8.05
Atlantic Blvd. Bridge	0.00	31.0
Bob Sikes Bridge	2.68	4.76
Brooks Bridge	0.00	1.90
CSX Railroad Bridge over Escambia Bay	0.00	0.00
Dupont Bridge	13.0	0.00
Gandy Bridge	24.0	0.00
Highway-90 Bridge over Escambia River	0.00	2.33
Interstate-10 Bridge over Escambia Bay	0.00	0.00
Navarre Beach Bridge	1.79	0.951
Pensacola Bay Bridge	0.00	0.768
Sister's Creek Bridge	0.00	6.48
Theo Baars Bridge	0.00	0.00

While many values of *PI* were smaller than 3.00×10^{-4}, the Acosta Bridge, Atlantic Blvd. Bridge, Bob Sikes Bridge, Dupont Bridge, Gandy Bridge, and the Sister's Creek Bridge were all associated with larger values of *PI*. In the case of the Bob Sikes Bridge, this was primarily due to the significant number of collision events that occurred in one direction (outbound). However, for the other five bridges, the main reason for the large values of *PI* was relatively low barge and tug traffic activity.

5.3 Modification Factors

To adjust for bridge site-specific conditions in the *BR* calibration process, the values of *PI* computed in the previous section were modified by several AASHTO-specified modification factors (through Eqn. 5.1). Each modification factor could only take a value of one or greater.

5.3.1 Bridge location

At certain bridge locations, the presence of a turn or bend in the waterway near the bridges necessitated the calculation of a bridge location modification factor (Table 5.4). This was accomplished through the methodology described in Chapter 3, along with relevant AASHTO (2014) design equations:

$$R_B = \left(1 + \frac{\theta}{45^\circ}\right) \tag{5.2}$$

$$R_B = \left(1 + \frac{\theta}{90^\circ}\right) \tag{5.3}$$

where, R_B is the bridge location modification factor and θ is the angle of the bend or turn in the waterway. Recall from Chapter 2 that Eqn. 5.2 is applied when a bridge is located directly within a turn or bend and Eqn. 5.3 is applied when a bridge is located adjacent to a turn or bend (i.e., within a 'transition' region). Many of the bridge locations included in this study were in relatively straight regions. However, the Acosta Bridge (Fig. 5.4), Brooks Bridge (Fig. 5.5), Dupont Bridge (Fig. 5.6), Highway-90 Bridge (Fig. 5.7), and the Sister's Creek Bridge (Fig. 5.8), were each located either within or adjacent to a waterway turn or bend. As shown in Table 5.4, estimated values of R_B ranged from 1.00 to 2.18.

Table 5.4 Estimated values of R_B

Bridge	Acosta Bridge	Atlantic Blvd. Bridge	Bob Sikes Bridge	Brooks Bridge	Dupont Bridge	Gandy Bridge	Highway-90 Bridge over Escambia River	Navarre Beach Bridge	Pensacola Bay Bridge	Sister's Creek Bridge
R_B (inbound)	2.18	1.00	1.00	1.56	2.07	1.00	1.91	1.00	1.00	1.21
R_B (outbound)	2.18	1.00	1.00	1.56	1.17	1.00	1.91	1.00	1.00	1.67

Note: The CSX Railroad Bridge, Interstate-10 Bridge, and Theo Baars Bridge had no recorded impact events, resulting in *PI* and *BR* estimates equal to zero. Consequently, R_B modification factors were not calculated for these three bridge locations.

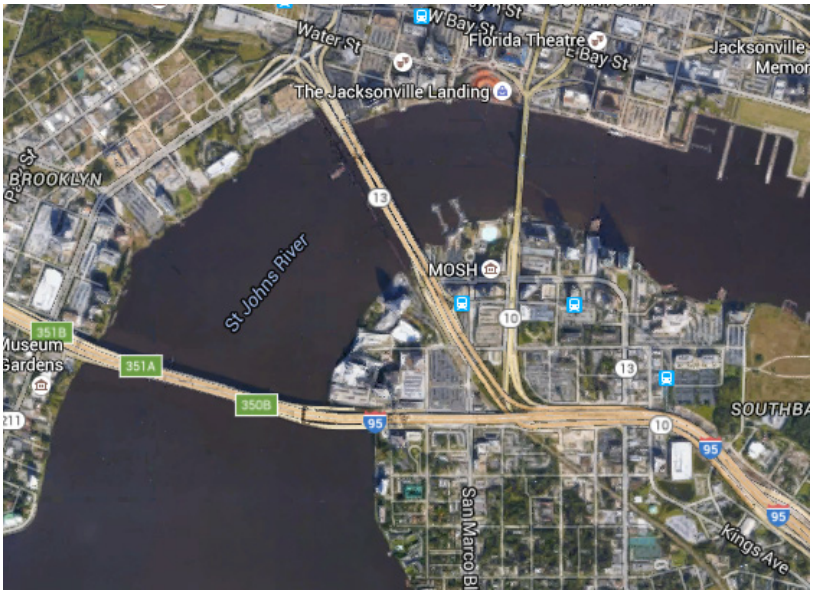

Figure 5.4 Curvature of waterway near Acosta Bridge (Source: Google)

Figure 5.5 Curvature of waterway near Brooks Bridge (Source: Google)

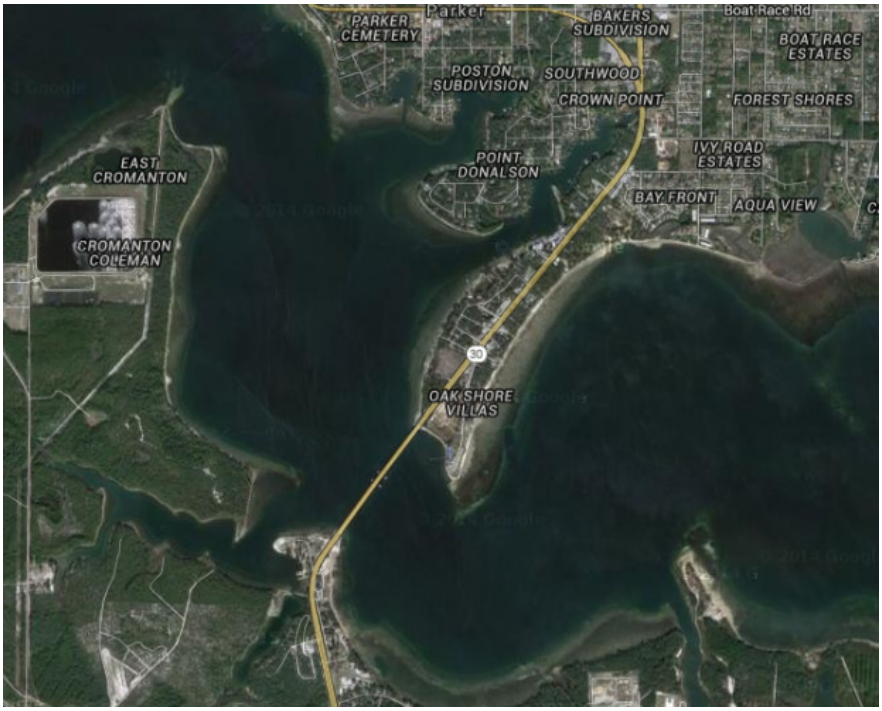

Figure 5.6 Curvature of waterway near Dupont Bridge (Source: Google)

Figure 5.7 Curvature of waterway near Highway-90 Bridge over Escambia River (Source: Google)

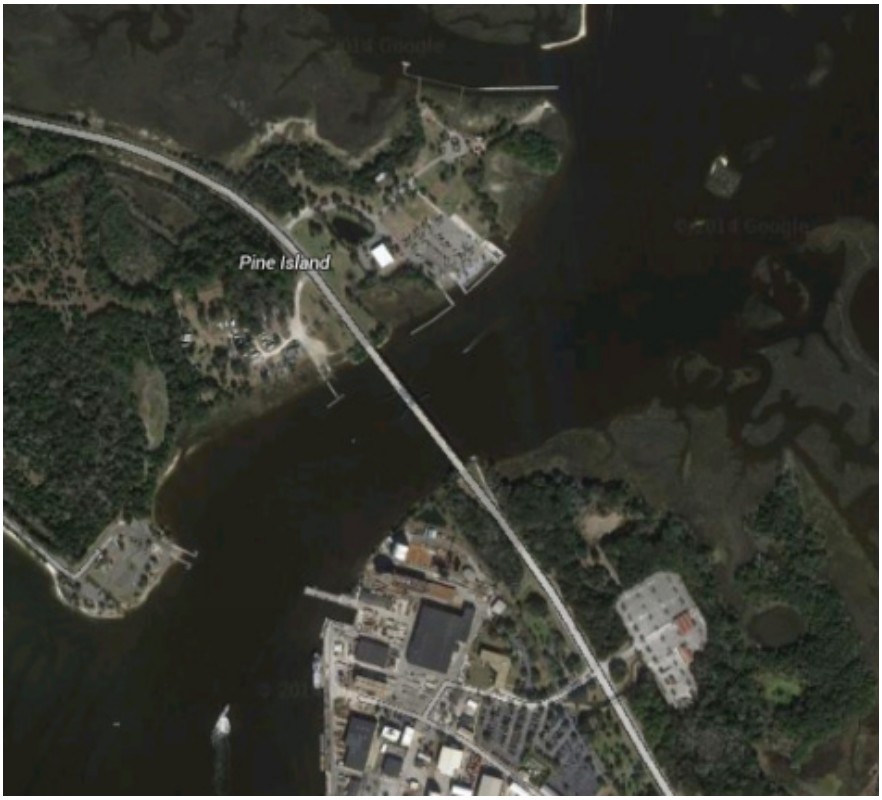

Figure 5.8 Curvature of waterway near Sister's Creek Bridge (Source: Google)

5.3.2 Current/crosscurrent

Two sources of data were used in conjunction with Eqns. 2.5 and 2.6 to compute modification factors associated with waterway flow: current velocities obtained from individual barge collision incident reports, and National Oceanic and Atmospheric Administration (NOAA) tidal current predictions. Modification factors determined from accident reports were calculated directly from the current magnitudes and current directions indicated in each report.

Modification factors determined from NOAA tidal current data were calculated by first averaging peak tidal currents collected over 52 weeks for the bridge site of interest and then using site-specific current directional information to calculate R_C and R_{XC}. For individual bridge sites, R_C and R_{XC} values were calculated for each available source of current data. For example, if a bridge site with NOAA tidal current predictions and two incident reports with current data were considered, three pairs of current modification factors would have been calculated. Note that, while several estimates of R_C and R_{XC} were calculated for bridge sites with multiple sources of current data, single estimates of R_C and R_{XC} were used in the *BR* calibration process (Table 5.5). The R_C and R_{XC} values shown in Table 5.5 were obtained by averaging R_C and R_{XC} values calculated from each source of data available at individual bridge sites.

Table 5.5 Estimated values of R_C and R_{XC}

Bridge	Acosta Bridge	Atlantic Blvd. Bridge	Bob Sikes Bridge	Brooks Bridge	Dupont Bridge	Gandy Bridge	Highway-90 Bridge over Escambia River	Navarre Beach Bridge	Pensacola Bay Bridge	Sister's Creek Bridge
R_C	1.22	1.42	1.26	1.14	1.04	1.11	1.43	1.22	1.20	1.06
R_{XC}	1.43	2.36	2.52	2.38	1.04	1.15	1.72	2.05	1.74	1.93

Note: The CSX Railroad Bridge, Interstate-10 Bridge, and Theo Baars Bridge had no recorded impact events, resulting in *PI* and *BR* estimates equal to zero. Consequently, R_C and R_{XC} modification factors were not calculated for these three bridge locations.

5.3.3 Vessel traffic density

In order to compute values of R_D, vessel density factors (*VDF*s) were first calculated (Tables 5.6 and 5.7):

$$VDF = \frac{\mu_N}{W} \tag{5.4}$$

where, μ_N is the average annual vessel traffic and W (ft) is the navigable width of the waterway near the bridge. It is important to note that, since all larger vessels can contribute significantly to vessel traffic density, all available vessel traffic data, including ship, barge, and tug traffic, were used in the computation of μ_N. To obtain a datum for which computed *VDF* values could be compared, an additional *VDF* of 5.87 was calculated for the LA-1 Bridge near Leeville, LA. Since a detailed risk assessment was performed on the LA-1 Bridge in the AASHTO (2009) guide specification for vessel collision design, a value of R_D was known for the this location. Recall from earlier discussions that R_D may take a value from 1.0 (low vessel traffic density) to 1.6 (high vessel traffic density). For the LA-1 Bridge, AASHTO (2009) specified a R_D value of 1.3, due to the width of the waterway and the number of vessel transits through the bridge site. Since the *VDF* calculated for the LA-1 Bridge was higher than the *VDF*s associated with the bridge sites in this study, R_D values for each investigated bridge were estimated (Table 5.8) by linearly interpolating between 1.0 and 1.3 using calculated *VDF*s.

Table 5.6 *VDF*s estimated for the inbound direction

Bridge	Acosta Bridge	Atlantic Blvd. Bridge	Bob Sikes Bridge	Brooks Bridge	Dupont Bridge	Gandy Bridge	HW-90 Bridge over Escambia River	Navarre Beach Bridge	Pensacola Bay Bridge	Sister's Creek Bridge
W (ft)	2174	732.0	2958	608.0	2672	6512	523.0	1284	9219	190.0
μ_N	218.0	92.00	2017	2017	366.0	189.0	2180	2017	2180	490.0
VDF	0.100	0.126	0.682	3.32	0.137	0.029	4.17	1.57	0.236	2.58

Table 5.7 *VDF*s estimated for the outbound direction

Bridge	Acosta Bridge	Atlantic Blvd. Bridge	Bob Sikes Bridge	Brooks Bridge	Dupont Bridge	Gandy Bridge	HW-90 Bridge over Escambia River	Navarre Beach Bridge	Pensacola Bay Bridge	Sister's Creek Bridge
W (ft)	1667	732.0	2958	608.0	2672	11540	523.0	1284	10420	190.0
μ_N	215.0	69.00	2067	2067	349.0	131.0	2168	2067	2168	553.0
VDF	0.129	0.094	0.699	3.40	0.131	0.011	4.14	1.61	0.208	2.91

Table 5.8 Estimated values of R_D

Bridge	Acosta Bridge	Atlantic Blvd. Bridge	Bob Sikes Bridge	Brooks Bridge	Dupont Bridge	Gandy Bridge	HW-90 Bridge over Escambia River	Navarre Beach Bridge	Pensacola Bay Bridge	Sister's Creek Bridge
R_D (inbound)	1.01	1.01	1.03	1.17	1.01	1.00	1.21	1.08	1.01	1.13
R_D (outbound)	1.01	1.00	1.04	1.17	1.01	1.00	1.21	1.08	1.01	1.15

Note: The CSX Railroad Bridge, Interstate-10 Bridge, and Theo Baars Bridge had no recorded impact events, resulting in *PI* and *BR* estimates equal to zero. Consequently, R_D modification factors were not calculated for these three bridge locations.

5.4 Additional Probabilities

To account for bridge geometry in the *BR* calibration process, *PG* and *PF* were calculated for individual bridge sites using the procedures described in Sections 3.4.3 and 3.4.4. Since the calculated values of both *PG* and *PF* were dependent on assumed flotilla sizes, four flotilla groups were selected for the investigated bridge sites to represent reasonable bounds on the length and width of barge flotillas in each region (Table 5.9). Specific flotilla dimensions for

individual bridge sites (see Appendix F) were determined using collected vessel traffic data and bridge drawings.

Table 5.9 Flotilla group classifications

Flotilla Group	FG-A	FG-B	FG-C	FG-D
Large dimension(s)	length	-	length, width	width
Small dimension(s)	width	length, width	-	length

5.4.1 Geometric probability

The range of *PG* values for individual bridges (Tables 5.10 and 5.11) depended primarily on the number and width of piers that fell within the waterway and the size of the flotillas which could pass underneath the bridge. In general, longer bridges and wider flotillas resulted in larger estimates of *PG*. Note that, aside from influencing the maximum size of barge flotillas, waterway widths were not included in the calculation of *PG* (per AASHTO [2014] specifications).

Table 5.10 Estimated values of *PG* (inbound direction)

Bridge	Acosta Bridge	Atlantic Blvd. Bridge	Bob Sikes Bridge	Brooks Bridge	Dupont Bridge	Gandy Bridge	HW-90 Bridge over Escambia River	Navarre Beach Bridge	Pensacola Bay Bridge	Sister's Creek Bridge
PG (FG-A)	0.158	0.356	0.552	0.193	0.367	0.405	0.558	0.561	0.674	0.299
PG (FG-B)	0.235	0.426	0.477	0.320	0.388	0.328	0.529	0.515	0.520	0.559
PG (FG-C)	0.274	0.688	0.950	0.431	0.887	0.522	0.861	0.910	0.959	0.469
PG (FG-D)	0.358	0.902	0.894	0.715	0.901	0.500	0.881	0.958	0.901	0.857

Note: The CSX Railroad Bridge, Interstate-10 Bridge, and Theo Baars Bridge had no recorded impact events, resulting in *PI* and *BR* estimates equal to zero. Consequently, *PG* estimates were not calculated for these three bridge locations.

Table 5.11 Estimated values of *PG* (outbound direction)

Bridge	Acosta Bridge	Atlantic Blvd. Bridge	Bob Sikes Bridge	Brooks Bridge	Dupont Bridge	Gandy Bridge	HW-90 Bridge over Escambia River	Navarre Beach Bridge	Pensacola Bay Bridge	Sister's Creek Bridge
PG (FG-A)	0.158	0.356	0.552	0.193	0.367	0.405	0.558	0.561	0.674	0.299
PG (FG-B)	0.235	0.426	0.477	0.320	0.388	0.328	0.529	0.515	0.520	0.559
PG (FG-C)	0.274	0.688	0.950	0.431	0.887	0.522	0.861	0.910	0.959	0.469
PG (FG-D)	0.358	0.902	0.894	0.715	0.901	0.500	0.881	0.958	0.901	0.857

Note: The CSX Railroad Bridge, Interstate-10 Bridge, and Theo Baars Bridge had no recorded impact events, resulting in *PI* and *BR* estimates equal to zero. Consequently, *PG* estimates were not calculated for these three bridge locations.

5.4.2 Protection factor

Bridge *PF* values were calculated (Tables 5.12 and 5.13) to account for waterway obstructions that could alter the navigational path of a barge flotilla prior to reaching a bridge. For this investigation, protective systems or obstructions immediately adjacent to a bridge pier (e.g., bridge fenders, neighboring bridges, etc.) were not represented in the *PF* calculation process since such obstructions were too close to the bridge to alter barge flotilla aberrancy rates in a meaningful way. Islands and shallow water regions were the primary sources of protection for investigated bridge sites.

Table 5.12 Estimated values of *PF* (inbound direction)

Bridge	Acosta Bridge	Atlantic Blvd. Bridge	Bob Sikes Bridge	Brooks Bridge	Dupont Bridge	Gandy Bridge	HW-90 Bridge over Escambia River	Navarre Beach Bridge	Pensacola Bay Bridge	Sister's Creek Bridge
PF (FG-A)	1.00	0.309	1.00	0.802	1.00	1.00	0.196	0.691	1.00	0.802
PF (FG-B)	1.00	0.571	1.00	0.883	1.00	1.00	0.443	0.978	1.00	0.887
PF (FG-C)	1.00	0.312	1.00	0.801	1.00	1.00	0.273	0.763	1.00	0.855
PF (FG-D)	1.00	0.536	1.00	0.888	1.00	1.00	0.563	0.985	1.00	0.917

Note: The CSX Railroad Bridge, Interstate-10 Bridge, and Theo Baars Bridge had no recorded impact events, resulting in *PI* and *BR* estimates equal to zero. Consequently, *PF* estimates were not calculated for these three bridge locations.

Table 5.13 Estimated values of *PF* (outbound direction)

Bridge	Acosta Bridge	Atlantic Blvd. Bridge	Bob Sikes Bridge	Brooks Bridge	Dupont Bridge	Gandy Bridge	HW-90 Bridge over Escambia River	Navarre Beach Bridge	Pensacola Bay Bridge	Sister's Creek Bridge
PF (FG-A)	0.705	0.141	1.00	0.802	1.00	1.00	0.239	0.637	1.00	0.802
PF (FG-B)	0.792	0.209	1.00	0.883	1.00	1.00	0.511	0.958	1.00	0.887
PF (FG-C)	0.734	0.139	1.00	0.801	1.00	1.00	0.301	0.714	1.00	0.855
PF (FG-D)	0.784	0.193	1.00	0.888	1.00	1.00	0.598	0.970	1.00	0.917

Note: The CSX Railroad Bridge, Interstate-10 Bridge, and Theo Baars Bridge had no recorded impact events, resulting in *PI* and *BR* estimates equal to zero. Consequently, *PF* estimates were not calculated for these three bridge locations.

5.5 Base Aberrancy Rate Calibration

Eqn. 5.1 was used to perform the *BR* calibration process for each bridge. As discussed earlier, four barge flotilla configurations were included in the calibration process. In addition, two levels of protection were considered: a protected state (using the *PF* values shown in Tables 5.12 and 5.13) and an unprotected state, in which all bridge piers in the waterway were considered fully exposed. Accordingly, eight estimates of *BR* were produced per bridge and direction. For the three bridge locations without any recorded collision events (CSX Railroad Bridge, Interstate-10 Bridge, and Theo Baars Bridge), *BR* estimates were taken as zero for each of the eight cases. Direction-specific estimates of bridge site *BR* values for each of the eight combinations of flotilla size and protection level were then averaged using a weighted approach based on the relative barge flotilla traffic in each direction; this process resulted in a single estimate of *BR* for each of the eight cases at each bridge site. Among all 13 bridges considered in this study, 104 total estimates of *BR* (Fig. 5.9) were produced. In order to provide a single estimate of *BR* that may be used in bridge design, mean values were computed for different subsets of the *BR* estimates (Table 5.14).

For each mean value calculated, confidence bounds were generated through a 'bootstrap' approach. In this approach, sets of *BR* values were resampled (with replacement) from the empirical *BR* distribution through Monte Carlo simulation. For each resampled data set, a mean *BR* was calculated so that a distribution of mean *BR* values could be formed and a 95% confidence interval could be calculated from the resulting normal distribution. As shown in Table 5.14, higher estimates of *BR* and wider confidence intervals were generated when bridges outside of the Florida panhandle were used in the calibration process. As discussed earlier, the Acosta Bridge, Atlantic Blvd. Bridge, Dupont Bridge, Gandy Bridge, and Sister's Creek Bridge had notably less recorded barge flotilla traffic than panhandle bridge sites, resulting in significantly larger estimates of *PI* (Table 5.3). Since the number of barge passages at these locations is possibly insufficient to form a reliable estimate of the *BR* parameter, it is recommended that only panhandle bridge sites (with the exception of the Dupont Bridge) be used

as the basis for calibration. As a consequence, a *BR* value of 5.4×10^{-5} is recommended as a characteristic design value for Florida bridges, which represents an approximate 55% decrease from the present AASHTO *BR* of 1.2×10^{-4} for barges. To show the relative effect of flotilla configuration on *BR* estimates, mean *BR* values were also calculated for each of the four flotilla configurations associated with the eight bridge locations used in the development of the recommended design value of *BR* (Table 5.15). It should be noted that the mean of the four flotilla-specific estimates shown in Table 5.15 is equivalent to the overall mean for the eight bridge locations (shown in Table 5.14).

Table 5.14 Summary of mean *BR* values

Region	Number of bridge sites	*BR* (mean)	95% confidence interval
All	13	5.2×10^{-4}	$3.6\times10^{-4} - 7.6\times10^{-4}$
Panhandle, Sister's Creek Bridge, and Acosta Bridge	11	1.5×10^{-4}	$1.2\times10^{-4} - 2.1\times10^{-4}$
Panhandle	9	1.1×10^{-4}	$7.5\times10^{-5} - 1.6\times10^{-4}$
Panhandle (except for Dupont Bridge)	8	5.4×10^{-5}	$4.0\times10^{-5} - 7.1\times10^{-5}$

Table 5.15 *BR* values associated with flotilla classifications for the eight design bridge locations

Flotilla classification	*BR* (mean)
FG-A	7.7×10^{-5}
FG-B	6.4×10^{-5}
FG-C	4.2×10^{-5}
FG-D	3.4×10^{-5}

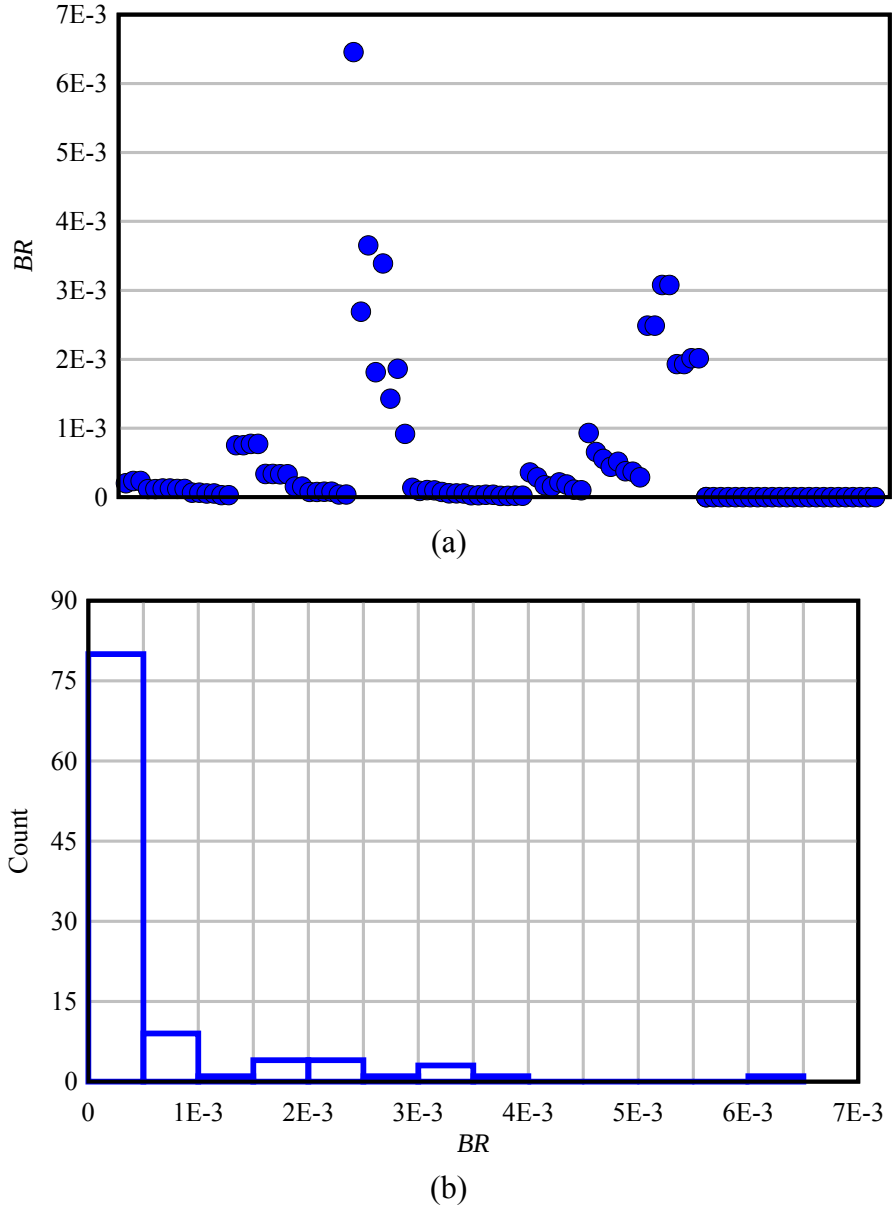

Figure 5.9 Estimates of *BR*: (a) scatterplot; (b) histogram

5.6 Risk Assessment

To illustrate the relative effect of the recalibrated *BR* parameter, annual frequency of collapse (*AF*) predictions were computed for the Bryant Grady Patton Bridge (Fig. 5.10) over Apalachicola Bay, FL, and the LA-1 Bridge near Leeville, LA (Fig. 5.11). Both of these structures were previously analyzed in detail as a part of FDOT project number BDK75-977-31 (see Consolazio et al. [2014] for specific calculations).

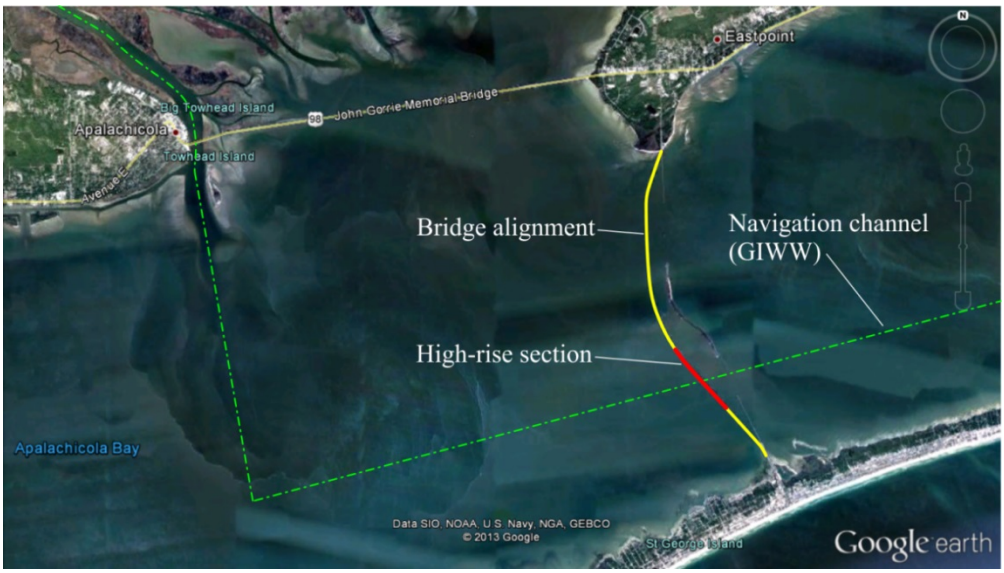

Figure 5.10 Bryant Grady Patton Bridge (SR-300) spanning Apalachicola Bay, Florida (Consolazio et al. 2014)

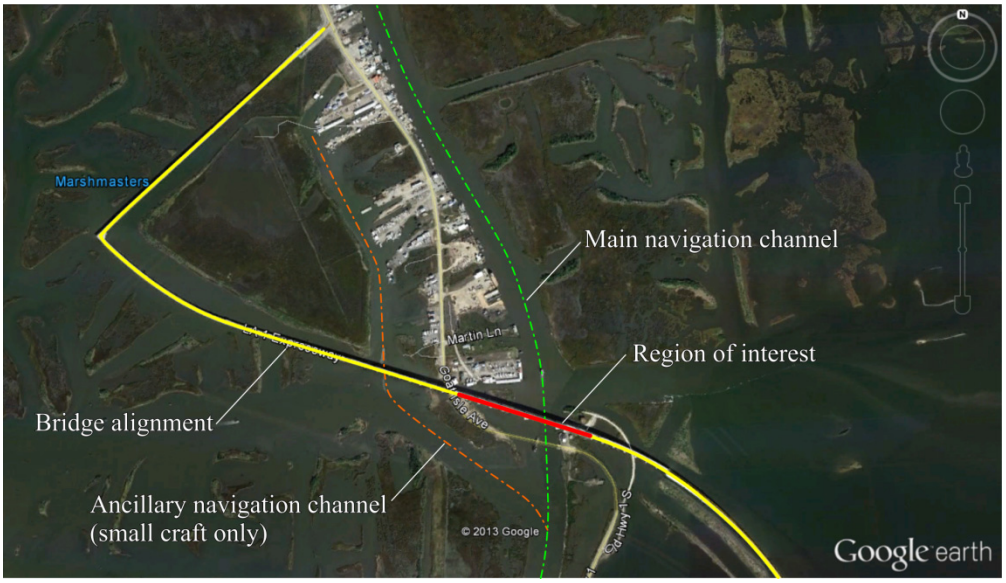

Figure 5.11 LA-1 Bridge near Leeville, Louisiana (Consolazio et al. 2014)

Risk assessments conducted under BDK75-977-31 were performed using current AASHTO specifications as well as with UF/FDOT-developed methods. Specific UF/FDOT methods employed included the coupled vessel impact analysis (CVIA) method (Consolazio and Cowan 2005), which incorporates dynamic amplification into the calculation of structural demand through time-history analysis. In addition, risk assessments conducted using UF/FDOT methods employed a revised barge force-deformation model (Getter and Consolazio 2011) which considers the influence of pier width and pier shape on peak impact force. Finally, UF/FDOT methods also incorporated a revised *PC* expression (Davidson et al. 2013) developed from an extensive reliability analysis. *AF* predictions determined using both AASHTO and UF/FDOT

methods were calculated by Consolazio et al. (2014); for convenience, these values have been re-tabulated here in Table 5.16. The values of *AF* computed by Consolazio et al. (2014) utilized the AASHTO design value for *BR* (1.2×10^{-4}). When the design value of *BR* determined in the present investigation (5.4×10^{-5}) was used instead, the UF/FDOT *AF* estimates decreased by 55%, resulting in the values shown in Table 5.17.

Table 5.16 *AF* estimates calculated by Consolazio et al. (2014)

Bridge name	*AF* estimate produced from AASHTO methods ($year^{-1}$)	*AF* estimate produced from UF/FDOT methods ($year^{-1}$)
Bryant Grady Patton Bridge	6.8×10^{-7} (return period of 1,460,000 years)	6.9×10^{-4} (return period of 1,448 years)
LA-1 Bridge	5.5×10^{-5} (return period of 18,060 years)	1.4×10^{-1} (return period of 7.3 years)

Table 5.17 *AF* estimates calculated in present study

Bridge name	*AF* estimate produced from AASHTO methods ($year^{-1}$)	*AF* estimate produced from UF/FDOT methods ($year^{-1}$)
Bryant Grady Patton Bridge	6.8×10^{-7} (return period of 1,460,000 years)	3.1×10^{-4} (return period of 3,226 years)
LA-1 Bridge	5.5×10^{-5} (return period of 18,060 years)	6.3×10^{-2} (return period of 15.9 years)

Despite the reduction in *BR* (i.e., from 1.2×10^{-4} to 5.4×10^{-5}), notable differences remained between *AF* values computed using UF/FDOT methods and those calculated from the AASHTO provisions. This result may be attributed to three primary differences between AASHTO and UF/FDOT methods:

- Load-prediction models: AASHTO design procedures make use of a barge bow force-deformation relationship—derived from experimental research conducted by Meier-Dörnberg (1983)—that does not consider the influences that pier width and pier shape have on peak impact force levels. However, numerous analytical and experimental studies [e.g., Consolazio et al. 2009, Kantrales et al. (2015)] have definitively demonstrated that both pier shape and size (i.e., 'pier geometry') affect barge bow force-deformation behavior and therefore impact load. Accordingly, the influence of pier geometry is directly accounted for in the UF/FDOT load-prediction model (Getter and Consolazio 2011) wherein flat-faced piers and pile caps generate higher peak crushing forces (and therefore larger loads) relative to round variants. Since both the Bryant Grady Patton Bridge and the LA-1 Bridge utilize wide, flat-faced pile caps, impact loads predicted by the UF/FDOT method are larger than those predicted by AASHTO. However, it has also been shown by Consolazio et al. (2014) that if the pile caps for these bridges were retrofitted (or had been originally designed) with rounded ends, *AF* estimates computed using the UF/FDOT procedures would decrease significantly.
- Dynamic amplification effects: Prior studies (e.g., Davidson et al. 2010) have demonstrated that during impact loading events, bridge pier design forces (moments, shears, etc.) are amplified—relative to static levels—as a result of mass-related

inertial effects. In contrast to the static design approach prescribed by AASHTO—which does not explicitly account for dynamic amplification—the UF/FDOT methods employ dynamic analysis procedures that account for such amplifications.

- Probability of collapse: The probability of collapse (*PC*) expression included in the current AASHTO provisions is intended to be applicable to both ship-to-bridge and barge-to-bridge collision events and was derived from ship-to-ship (not vessel-to-bridge) collision data. In contrast, UF/FDOT methods make use of an updated probability of collapse (*PC*) expression that was developed (Davidson et al. 2013) through rigorous reliability analyses involving thousands of dynamically simulated barge-to-bridge impact events. Over the entire feasible range of pier demand-to-capacity (D/C) ratios, the UF/FDOT *PC* expression yields collapse probabilities that are larger than those predicted by the AASHTO *PC* expression. Consequently annual frequency of collapse (*AF*) values determined from the UF/FDOT methods are accordingly larger than those determined using the AASHTO provisions.

5.7 Discussion

Of the Florida bridge locations analyzed in this study, it was noted that locations with low volumes of barge traffic correlated with very high estimates of the probability of impact (*PI*), as well as *BR*. Since this was a statistical investigation, the number of recorded observations per bridge site—represented by barge flotilla passages—directly related to the accuracy of the predicted *BR* parameter. Consequently, only Florida bridges with more significant volumes of barge flotilla traffic were included in the calibration procedures used to produce the recommended design value of *BR*. However, other bridge locations exist outside of the state of Florida which have even more elevated levels of barge traffic than the bridges that were considered in this investigation. Consistent with the findings from this study, if such locations were included in a similar *BR* recalibration effort, the resulting design value could potentially be much smaller than the design value of *BR* computed strictly from Florida bridge data.

During the initial phases of this study, barge-to-bridge collision data were requested from the USCG for the entire United States, rather than just for bridges located in Florida. In response to this initial nationwide request, the USCG indicated that such a request would not be feasible to fulfill. Therefore, since this research was intended to produce a design expression specifically applicable to the analysis and design of bridges in Florida waterways, a more restricted subset of data—consisting only of barge-to-bridge collision data for bridges located in Florida—was requested and received from the USCG. Moreover, during discussions with the USCG relating to the collection of barge-to-bridge collision *casualty data*, the UF research team was directed to the USACE Waterborne Commerce Statistics Center (WCSC) for collection of barge and tug *traffic data* corresponding to Florida bridge locations. Accordingly, this USACE center was consulted to obtain all traffic data sets used in this investigation (a process that took more than six (6) months to complete).

For bridges sites located near locks, an additional source of barge traffic data exists—the USACE Lock Performance Monitoring System (LPMS). LPMS data are associated with barge flotilla transits through USACE owned and operated *lock and dam structures*, and are more accurate (e.g. with respect to flotilla sizes and configurations) and more accessible than data provided by the Waterborne Commerce Statistics Center. However, since LPMS data are

associated with river locks and dams, and since there are few of these structures in the state of Florida, no LPMS data were available for the (mostly coastal) Florida bridges considered in the present investigation. Nevertheless, additional coastal states neighboring Florida, such as Louisiana, contain waterways with higher volumes of barge traffic and a number of lock and dam systems. Consequently, if out-of-state USACE LPMS barge traffic data associated with highly-trafficked bridge locations were combined with corresponding USCG-provided collision data, a subsequent statistical recalibration effort could yield significantly lower estimates of *BR* relative to the presently computed estimates.

CHAPTER 6
CONCLUSIONS AND RECOMMENDATIONS

6.1 Concluding Remarks

Present AASHTO bridge design specifications include, as a critical component, a risk-based approach for the design of waterway bridges to resist vessel impact loads. This approach includes expressions for quantifying the severity of ship and barge impact loads as well as expressions for predicting the likelihood that an impact event will occur. The existing AASHTO probability expressions, used to estimate the frequency of impact events, are based on a limited number of investigations conducted prior to the 1990s, when vessel navigational technology was significantly less developed than in more recent decades. Moreover, the AASHTO expressions for estimating barge-to-bridge impact probabilities are based on data sets that included other types of vessel casualties, such as vessel groundings and strandings, which did not result in a collision event with a bridge structure.

In the present investigation, the current state of maritime technology—both navigational and mechanical—was reviewed to determine the influence of technological advances on the barge towing industry since the year 1990. Based on interviews with various industry professionals, it was determined that due to improvements in technologies, such as global positioning systems (GPS), and with the advent of newer technologies, such as automatic identification systems (AIS), navigation in inland waterways and coastal areas has improved since the 1990s. Consequently, it was determined that the updated barge impact probability expression developed herein needed to incorporate recent barge-to-bridge collision data, thus implicitly considering these new and improved navigational technologies. Using such data, a recalibration of the AASHTO base aberrancy rate (*BR*) associated with barge flotillas was performed.

To facilitate the development of the revised *BR* expression, barge traffic data and barge-to-bridge collision data were collected for bridges in waterways throughout the state of Florida. In total, 13 bridges from three general regions in Florida were utilized in this study; additional bridges were considered, but were not incorporated into the recalibration process due to an insufficient level of barge flotilla traffic. Using site-specific information (e.g., bridge layouts, water current information, waterway charts, etc.) for investigated bridge locations, AASHTO expressions needed in the recalibration process—*PG*, *PF*, R_B, R_C, R_{XC}, and R_D—were computed. These expressions were then employed in conjunction with probability of impact (*PI*) estimates, computed from collected barge traffic and collision data, to produce a range of recalibrated *BR* values associated with each bridge location. A design value of *BR* was produced by computing the mean of *BR* estimates from a subset of bridge locations considered in this study. The revised estimate of *BR* (5.4×10^{-5}) represents a 55% decrease from the *BR* value presently employed in AASHTO (1.2×10^{-4}). Using the new *BR* estimate, updated risk assessments were performed on two bridge locations—the Bryant Grady Patton Bridge over Apalachicola Bay, FL, and the LA-1 Bridge in Leeville, LA. *AF* values computed using the new *BR* expressions, in conjunction with additional UF/FDOT analysis methodologies, load models, and design parameters, were larger than *AF* values computed from existing AASHTO procedures.

As discussed in this report, a correlation was noted between the volume of barge traffic associated with a bridge location and the recalibrated value of *BR*. Specifically, of the Florida

bridges considered in this investigation, bridges with very low volumes of barge traffic had very high estimates of *BR*. This result was likely a consequence of a reduction in the accuracy of *BR* predictions correlative with the utilization of fewer barge trips in the statistical analysis procedures. Consequently, only those Florida bridge locations with more significant levels of barge traffic were included in the recalibration process that produced the recommended design value of *BR*. However, additional out-of-state bridge locations exist with even higher volumes of barge flotilla traffic. In addition, a comprehensive and readily available source for barge flotilla traffic data—the USACE Lock Performance Monitoring System (LPMS)—is available for waterways with lock and dam structures in place. Since Florida has few bridge structures with nearby locks, LPMS data were not available for the Florida bridge locations considered in this study. However, several neighboring coastal states contain lock and dam systems for which LPMS data may be obtained. Consequently, if out-of-state LPMS barge traffic data associated with highly-trafficked bridge locations were combined with corresponding USCG-provided collision data, a subsequent statistical recalibration effort could yield a significantly lower estimate of *BR* relative to the presently computed value.

6.2 Design Recommendations

- It is recommended that a *BR* for barges of 5.4×10^{-5} be used in risk assessments of waterway bridge structures in the state of Florida, in lieu of the present AASHTO-specified value of 1.2×10^{-4} .
- It is recommended that the code provisions detailed in Appendix G be utilized to supplement existing AASHTO procedures for the analysis and design of waterway bridges in the state of Florida.

6.3 Recommendations for Future Research

- It is recommended that additional bridges located outside of Florida, preferably on waterways with high levels of barge traffic, be incorporated into a follow-up, expanded effort to recalibrate *BR*.
- It is recommended that additional investigation of the AASHTO *PG* expression be conducted, both with respect to the defining characteristics of the *PG* distribution and with respect to its interpretation to bridges with narrow waterways.

REFERENCES

American Association of State Highway and Transportation Officials (AASHTO). (2009). *Guide specification and commentary for vessel collision design of highway bridges*, 2nd Ed., Washington, DC.

AASHTO. (2014). *LRFD bridge design specifications,* 7th Ed., Washington, DC.

Bridge Software Institute (BSI). (2010). *FB-MultiPier user's manual*, Univ. of Florida, Gainesville, FL.

Consolazio, G. R., and Cowan D. R. (2005). "Numerically efficient dynamic analysis of barge collisions with bridge piers." *J. Struct. Eng.*, 131(8), 1256-1266.

Consolazio, G.R., Cowan, D.R., Biggs, A., Cook, R.A., Ansley, M., and Bollmann, H.T. (2005). "Full-scale experimental measurement of barge impact loads on bridge piers." *Transportation Research Record* 1936, Transportation Research Board, Washington, D.C., 81-93.

Consolazio, G. R, and Davidson, M. T. (2008). "Simplified dynamic barge collision analysis for bridge design." *Transportation Research Record 2050*, Transportation Research Board, Washington, DC, 13-25.

Consolazio, G. R., McVay, M. C., Cowan, D. R., Davidson, M. T., and Getter, D. J. (2008). *Development of improved bridge design provisions for barge impact loading.* Structures Research Report No. 51117, Engineering and Industrial Experiment Station, Univ. of Florida, Gainesville, FL.

Consolazio, G. R., Davidson, M. T., and Cowan, D. R. (2009). "Barge bow force-deformation relationships for barge-bridge collision analysis." *Transportation Research Record 2131*, Transportation Research Board, Washington, DC, 3–14.

Consolazio, G. R., Davidson, M. T., and Getter D. J. (2010). *Vessel crushing and structural collapse relationships for bridge design*. Structures Research Report No. 72908/74039, Engineering and Industrial Experiment Station, Univ. of Florida, Gainesville, FL.

Consolazio, G.R., Getter, D.J., and Kantrales, G.C. (2014). *Validation and implementation of bridge design specifications for barge impact loading.* Structures Research Report No. 2014/87294, Univ. of Florida, Gainesville, FL.

Davidson, M. T., Consolazio, G. R., Getter, D. J., (2010). "Dynamic Amplification of Pier Column Internal Forces Due to Barge-Bridge Collision." *Transportation Research Record 2172*, Transportation Research Board, Washington, DC, 11–22.

Davidson, M. T., Consolazio, G. R., Getter, D. J., and Shah, F. D. (2013). "Probability of collapse expression for bridges subject to barge collision." *J. Bridge Eng.*, 18(4), 287-296.

European Committee for Standardization (CEN). (2006). *Eurocode 1: Actions on structures – Part 1-7: General actions – Accidental actions (EN 1991-1-7:2006)*, Brussels, Belgium.

Friis-Hansen, P., and Simonsen, B.C. (2002). "GRACAT: software for grounding and collision risk analysis." *Marine Structures*, 15(4-5), 383-401.

Getter, D. J., and Consolazio, G. R. (2011). "Relationships of barge bow force-deformation for bridge design: Probabilistic consideration of oblique impact scenarios." *Transportation Research Record 2251*, Transportation Research Board, Washington, DC, 3-15.

Gucma, L. (2003). "Combination of photogrammatic and simulation method for safety evaluation of ships passage through bridges." *Proc., XI Int. Navigational Congress, International Association of Institutes of Navigation*, Berlin.

Hutchison, B.L., Gray, D.L., and Mathai, T. (2003). "Maneuvering simulations – an application to waterway navigability." *Proc., 1st World Maritime Technology Conference*, The Society of Naval Architects and Marine Engineers, San Francisco.

Kantrales G.C., G.R. Consolazio, D. Wagner, and S. Fallaha. (2015). "Experimental and analytical study of high-level barge deformation for barge-bridge collision design." *J. Bridge Eng.,* 21(2).

Kumar, S. and Moore, K.B. (2002). "The evolution of global positioning systems (GPS) technology." *J. of Sci. Ed. And Tech,* 11(1), 59-80.

Kunz, C.U. (1998). "Ship bridge collision in river traffic, analysis and design practice." *Ship Collision Analysis*, Balkema, Rotterdam, Netherlands, 13-21.

Larsen, O.D. (1993). "Ship collision with bridges: interaction between vessel traffic and bridge structures." *Structural Engineeing Documents*, SED 4, International Association for Bridge and Structural Engineering (IABSE), Switzerland.

Leys, C., Ley, C., Klein, O., Bernard, P., and Licata, L. (2013). "Detecting outliers: do not use standard deviation around the mean, use absolute deviation around the median." *J. Exp. Soc. Psychol.*, 49, 764-766.

Meier-Dörnberg, K. E. (1983). *Ship collisions, safety zones, and loading assumptions for structures in inland waterways*. Verein Deutscher Ingenieure (Association of German Engineers) Report No. 496, Düsseldorf, Germany, 1–9.

National Transportation Safety Board (NTSB). (2004). *U.S. Towboat Robert Y. Love Allision with Interstate 40 Highway Bridge Near Webbers Falls, Oklahoma, May 26, 2002*. Highway/Marine Accident Report NTSB/HAR-04/05, NTSB, Washington, D.C.

Tukey, J. (1977). *Exploratory Data Analysis*, Pearson, New York, NY.

United States Army Corps of Engineers (USACE). (2012). *Waterborne Commerce of the United States, Part 2—Waterways and Harbors, Gulf Coast, Mississippi Rivr System, Antilles*, Institute for Water Resources, U.S. Army Corps of Engineers, Alexandria, VA.

Wang, J., and Wang, W. (2014). "Estimation of Vessel-Bridge Collision Probability for Complex Navigation Channels." *J. Bridge Eng.*

Zhang, S. (2013). "Studies on the Probabilistic Model for Ship-Bridge Collisions." *Int. J. of Statistics and Probability*, 2(1), 16-23.

Zhou, L., Liu, M., and Liu, J. (2011) "Research on Probability of Ship Collision with Bridge in Different Wind and Draft." *Proc., 1st International Conference on Transportation Information and Safety (ICTIS),* American Society of Civil Engineers, Wuhan, China, 2490-2500.

APPENDIX A: ADDITIONAL DESIGN PROVISIONS

A.1 Introduction

This appendix summarizes design provisions in both AASHTO (2014) as well as CEN (2006) which cover the calculation of barge impact forces and the prediction of structural collapse probabilities. UF/FDOT-developed relationships covering these topics are discussed in Appendix B.

A.2 AASHTO Provisions

In order to perform a comprehensive risk assessment on a new or existing bridge structure, it is not only necessary to compute the probability that such an event would occur (probability of impact), but also the loads associated with the vessel-structure impact event, and the probability of structural collapse. This section summarizes AASHTO (2014) calculation procedures for quantifying the latter two components: barge-to-bridge impact loads (forces), and the probability of structural collapse

A.2.1 Barge impact forces

Barge-to-bridge impact forces computed using the procedures detailed in AASHTO (2014) are applied as static design forces, and are determined in three stages. The first stage is the calculation of kinetic energy associated with an impacting vessel:

$$KE = \frac{C_H W (V)^2}{29.2} \tag{A.1}$$

where KE is the vessel collision energy (kip-ft), C_H is the hydrodynamic mass coefficient (unitless), W is the vessel displacement tonnage (tonne), and V is the vessel impact speed (ft/s). Note that the divisor in Eqn. A.1 is related to gravitational acceleration. For barge tows, W is calculated using the combined mass of the tug/towing vessel and the total number of barges in one string of the tow. AASHTO recommends that the mass of adjacent (non-impacting) strings in a multi-string barge tow should be neglected in the computation of vessel tonnage, based on the assumption that the lashings between strings will fail during impact, causing these strings to break away, and thereby not contribute to the impacting mass of the barge tow. In addition to the mass of the impacting vessels, the mass of the water volume moving with the vessel immediately prior to impact must be approximated in the calculation process. AASHTO (2014) satisfies this requirement through implementation of a hydrodynamic mass coefficient C_H. C_H can take on multiple values, based on the vessel underkeel clearance, which is the distance between the bottom of the vessel and the bottom of the waterway:

- $C_H = 1.05$ if the vessel underkeel clearance exceeds 50% of the vessel draft
- $C_H = 1.25$ if the vessel underkeel clearance is less than 10% of the vessel draft

For intermediate values of underkeel clearance, C_H may be calculated through linear interpolation.

After calculating the kinetic energy associated with the impacting vessel, AASHTO requires the determination of a barge bow damage depth, which is the depth of deformation into the barge bow in the direction of impact (i.e., crush depth) (AASHTO 2014):

$$a_B = 10.2\left(\sqrt{1+\frac{KE}{5672}}-1\right) \tag{A.2}$$

where a_B is the barge bow damage depth (ft), and KE is the vessel collision energy (kip-ft), calculated using Eqn. A.1. The crush depth a_B is then used to determine a final design barge impact force (AASHTO 2014):

$$P_B = 4112a_B \text{ for } a_B < 0.34 \text{ ft} \tag{A.3}$$

$$P_B = 1349 + 110a_B \text{ for } a_B \geq 0.34 \text{ ft} \tag{A.4}$$

where P_B is a design barge impact force (kip), and a_B is the barge bow damage depth (ft), calculated using Eqn. A.2. When plotted as a piece-wise linear function, Eqns. A.3 and A.4 produce a bilinear load-deformation (force-crush) curve (Fig. A.1).

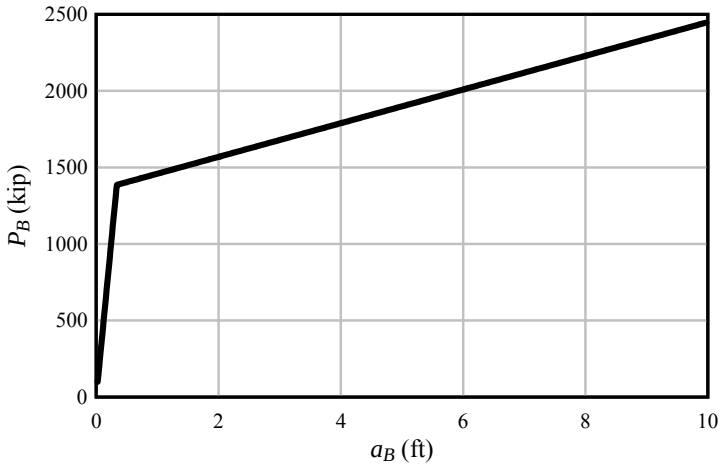

Figure A.1 Equivalent-static barge impact force-deformation relationship utilized in AASHTO (2014) design specifications

Eqns. A.2-A.4 were adapted by AASHTO from research conducted by Meier-Dörnberg (1983), in which dynamic impact experiments and a static crush experiment were performed on reduced-scale European pontoon barges. Dynamic impact tests were performed with both round and pointed impact hammers. Results from the static crush test (Fig. A.2) were later scaled to full-scale and adapted for use in design.

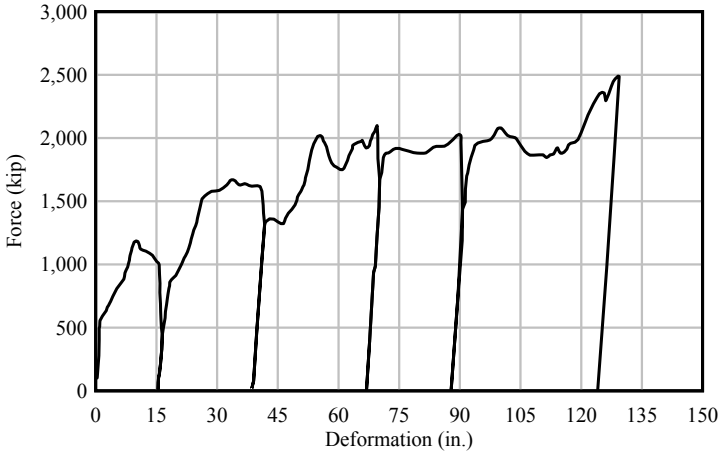

Figure A.2 Results from static crush test conducted by Meier-Dörnberg (1983) showing monotonic system hardening (Adapted from: Meier-Dörnberg 1983)

A.2.2 Probability of collapse

Intended to be used within the larger AASHTO *AF* expression, the probability of collapse (*PC*) expression is used to quantify the probability that a structural element will collapse given that an impact event has occurred. This expression (shown graphically in Fig. A.3) may take on one of the following forms, depending on the ratio of structural capacity (*H*) to structural demand (*P*) (AASHTO 2014):

$$PC = 0.1 + 9\left(0.1 - H/P\right) \quad \text{for } 0.0 \le H/P < 0.1 \tag{A.5}$$

$$PC = 0.111\left(1 - H/P\right) \quad \text{for } 0.1 \le H/P < 1.0 \tag{A.6}$$

$$PC = 0.0 \quad \text{for } H/P \ge 1.0 \tag{A.7}$$

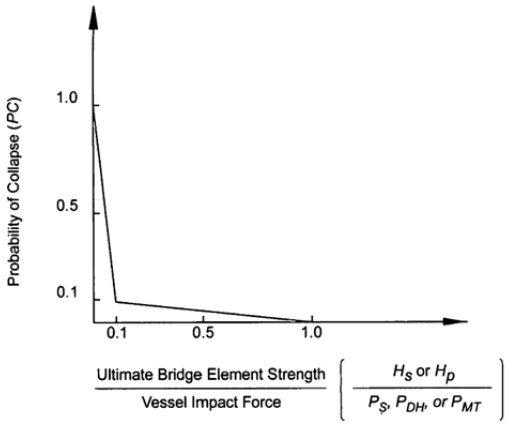

Figure A.3 AASHTO relationship between structural demand, impact force, and the probability of collapse (*PC*) (Source: AASHTO 2009)

A.3 Eurocode Provisions

Coupled with an outline of the methodology for performing a risk assessment in the context of a vessel-structure impact event, Eurocode provisions in EN 1991 (CEN 2006) also provide guidance on the computation of vessel impact forces. This section details the methods which are used to quantify these design forces as well as the basis for the approach taken by EN 1991.

A.3.1 Load cases

EN 1991 requires that two independent load cases be considered for barge-to-bridge impact design (Fig. A.4). These include: (1) a frontal (i.e., head-on) impact force (F_{dx}), and (2) a lateral impact force (F_{dy}) to be applied in conjunction with a friction force $\left(F_R = \mu F_{dy}\right)$. Note that the friction coefficient relating F_{dy} and F_R may be specified in a national annex, but is recommended to be taken as 0.4 in the main EN 1991 provisions.

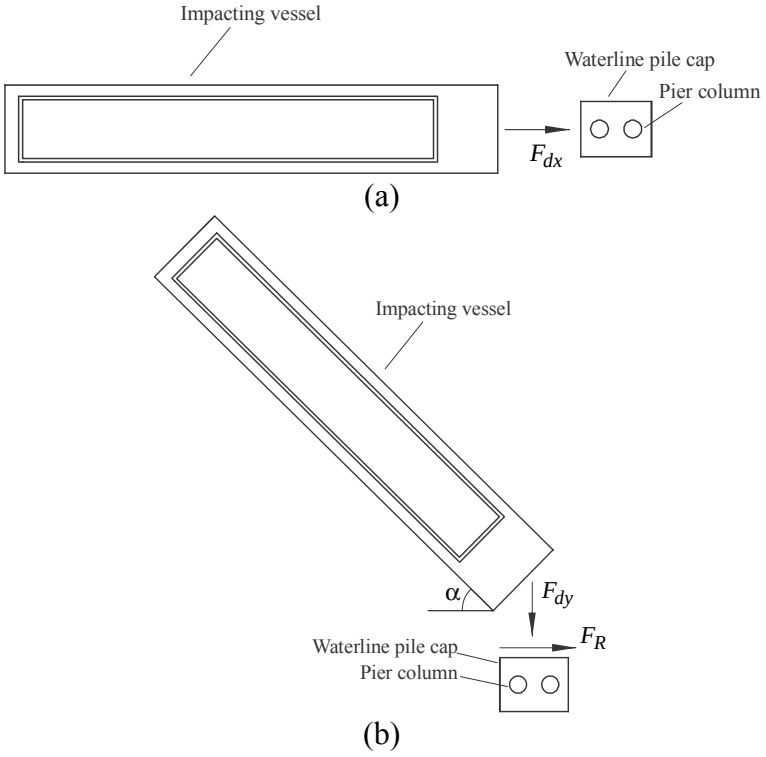

Figure A.4 Direction of dynamic impact forces for (a) frontal impacts); (b) lateral impacts

A.3.2 Barge impact forces

Similar to the AASHTO P_B expression, EN 1991 presents a method for computing barge impact forces that is based on findings from the reduced-scale gravity hammer experiments conducted by Meier-Dörnberg. The method presented in EN 1991 involves computing the energy of deformation $\left(E_{def}\right)$, which is the *total* (combined elastic and plastic) energy absorbed by the barge on impact with a bridge pier or waterline pile cap. Since the bridge element is

assumed to behave rigidly during an impact event, E_{def} is simply equal to the kinetic energy of the vessel prior to impact (CEN 2006):

$$E_{def} = \frac{1}{2} m \left(v_{rd} \right)^2 \tag{A.8}$$

where m is the combined effective mass of the impacting vessel and the hydrodynamic mass of the water volume in the immediate vicinity of the vessel prior to impact, and v_{rd} is the impact velocity. Additionally, for the case of a lateral impact at an angle α, with respect to the impacted face of the bridge element (Fig. A.4b), the energy of deformation may be computed as follows (CEN 2006):

$$E_{def} = \frac{1}{2} m \left(v_{rd} \right)^2 \left(1 - \cos(\alpha) \right) \tag{A.9}$$

In the event that the angle α is not known, EN 1991 recommends that a value of 20° be used in conjunction with Eqn. A.9.

While EN 1991 does provide some guidance on the calculation of hydrodynamic mass—it is taken as 10% of the vessel mass for frontal impacts, and 40% of the vessel mass for side impacts—no guidance is provided in regard to calculating the effective mass of an impacting barge tow. Instead, EN 1991 recommends using the values shown in Tables A.1 and A.2, or similar values that may be obtained from individual national annexes.

Table A.1 Recommended EN 1991 design values for vessels common to inland waterways (Source: CEN 2006)

CEMT[a] Class	Reference type of ship	Length ℓ (m)	Mass m (ton)[b]	Force F_{dx}[c] (kN)	Force F_{dy}[c] (kN)
I		30-50	200-400	2 000	1 000
II		50-60	400-650	3 000	1 500
III	"Gustav König"	60-80	650-1 000	4 000	2 000
IV	Class „Europe"	80-90	1 000-1 500	5 000	2 500
Va	Big ship	90-110	1 500-3 000	8 000	3 500
Vb	Tow + 2 barges	110-180	3 000-6 000	10 000	4 000
VIa	Tow + 2 barges	110-180	3 000-6 000	10 000	4 000
VIb	Tow + 4 barges	110-190	6 000-12 000	14 000	5 000
VIc	Tow + 6 barges	190-280	10 000-18 000	17 000	8 000
VII	Tow + 9 barges	300	14 000-27 000	20 000	10 000

[a] CEMT: European Conference of Ministers of Transport, classification proposed 19 June 1992, approved by the Council of European Union 29 October 1993.

[b] The mass m in tons (1 ton = 1 000 kg) includes the total mass of the vessel, including the ship structure, the cargo and the fuel. It is often referred to as the displacement tonnage.

[c] The forces F_{dx} and F_{dy} include the effect of hydrodynamic mass and are based on background calculations, using expected conditions for every waterway class.

Table A.2 Recommended EN 1991 design values for ocean-going vessel classifications (Source: CEN 2006)

Class of ship	Length ℓ= (m)	Mass m[a] (ton)	Force F_{dx}[b,c] (kN)	Force F_{dy}[b,c] (kN)
Small	50	3 000	30 000	15 000
Medium	100	10 000	80 000	40 000
Large	200	40 000	240 000	120 000
Very large	300	100 000	460 000	230 000

[a] The mass m in tons (1 ton = 1 000 kg) includes the total mass of the vessel, including the ship structure, the cargo and the fuel. It is often referred to as the displacement tonnage. It does not include the added hydraulic mass.

[b] The forces given correspond to a velocity of about 5,0 m/s. They include the effects of added hydraulic mass.

[c] Where relevant the effect of bulbs should be accounted for.

For broadside impacts, EN 1991 recommends that the total mass used in Eqn. A.8 be taken as one-third of the combined mass of the vessel and the surrounding water volume (hydrodynamic mass). In the absence of vessel-specific information, it is recommended that v_{rd} be taken as 3 m/s (~10 ft/s). Furthermore, in the event that the vessel is transiting through a harbor, EN 1991 states that the impact velocity may be lowered to 1.5 m/s (~5 ft/s).

Using the computed deformation energy, the dynamic design impact force may be computed as follows (CEN 2006):

If $E_{def} \leq 0.21$ MNm

$$F_{dyn} = 10.95\sqrt{E_{def}} \tag{A.10}$$

If $E_{def} > 0.21$ MNm

$$F_{dyn} = 5.0\sqrt{1 + 0.128 \cdot E_{def}} \tag{A.11}$$

where F_{dyn} is the dynamic design impact force (MN), and E_{def} is the energy of deformation of the impacting vessel (MNm). It is intended that Eqn. A.10 be employed for elastic impact events (i.e., events which cause no permanent deformation to the impacting vessel); otherwise, Eqn. A.11 should be used. In the event that, under certain conditions, a dynamic analysis cannot be conducted, EN 1991 recommends that the dynamic design forces computed from Eqns. A.10 and A.11 be amplified by an appropriate dynamic amplification factor—1.3 for frontal impacts and 1.7 for lateral impacts—to produce an equivalent static design force.

In the context of a dynamic analysis, EN 1991 recommends that all utilized force time-histories (examples shown in Fig. A.5) be formed *a priori*. Note that the shape of each individual time-history is dependent on whether or not the computed dynamic impact force exceeds a Eurocode-specified plastic limit (5 MN). Guidance regarding the computation of specific temporal values (e.g., t_r) is not provided in EN 1991.

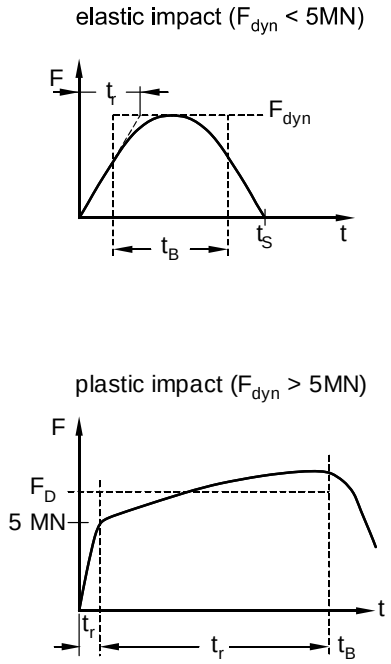

Figure A.5 Example force time-histories for use in dynamic analysis according to EN 1991 provisions (Reproduced from: CEN 2006)

APPENDIX B: PREVIOUS UF/FDOT BARGE-TO-BRIDGE IMPACT RESEARCH

B.1 Introduction

Researchers at the University of Florida, working in conjunction with the FDOT, have conducted numerous past investigations into barge-to-bridge impact behavior. All of these investigations were targeted toward addressing specific limitations of the current AASHTO (2014) bridge design provisions. This appendix summarizes the most pertinent findings from these past studies.

B.2 Development of Barge Bow Force-Deformation Relationships

In connected studies (Consolazio et al. 2009, Getter and Consolazio 2011) dynamic simulations of high-resolution barge models were conducted to quantify the force-deformation behavior of barge bows during barge-to-bridge impacts. One of the most important findings from these investigations was that barge impacts against rounded bridge piers generate smaller forces than corresponding impacts (i.e., at an equivalent energy level) against rectangular piers. This outcome relates to the manner in which 'stiffening-trusses' inside the bow of a barge are engaged and buckle during impact. Using numerical simulations, parametric studies were conducted that spanned a wide range of pier shapes (e.g., rounded, rectangular, etc.), pier sizes (e.g., diameters, widths), and vessel impact angles. Simulation results were subsequently used to develop a barge bow force-deformation model (Fig. B.1) that enables bridge designers to account for pier shape and size when computing impact loads—a feature not presently incorporated into widely used design standards (e.g., AASHTO 2014). Also of direct relevance to bridge design, the analytical studies indicated that jumbo hopper barges and tanker barges, both common to U.S. waterways, have comparable force-deformation relationships due to design similarities. Moreover, it was determined that for both barge types, a simplified elastic, perfectly-plastic (i.e., limited load) barge force-deformation relationship is adequate for use in bridge design.

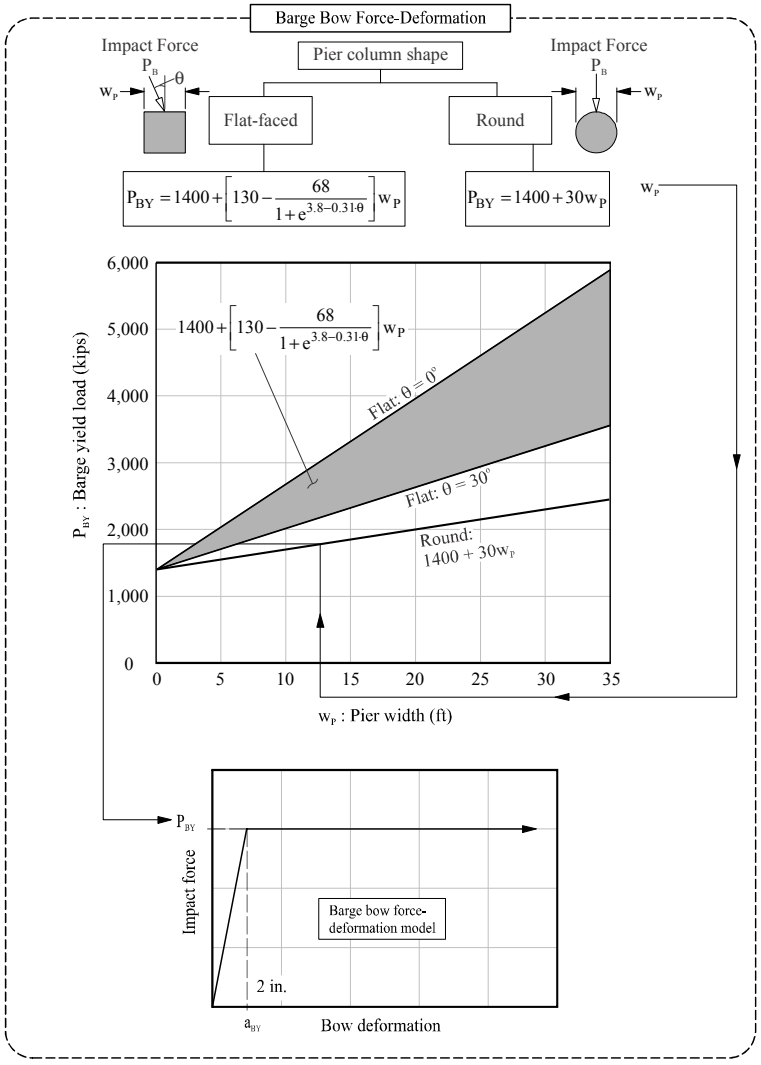

Figure B.1 UF/FDOT barge bow force-deformation model
(Source: Getter and Consolazio 2011)

B.3 Validation of Barge Bow Force Deformation Relationships

Given that the UF/FDOT barge bow force-deformation model was developed through numerical simulation, experimental validation of the analytical models was necessary. Validation was achieved through two investigations: (1) a full-scale experimental study which achieved moderate levels of barge bow deformation; and (2) a reduced-scale experimental study that achieved high levels of barge bow deformation.

Validation of the FE modeling and analysis techniques utilized in the previously mentioned studies (Consolazio et al. 2009, Consolazio and Getter 2011) was achieved up to moderate deformation levels (less than 20 in.) through a full-scale experimental investigation conducted by Consolazio et al. (2005). These experiments, conducted on a decommissioned causeway bridge near St. George Island, Florida, involved multiple impacts from a full-size barge striking concrete bridge piers. Tests were conducted on two different stand-alone piers (Fig. B.2a), as well as a pier with the superstructure in-place (Fig. B.2b). Impact forces and barge

bow deformations were quantified for each test. Due to environmental restrictions, structural collapse of the piers was not permissible; consequently, tests were limited to moderate impact energies. Data relating to the full-scale force-deformation behavior of barges during head-on barge-to-bridge collisions were obtained from this study and used to validate modeling and simulation techniques employed in complementary analytical studies (Consolazio et al. 2009, Getter and Consolazio 2011).

a) b)

Figure B.2 Full-scale barge impact experiments at St. George Island, Florida: a) Stand-alone pier impact (superstructure removed), and b) Intact bridge impact
(Source: Consolazio et al. 2005)

In addition, the experimental measurements revealed that inertial effects in the bridge—particularly from the superstructure—increase pier column member demands (i.e. shears, moments) relative to what the AASHTO-prescribed static analysis procedures would predict. Using dynamic finite element analysis models to simulate the experimental impact conditions, Consolazio et al. (2005) demonstrated that immediately after impact, superstructure mass provides inertial resistance, which can cause significant dynamic amplification of column forces. Additionally, once the superstructure is accelerated to its maximum velocity and begins decelerating, the superstructure mass may also force the pier to sway beyond the pier-top displacement predicted by AASHTO static analysis, once again producing dynamic amplification of column forces. Consequently, while the utilization of AASHTO procedures would result in similar barge impact forces applied to a structure, internal structural demands resulting from a static structural analysis would underpredict actual demands experienced during the dynamic response of the structure.

Complementing the full-scale test series at St. George Island, Consolazio et al. (2014) conducted two series of reduced-scale (40%) barge bow impact experiments using the FDOT pendulum impact facility (Fig. B.3). Located at the FDOT Marcus H. Ansley Structures Research Center in Tallahassee, Florida, the pendulum impact facility is comprised of a 34-ft wide, 20-ft long, 3-ft thick, concrete foundation (heavily reinforced internally with structural shapes) and three 50-ft tall structural steel towers. One of the towers serves to pull an impactor (i.e., a nearly-rigid impact block) up to the desired drop height while the remaining two towers support the impactor through the downward swinging motion that occurs during an impact test.

Figure B.3 FDOT pendulum impact facility in Tallahassee, Florida
(Source: Kantrales et al. 2015)

To experimentally confirm that pier shape influences the magnitude of force imparted to a bridge during impact, two separate series of pendulum impact tests were conducted: one with a round nose impactor and one with a flat-faced impactor. The target barge deformation level to be achieved during each test series was 4 ft, which corresponds to approximately 10 ft of equivalent deformation at full-scale, a reasonably conservative upper level of crush depth for barge collisions with bridge structures.

Following completion of the experimental portion of the investigation, a corresponding analytical study was carried out, wherein each impact experiment in both the round and flat test series was replicated analytically using high-fidelity finite element modeling and analysis techniques. Importantly, the same modeling and analysis techniques employed previously at full-scale to quantify bridge design loads (Consolazio et al. 2009, Getter and Consolazio 2011) were used in this study to model the reduced-scale pendulum impact experimental test conditions. Barge components were modeled at reduced (40%) geometric size, and both dynamic buckling and strain rate effects were directly taken into account, as appropriate at reduced-scale. Validation of the modeling and simulation techniques was carried out by comparing results from the impact simulations to corresponding experimental test data (Figs. B.4 and B.5), with good agreement observed.

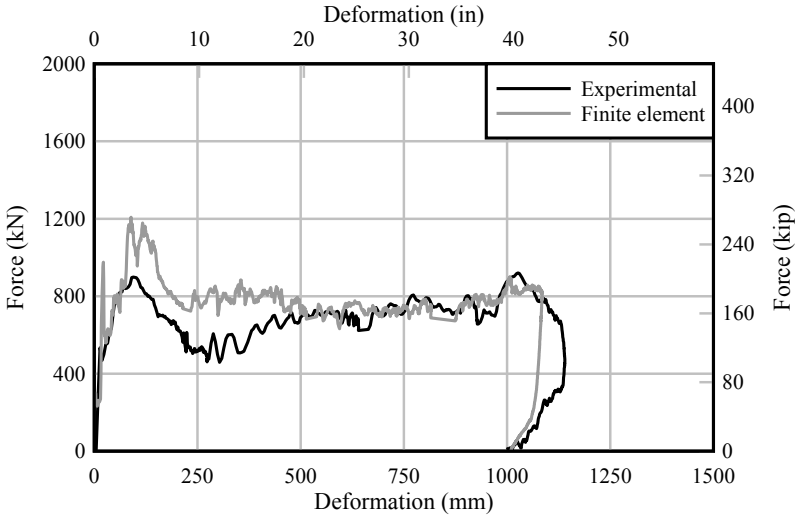

Figure B.4 Comparison of analytical and experimental force-deformation relationships for round impactor test series (Source: Kantrales et al. 2015)

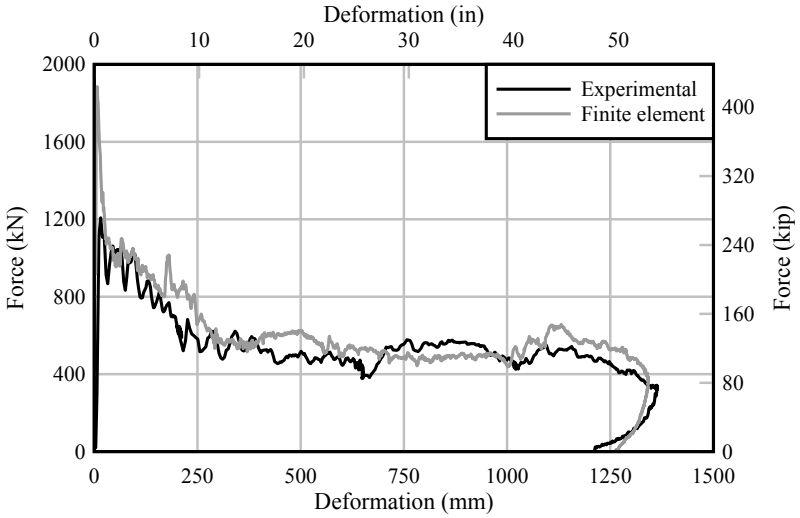

Figure B.5 Comparison of analytical and experimental force-deformation relationships for flat impactor test series (Source: Kantrales et al. 2015)

B.4 Coupled Vessel Impact Analysis (CVIA)

During the full-scale barge-to-bridge impact experiments conducted by Consolazio et al. (2005), it was discovered that the dynamic response of the bridge during impact can amplify structural demands. This behavior is related to either inertial restraint afforded by the mass of the bridge superstructure, or a momentum-driven sway response mode (Davidson et al. 2010) initiated by pier motion. Due to these mechanisms, it was determined that only a dynamic analysis which treats the barge and bridge as a coupled system is appropriate for predicting

barge-to-bridge impact behavior. To address this issue, Consolazio and Cowan (2005) developed the coupled vessel impact analysis (CVIA) method (Fig. B.6).

CVIA considers a barge-to-bridge impact event as a coupled system, where the impacting barge is treated as a SDOF mass, and the bridge is modeled as a MDOF system. The crushing behavior of the barge bow is represented by a nonlinear spring, which couples the barge and bridge models, while soil behavior is accounted for through a series of nonlinear springs defining soil-foundation interactions. To conduct a CVIA analysis, the SDOF barge mass is given an initial velocity, and the dynamic interactions between the barge and the bridge are calculated and updated at each time step.

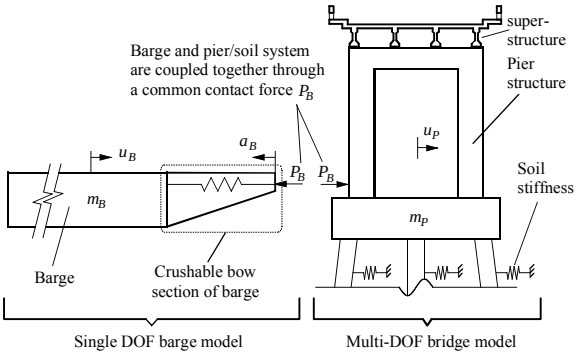

Figure B.6 Coupled vessel impact analysis (CVIA) (Source: Consolazio and Cowan 2005)

Since modeling an entire bridge structure as a MDOF system can be computationally demanding for a common workstation computer, Consolazio and Davidson (2008), developed a simplified approach whereby the bridge is modeled as one pier and two spans. In this one-pier-two-spans (OPTS) model, the remaining portions of the bridge are represented as single spring and mass systems placed at either end of the modeled spans.

Results from CVIA analyses have been validating against experimental data obtained from full-scale barge to bridge impacts (Consolazio and Cowan 2005). In addition, the combined CVIA-OPTS approach for considering barge-to-bridge impact events has been incorporated into FB-Multipier (BSI 2010), which is a comprehensive finite element analysis program commonly employed for bridge design.

B.5 Revised Probability of Collapse (*PC*) Expression

Since AASHTO (2014) was initially developed prior to a period where barge-to-bridge collision data were widely available, the current AASHTO probability of collapse (PC) expression was developed from historical ship-to-ship collision data. Due to notable differences in the vessels and structures involved in a barge-to-bridge collision versus a ship-to-ship collision, UF, working with the FDOT, has developed a revised PC expression that is specifically tailored for the analysis of barge-to-bridge impact events (Consolazio et al. 2010, Davidson et al. 2013). The UF/FDOT PC expression was developed through sophisticated statistical analysis of thousands of CVIA analysis conducted on ten different bridge structures. In this study, sources of variability in both the impacting barge and the impacted structure were considered. For each analysis, a PC estimate and a mean demand-to-capacity (*D/C*) ratio were

calculated, and curve fitting techniques were employed to produce a general expression capable of calculating PC based on a provided D/C ratio (Fig. B.1).

$$PC = 2.33\times10^{-6}\cdot e^{13\cdot D/C} \le 1.0 \tag{B.1}$$

Curve fitting techniques utilized in this investigation used 95% confidence upper bounds (Fig. B.7) in order to ensure that the revised expression will produce conservative estimates of the probability of collapse.

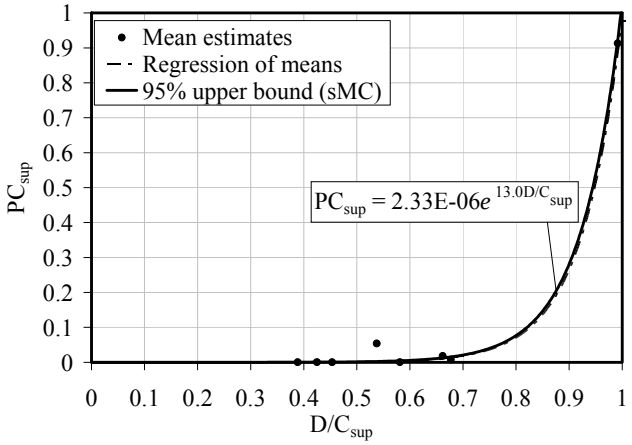

Figure B.7 Revised probability of collapse (*PC*) expression (Source: Consolazio et al. 2010)

APPENDIX C: SUMMARY OF BARGE ACCIDENT DATA COLLECTED

This appendix contains a listing of all barge-to-bridge impact events for which USCG accident reports were requested (Table C.1). For each event, USCG activity IDs are provided, along with the date and location of the barge impact.

Table C.1 Barge accident data summary

MISLE activity ID	Approximate date of event (obtained from MISLE records)	USCG district	Name of impacted Florida bridge
2946400	5/29/2007	7	Mantanzas Pass Bridge
1775418	2/9/2003	7	Sanibel Causeway Bridge
2039362	4/9/2004	7	Sanibel Causeway Bridge
2153420	7/30/2004	7	Sanibel Causeway Bridge
2241315	11/13/2004	7	Sanibel Causeway Bridge
2307385	3/8/2005	7	Sanibel Causeway Bridge
2533243	10/1/2005	7	Sanibel Causeway Bridge
2539078	10/26/2005	7	Sanibel Causeway Bridge
2578208	8/19/2005	7	Sanibel Causeway Bridge
2598508	3/3/2006	7	Sanibel Causeway Bridge
2794928	8/1/2006	7	Sanibel Causeway Bridge
2546182	12/5/2005	7	Venetian Causeway
2030257	3/24/2004	7	Atlantic Blvd. Bridge
4766432	12/4/2013	7	Atlantic Blvd. Bridge
2225557	10/21/2004	7	Sisters Creek Bridge
2290720	2/10/2005	7	Sisters Creek Bridge
2989716	6/2/2007	7	CSX Railroad Bridge
2408766	6/29/2005	7	Longboat Pass Bridge
2911460	4/19/2007	7	Longboat Pass Bridge
3318470	9/5/2008	7	Longboat Pass Bridge
3659489	12/31/2009	7	Longboat Pass Bridge
2287878	7/6/2004	7	Dick Misener Bridge
2712795	7/13/2006	7	Dick Misener Bridge
2965566	6/17/2007	7	John’s Pass Bridge
3325240	9/14/2008	7	John’s Pass Bridge
3363132	11/14/2008	7	John’s Pass Bridge
3002430	7/21/2007	7	Memorial Causeway
14692	7/5/1996	8	Dupont Bridge
181578	7/2/1996	8	Dupont Bridge
1842150	5/9/2003	8	Dupont Bridge
1900158	9/7/2003	8	Dupont Bridge
3710171	4/4/2010	8	Dupont Bridge
2408780	6/26/2005	8	Brooks Bridge

Table C.1 (continued) Barge accident data summary

2973391	6/22/2007	8	Brooks Bridge
104061	3/4/2000	8	Navarre Beach Bridge
2433189	7/3/2005	8	Navarre Beach Bridge
2547589	12/3/2005	8	Navarre Beach Bridge
10924	1/8/2000	8	Bob Sikes Bridge
29659	11/27/2001	8	Bob Sikes Bridge
115324	10/10/1999	8	Bob Sikes Bridge
2074374	5/16/2004	8	Bob Sikes Bridge
2294661	2/7/2005	8	Bob Sikes Bridge
2408097	5/5/2005	8	Bob Sikes Bridge
2604457	1/21/2006	8	Bob Sikes Bridge
3641673	11/28/2009	8	Bob Sikes Bridge
3710480	4/3/2010	8	Bob Sikes Bridge
26888	9/16/1998	8	Gulf Beach Bridge
2306623	2/23/2005	8	Gulf Beach Bridge
2591278	1/30/2006	8	Pensacola Bay Bridge
146084	10/26/2000	8	HW-90 Bridge over Escambia River
2026361	1/21/2004	8	HW-90 Bridge over Escambia River
3673300	1/27/2010	8	HW-90 Bridge over Escambia River

APPENDIX D: SUMMARY OF BARGE TRAFFIC DATA COLLECTED

This appendix contains a listing of all waterways and mile marker locations for which USACE barge traffic data were obtained (Table D.1). For each location, the years for which data were obtained and the type of information sought is provided.

Table D.1 Barge traffic data summary

Waterway name	Mile marker	Years	Type of data
Gulf Intracoastal Waterway, Pensacola Bay, FL to Mobile Bay, AL	172	2002, 2004, 2006, 2008, 2010, 2012, 2013	Upstream and downstream barge traffic
Gulf Intracoastal Waterway, Panama City to Pensacola Bay, FL	189	2002, 2004, 2006, 2008, 2010, 2012, 2013	Upstream and downstream barge traffic
Gulf Intracoastal Waterway, Panama City to Pensacola Bay, FL	284	2002, 2004, 2006, 2008, 2010, 2012, 2013	Upstream and downstream barge traffic
Escambia and Conecuh Rivers, FL and AL; Escambia Bay, FL	5	2002, 2004, 2006, 2008, 2010, 2012, 2013	Upstream and downstream barge traffic
Gulf Intracoastal Waterway, Apalachee Bay to Panama City, FL	295	2002, 2004, 2006, 2008, 2010, 2012, 2013	Upstream and downstream barge traffic
Atlantic Intracoastal Waterway between Norfolk, VA, and the St. Johns River, FL (Jacksonville District)	738	2002, 2004, 2006, 2008, 2010, 2012, 2013	Upstream and downstream barge traffic
Intracoastal Waterway, Jacksonville to Miami, FL	745	2002, 2004, 2006, 2008, 2010, 2012, 2013	Upstream and downstream barge traffic
St. John's River, FL (Jacksonville to Lake Harney)	1	2002, 2004, 2006, 2008, 2010, 2012, 2013	Upstream and downstream barge traffic
Tampa Channel Access, FL	8	2002, 2004, 2006, 2008, 2010, 2012, 2013	Upstream and downstream barge traffic

APPENDIX E: VESSEL TRAFFIC CURVE FITS

This appendix contains curve fits that were applied to barge and tug traffic data. These include fits used to replace outlying barge-to-tug ratios (Figs. E.1, E.2, E.3, and E.4) and fits used to make predictions of barge flotilla traffic for years where data were not available (due scope-of-request constraints) from the USACE (Figs. E.5, E.6, E.7, E.8, E.9, E.10, and E.11).

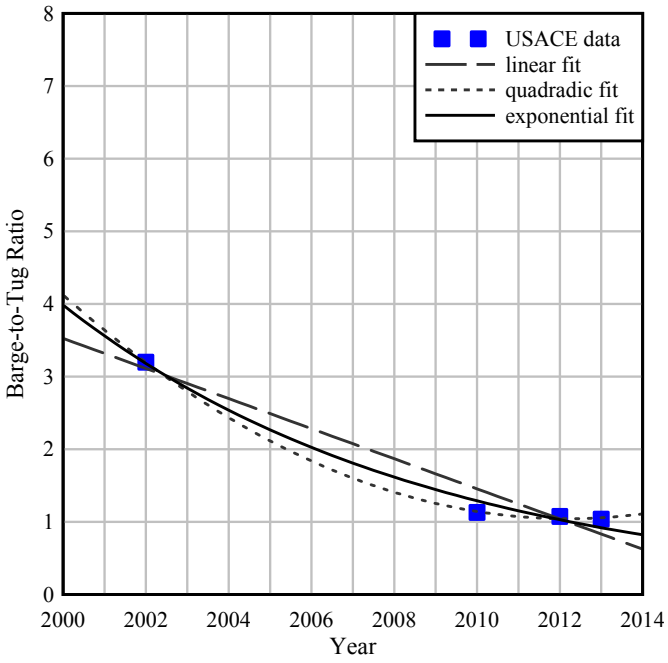

(a)

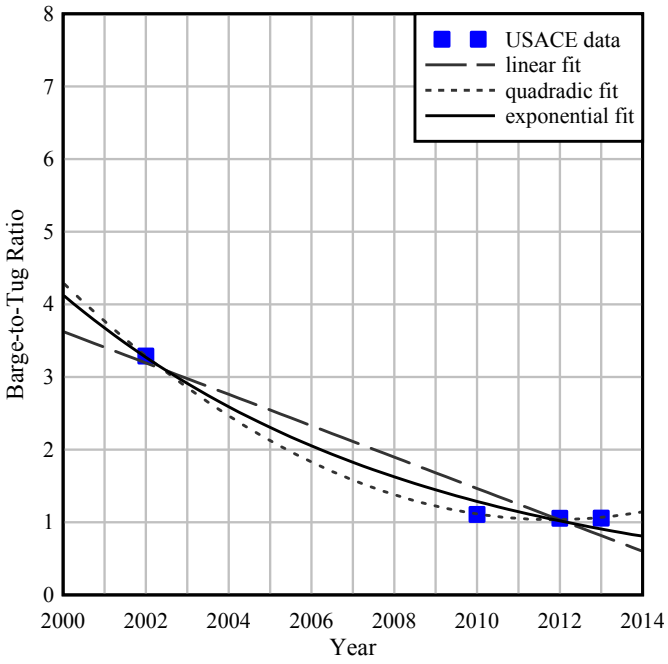

(b)

Figure E.1 Curve fits used to replace outlying barge-to-tug ratios for Highway-90 Bridge over Escambia River and Pensacola Bay Bridge: (a) inbound direction; (b) outbound direction

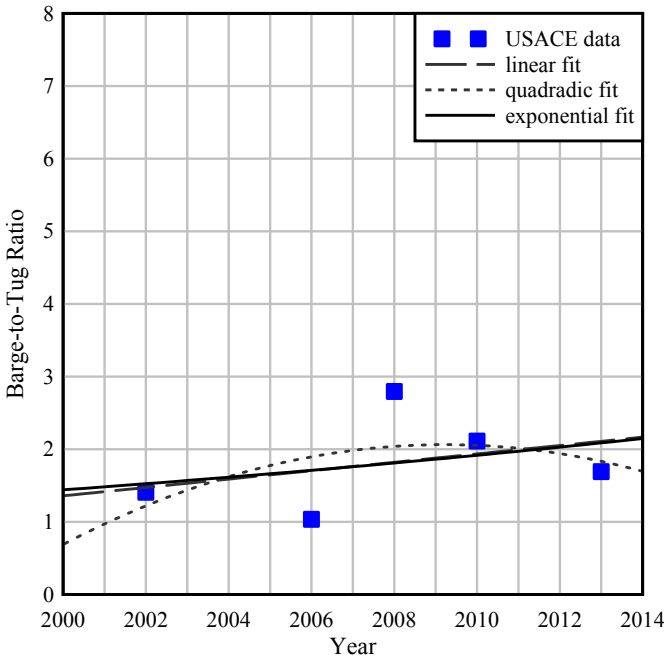

(a)

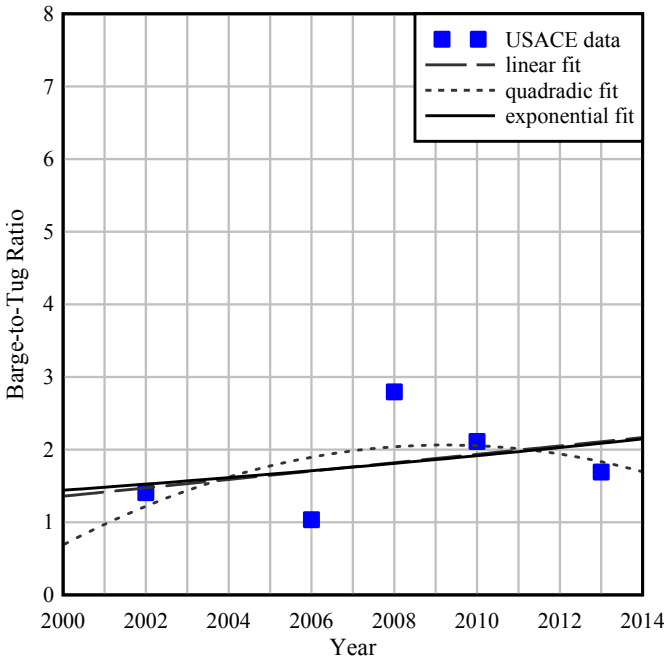

(b)

Figure E.2 Curve fits used to replace outlying barge-to-tug ratios for Dupont Bridge: (a) inbound direction; (b) outbound direction

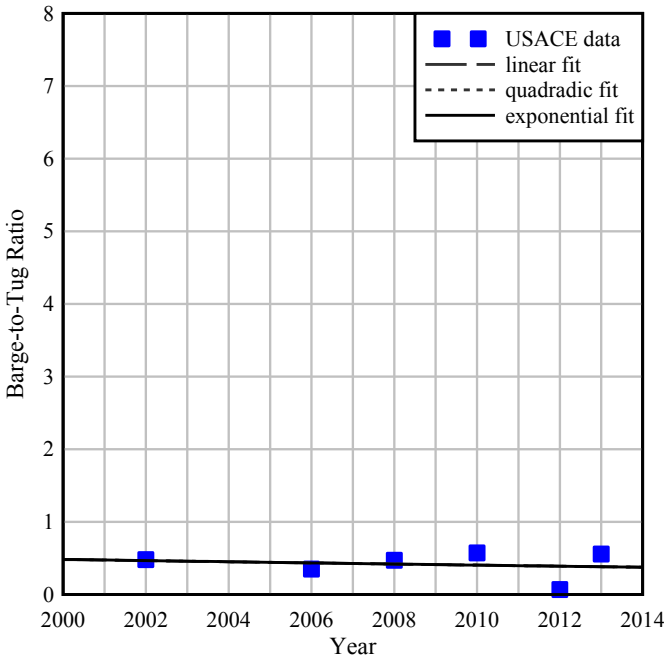

(a)

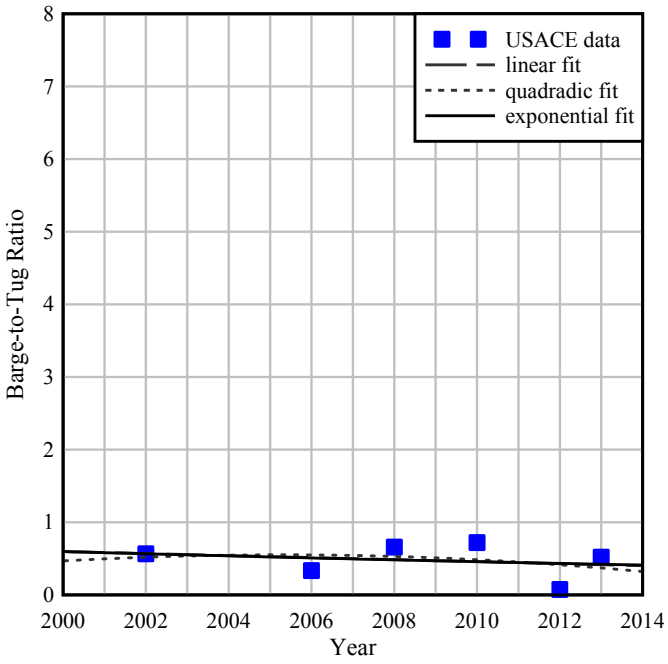

(b)

Figure E.3 Curve fits used to replace outlying barge-to-tug ratios for Atlantic Blvd. Bridge: (a) inbound direction; (b) outbound direction

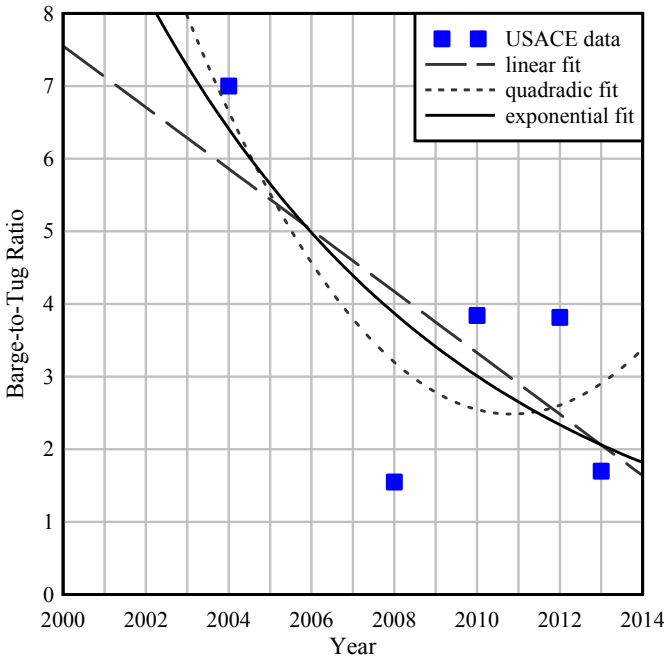

(a)

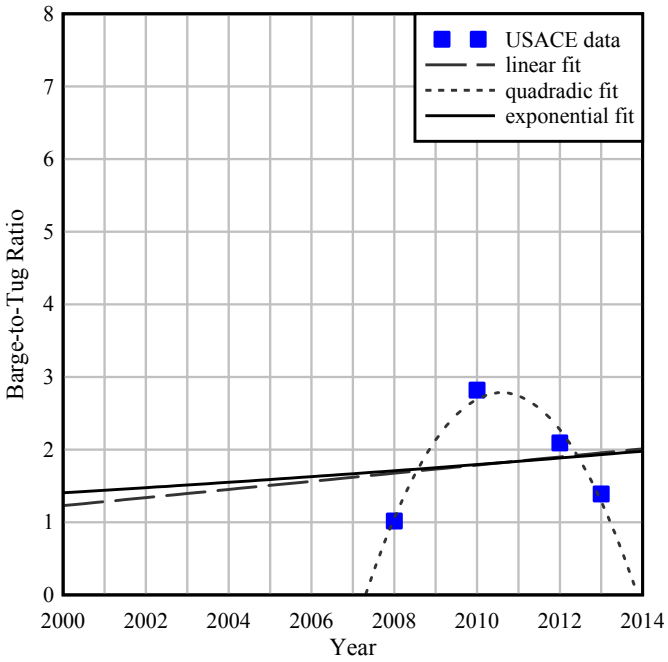

(b)

Figure E.4 Curve fits used to replace outlying barge-to-tug ratios for Gandy Bridge: (a) inbound direction; (b) outbound direction

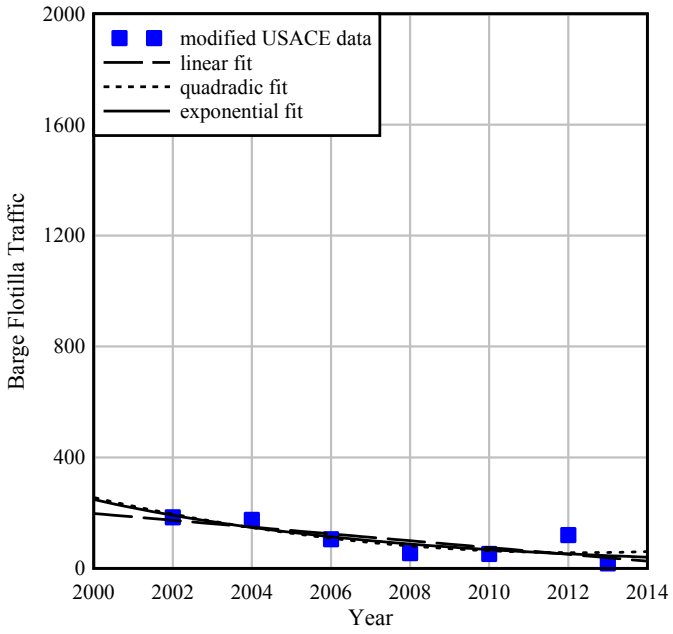

(a)

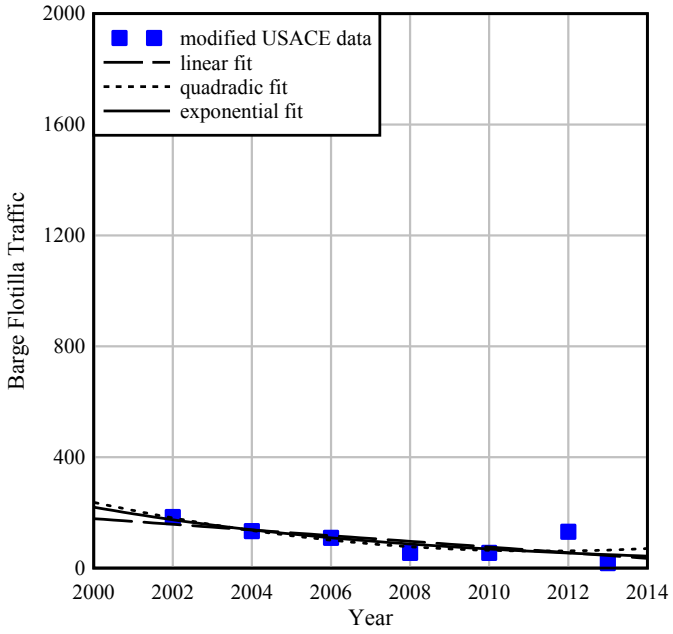

(b)

Figure E.5 Curve fits used to produce estimates of barge flotilla traffic for Acosta Bridge: (a) inbound direction; (b) outbound direction

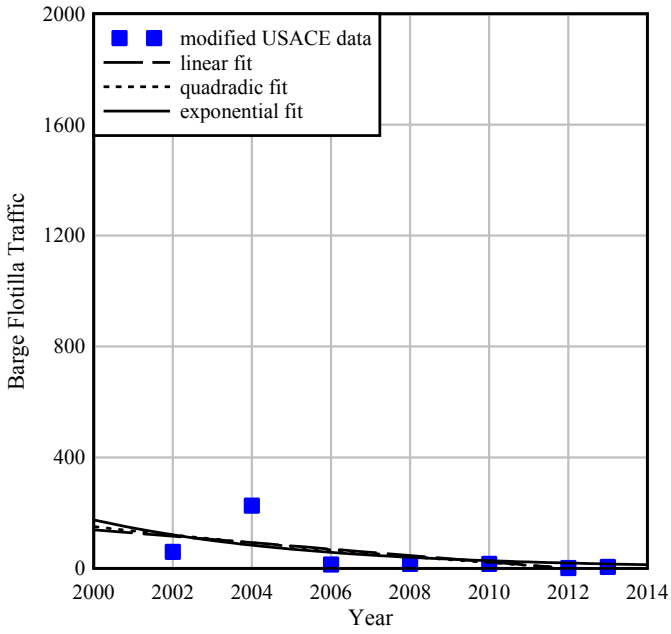

(a)

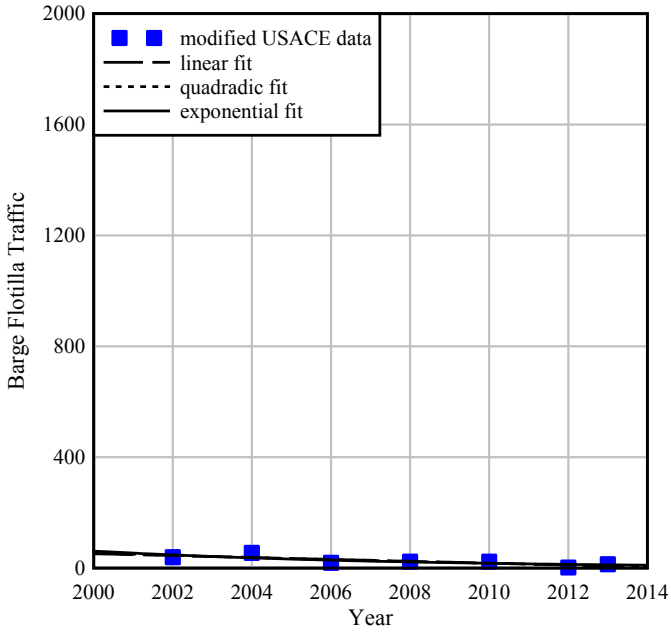

(b)

Figure E.6 Curve fits used to produce estimates of barge flotilla traffic for Atlantic Blvd. Bridge: (a) inbound direction; (b) outbound direction

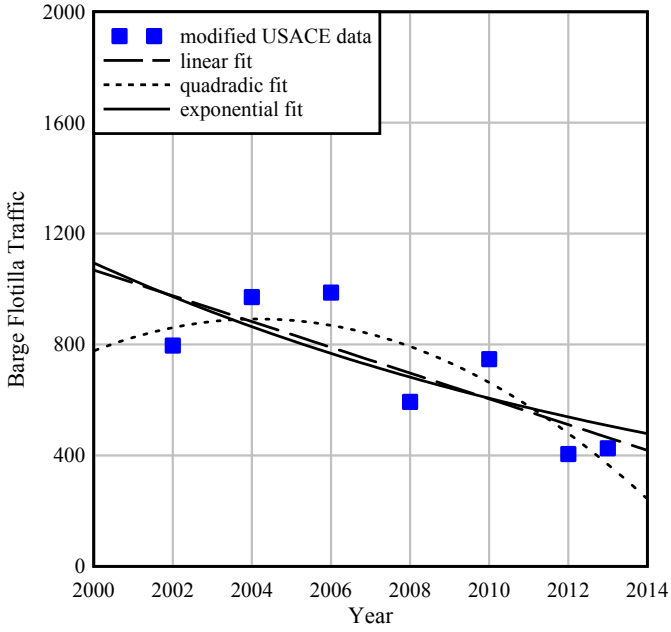

(a)

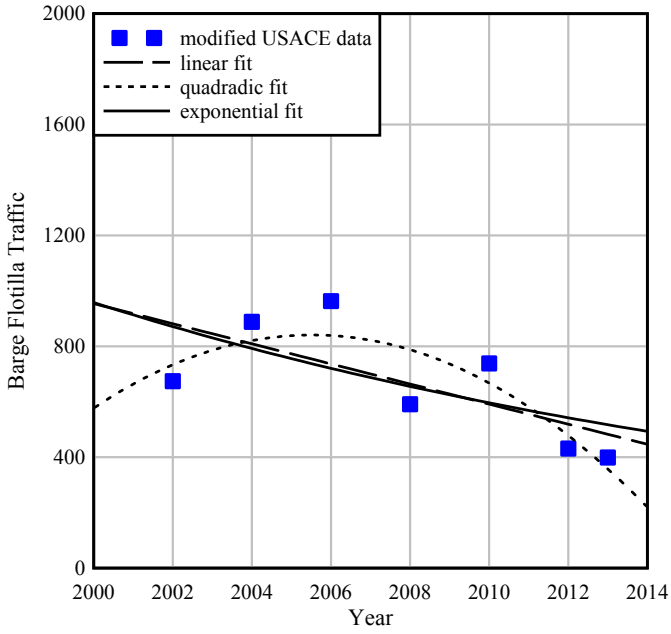

(b)

Figure E.7 Curve fits used to produce estimates of barge flotilla traffic for Bob Sikes Bridge, Brooks Bridge, and Navarre Beach Bridge: (a) inbound direction; (b) outbound direction

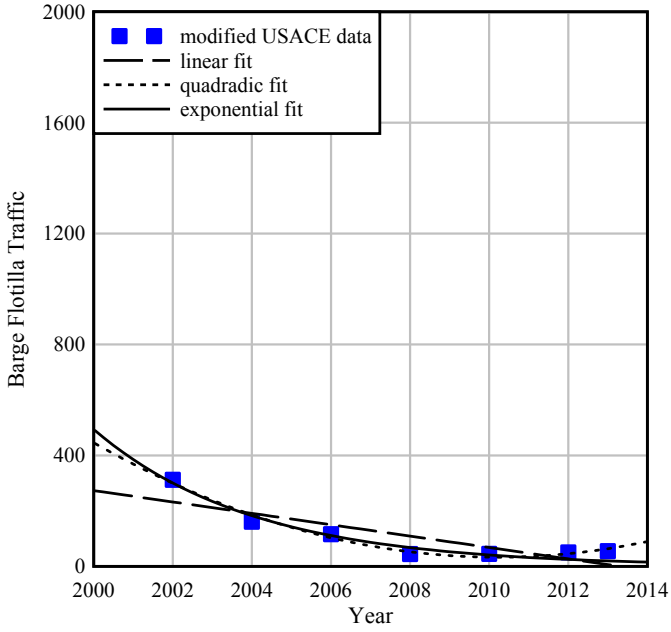

(a)

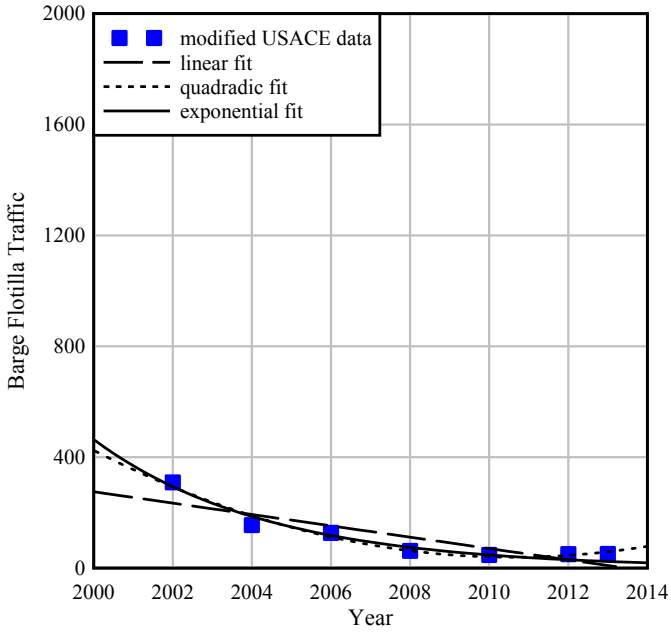

(b)

Figure E.8 Curve fits used to produce estimates of barge flotilla traffic for Dupont Bridge: (a) inbound direction; (b) outbound direction

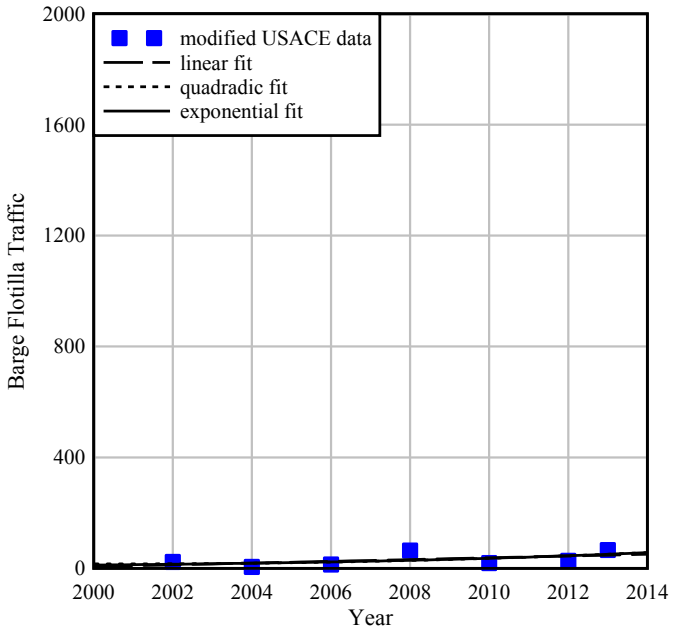

(a)

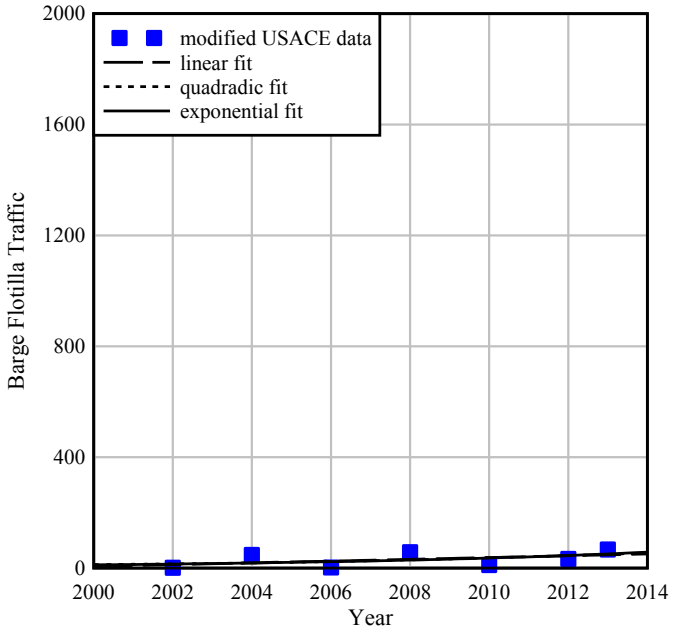

(b)

Figure E.9 Curve fits used to produce estimates of barge flotilla traffic for Gandy Bridge: (a) inbound direction; (b) outbound direction

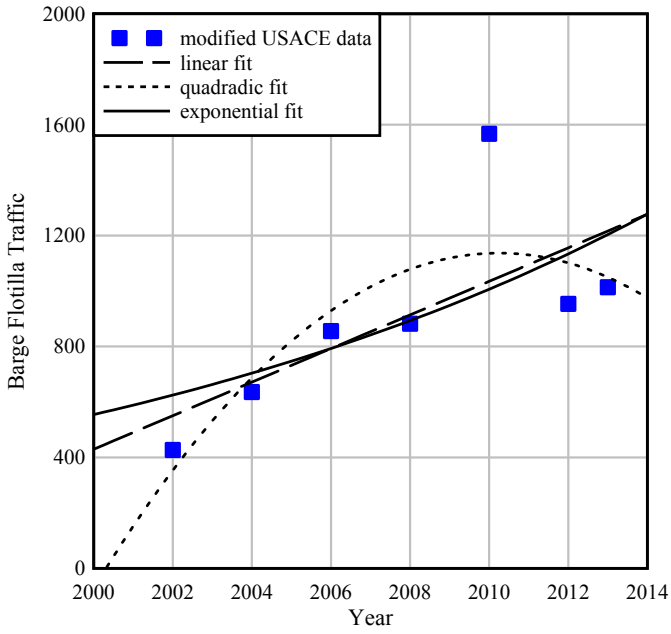

(a)

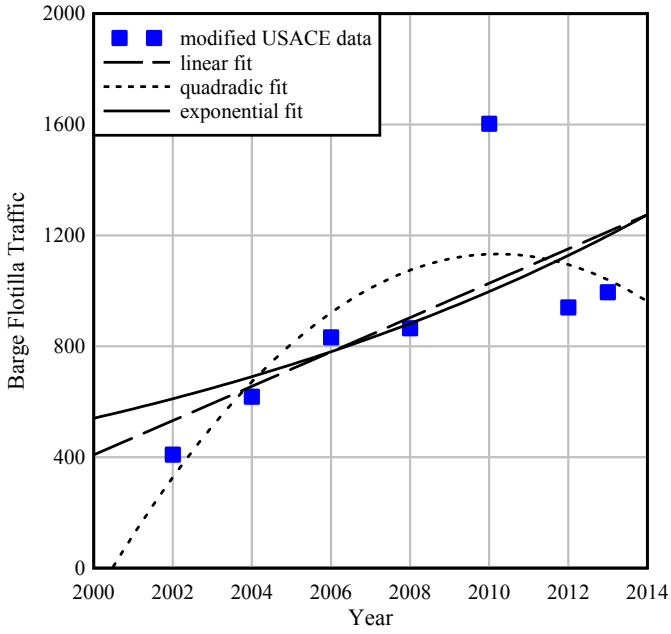

(b)

Figure E.10 Curve fits used to produce estimates of barge flotilla traffic for Highway-90 Bridge over Escambia River and Pensacola Bay Bridge: (a) inbound direction; (b) outbound direction

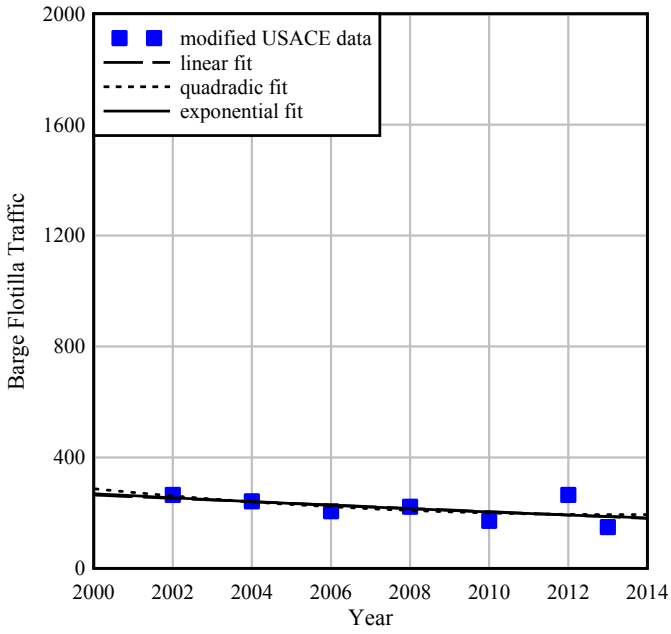

(a)

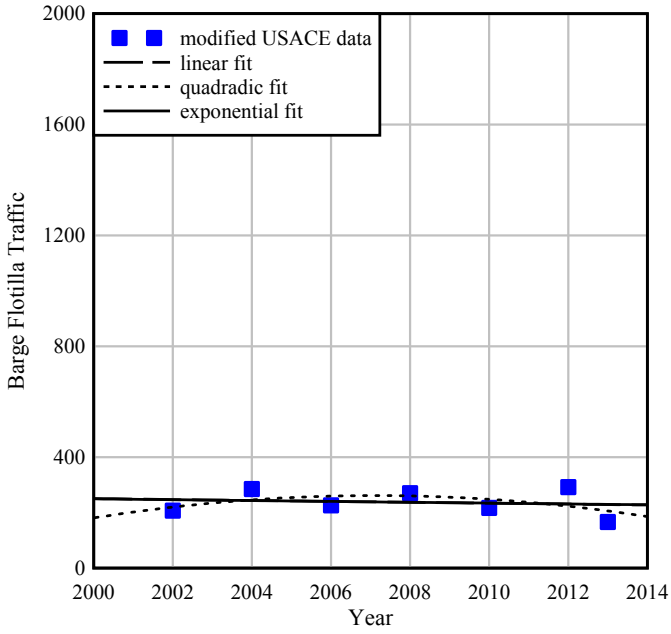

(b)

Figure E.11 Curve fits used to produce estimates of barge flotilla traffic for Sister's Creek Bridge: (a) inbound direction; (b) outbound direction

APPENDIX F: BARGE FLOTILLA DIMENSIONS

This appendix describes the four representative barge flotilla sizes that were used to evaluate *PG* and *PF* at individual bridge locations. Flotilla dimensions were selected to approximate large and small barge flotillas that could reasonably be expected to pass through a given bridge site. A single 'design' tug length was determined for each location through a weighted averaging of tug lengths using the number of observed passages as weighting factors. Note that certain bridges shared waterways (e.g., Highway-90 Bridge over Escambia River and Pensacola Bay Bridge); as a consequence, representative flotilla sizes were the same for these locations.

Table F.1 Flotilla sizes for Acosta Bridge

Classification	Length (ft)	Width (ft)	Description
FG-A	647	35	Three jumbo hopper barge (one column) and a 62-ft tug
FG-B	257	35	One jumbo hopper barge and a 62-ft tug
FG-C	452	70	Four jumbo hopper barges (two columns, two rows) and a 62-ft tug
FG-D	257	70	Two jumbo hopper barges (one row) and a 62-ft tug

Table F.2 Flotilla sizes for Atlantic Blvd. Bridge

Classification	Length (ft)	Width (ft)	Description
FG-A	656	35	Three jumbo hopper barge (single column) and a 71-ft tug
FG-B	191	30	One small hopper barge and a 71-ft tug
FG-C	611	78	Ocean-going barge and a 71-ft tug
FG-D	206	80	Two small tank barges (one row) and a 71-ft tug

Table F.3 Flotilla sizes for Bob Sikes Bridge, Brooks Bridge, and Navarre Beach Bridge

Classification	Length (ft)	Width (ft)	Description
FG-A	660	35	Three jumbo hopper barge (one column) and a 75-ft tug
FG-B	270	35	One jumbo hopper barge and a 75-ft tug
FG-C	655	106	Four oversize tank barges (two columns, two rows) and a 75-ft tug
FG-D	270	105	Three jumbo hopper barges (one row) and a 75-ft tug

Table F.4 Flotilla sizes for Gandy Bridge

Classification	Length (ft)	Width (ft)	Description
FG-A	688	35	Three jumbo hopper barges (one column) and a 103-ft tug
FG-B	223	30	One small hopper barge and a 103-ft tug
FG-C	683	53	Two oversize tank barges (one column) and a 103-ft tug
FG-D	393	53	One oversize tank barges (one row) and a 103-ft tug

Table F.5 Flotilla sizes for Highway-90 Bridge over Escambia River and Pensacola Bay Bridge

Classification	Length (ft)	Width (ft)	Description
FG-A	653	35	Three jumbo hopper barge (one column) and a 68-ft tug
FG-B	263	35	One jumbo hopper barge and a 68-ft tug
FG-C	648	106	Four oversize tank barges (two columns, two rows) and a 68-ft tug
FG-D	263	105	Three jumbo hopper barges (one row) and a 68-ft tug

Table F.6 Flotilla sizes for Sister's Creek Bridge

Classification	Length (ft)	Width (ft)	Description
FG-A	656	35	Three jumbo hopper barge (single column) and a 71-ft tug
FG-B	191	30	One small hopper barge and a 71-ft tug
FG-C	562	76	Ocean-going barge and a 71-ft tug
FG-D	206	80	Two small tank barges (one row) and a 71-ft tug

APPENDIX G: PROPOSED BRIDGE DESIGN SPECIFICATIONS FOR BARGE COLLISION EVENTS

G.1 Introduction

This document is intended to be used as a supplement to sections of the American Association of State Highway and Transportation Officials (AASHTO) Bridge Design Specifications (AASHTO 2014) pertaining to the analysis and design of bridge structures for barge impact loading. Sections of AASHTO (2014) that are superseded by this document are indicated where applicable.

G.2 Barge Collision Demands

The methodology for evaluating structural demands associated with barge-to-bridge collision events is described in this section. These procedures are intended to replace the equivalent static approach presented in Section 3.14.11 of AASHTO (2014).

In general, design barge impact forces and moments shall be determined through an appropriate analysis procedure capable of accounting for dynamic interactions between the impacting barge and the impacted structure. Such interactions typically result in dynamic amplification of imparted structural demands. Consequently, in order to properly represent this behavior, the barge and bridge may be modeled as independent masses joined by a spring for purposes of dynamic load computation. The stiffness of the spring, modeled as a bi-linear (elastic, perfectly-plastic) force-deformation relationship (Fig. G.2.1), shall represent the static resistance of a barge bow. The peak force (P_{BY}) of the barge force-deformation relationship shall be dependent on the shape of the impacted bridge pier, and, if a flat-faced pier is considered, the incident angle between the pier and the bow of the barge (Fig. G.2.2):

For flat-faced piers,

$$P_{BY} = 1400 + \left[130 - \frac{68}{1 + e^{3.8 - 0.31\theta}} \right] w_P \qquad \text{(G.2.1)}$$

For round piers,

$$P_{BY} = 1400 + 30 w_P \qquad \text{(G.2.2)}$$

where:

P_{BY} = barge yield load (kip);

θ = incident angle (deg, Fig. G.2.2); and

w_P = bridge pier width (ft).

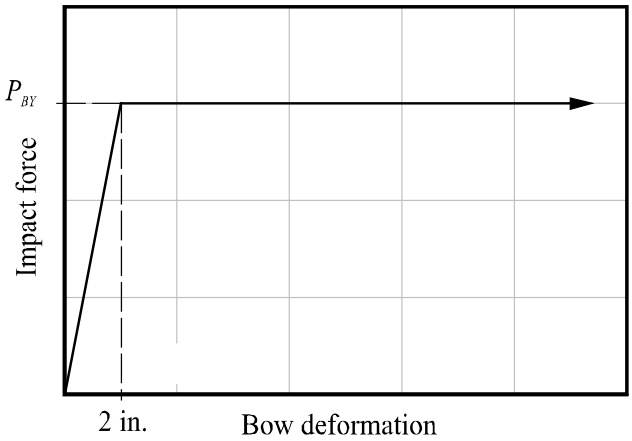

Figure G.2.1 Barge bow force-deformation relationship
(Adapted from: Getter and Consolazio 2011)

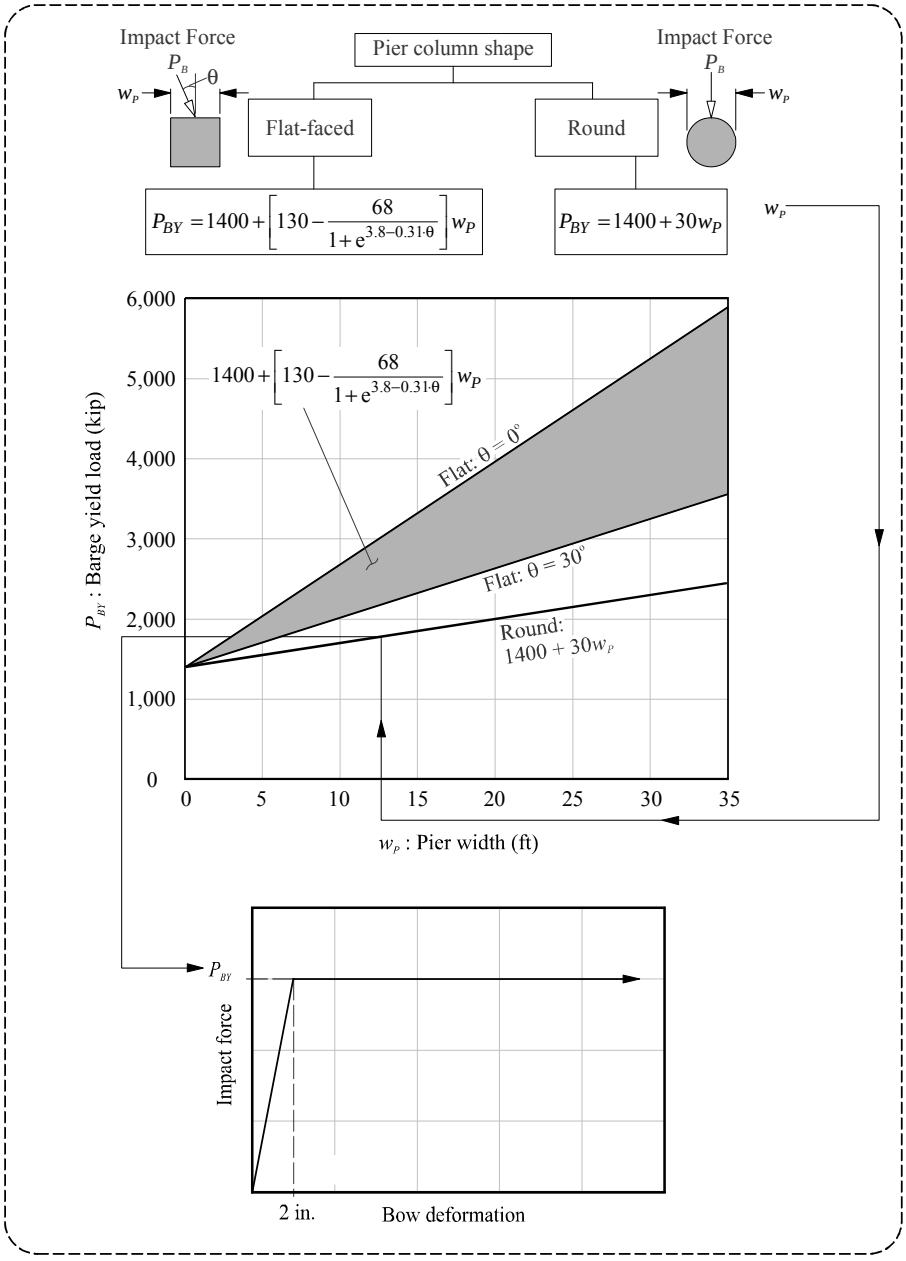

Figure G.2.2 Flowchart for computation of P_{BY} (Adapted from: Getter and Consolazio 2011)

G.3 Probability of Collapse (*PC*)

The provisions discussed in this section relate to the computation of a probability of bridge collapse (*PC*) term. These procedures are intended to be used in conjunction with the AASHTO methodology (see Section 3.14.5 of AASHTO [2014]) for computing the annual frequency of collapse (*AF*) for a new or existing bridge structure:

$$AF = (N)(PA)(PG)(PC)(PF) \tag{G.3.1}$$

where:

AF = annual frequency of bridge element collapse due to vessel collision;

N = annual number of vessels classified by type, size, and loading condition that can strike the bridge element;

PA = probability of vessel aberrancy;

PG = geometric probability of collision between an aberrant vessel and a bridge pier or span;

PC = probability of bridge collapse due to collision with an aberrant vessel; and

PF = adjustment factor to account for protection of the piers from vessel collision due to the presence of upstream or downstream land masses, or other structures, that block the vessel.

Discussions for the determination of *N*, *PG*, and *PF* may be found in relevant sections of AASHTO (2014). *PA* is determined through the provisions discussed in Section G.4.

Given that a vessel-structure impact event has occurred, the probability of bridge collapse (*PC*) shall be calculated using Eq. G.3.2, which is intended to replace Eqs. 3.14.5.4-1, 3.14.5.4-2, and 3.14.5.4-3 in the AASHTO (2014) provisions:

$$PC = 2.33\times10^{-6}\cdot e^{13\cdot D/C} \le 1.0 \tag{G.3.2}$$

where:

PC = probability of collapse

D/C = demand-capacity ratio

The magnitude of *D/C* indicates the severity of a loading condition relative to a state of structural collapse (*D/C* = 1.0). Since collapse can only occur once the reserve capacity of all affected members is exhausted, *D/C* should be computed based on the proximity of each bridge pier component to a state of collapse. Furthermore, because collapse may occur in the foundation

system as well as the bridge superstructure, Eq. G.3.3 may be used to evaluate *D/C* for both pier column and foundation components; the larger of these two *D/C* ratios may then be employed in Eq. G.3.2.

$$D/C = \frac{1}{m \cdot n} \sum_{i=1}^{m} \sum_{j=1}^{n} (D/C)_{ij} \tag{G.3.3}$$

where:

D/C = demand-capacity ratio

m = number of members associated with a possible collapse mechanism

n = number of local mechanisms (e.g. plastic hinges) per member necessary to form a potential global collapse mechanism

$(D/C)_{ij}$ = j'th largest element demand-capacity ratio associated with member i.

G.4 Probability of Aberrancy (PA) for Barges

The probability of vessel aberrancy (*PA)* is determined through the evaluation of several component expressions outlined in AASHTO (2014):

$$PA = BR(R_B)(R_C)(R_{XC})(R_D) \tag{G.4.4}$$

where:

PA = probability of aberrancy;

BR = base aberrancy rate;

R_B = correction factor for bridge location;

R_C = correction factor for currents acting parallel to vessel transit path;

R_{XC} = correction factor for crosscurrents acting perpendicular to vessel transit path; and

R_D = correction factor for vessel traffic density

Through a study of several Florida bridge locations, the following estimate of *BR*, *specific to barges*, was developed:

$$BR = 5.4 \times 10^{-5} \tag{G.4.5}$$

R_B shall be calculated by first examining the geometry of the waterway in the vicinity of the

bridge structure to determine whether or not the bridge is located within, or immediately adjacent to, either a turn or a bend in the waterway. If the bridge is located immediately adjacent to either a turn or a bend, then it shall be classified as being in a 'transition region' of the waterway (Fig. G.4.1). The angle of the turn or bend (θ , degrees) is calculated (as shown in Fig. G.4.1) and used in one of the following equations (AASHTO 2014):

For a bridge located in a straight region,

$$R_B = 1.0 \tag{G.4.6}$$

For a bridge located within a turn or bend,

$$R_B = \left(1 + \frac{\theta}{45^\circ}\right) \tag{G.4.7}$$

For a bridge located in a transition region,

$$R_B = \left(1 + \frac{\theta}{90^\circ}\right) \tag{G.4.8}$$

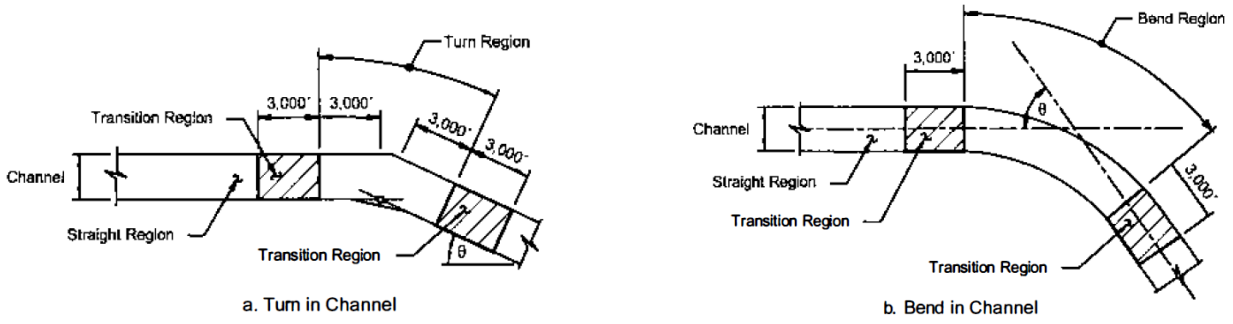

Figure G.4.1 Methodology for determining the region and angle of a turn or bend in a waterway (Source: AASHTO 2014)

Correction factors which account for water velocity (current) conditions may be computed through the use of the following equations:

For currents acting parallel to the transit path of the vessel,

$$R_C = \left(1 + \frac{V_C}{10}\right) \tag{G.4.9}$$

For currents acting perpendicular to the transit path of the vessel,

$$R_{XC} = \left(1 + V_{XC}\right) \tag{G.4.10}$$

where:

V_C = water velocity parallel to the vessel transit path (knots)

V_{XC} = water velocity perpendicular to the vessel transit path (knots)

The correction factor for vessel traffic density (R_D) is selected through an evaluation of the frequency at which vessels encounter (cross paths with or pass by) each other in the vicinity of the bridge. AASHTO (2014) procedures provide for three broad categories of vessel traffic density with corresponding values for R_D:

For low vessel traffic density conditions,

$$R_D = 1.0 \tag{G.4.11}$$

For average vessel traffic density conditions,

$$R_D = 1.3 \tag{G.4.12}$$

For high vessel traffic density conditions,

$$R_D = 1.6 \tag{G.4.13}$$